Analysis of sediment dynamics in the Bill Williams River, Arizona

Andrew C. Wilcox and Franklin Dekker
Department of Geosciences
Center for Riverine Science and Stream Renaturalization
University of Montana
Missoula, MT 59812-1296

Paul Gremillion (Northern Arizona University) and David Walker (University of Arizona)

Collaborators: Patrick Shafroth (USGS), Cliff Riebe (University of Wyoming), Kyle House (USGS), John Stella (State University of New York)
Report prepared for U.S. Fish and Wildlife Service, via Rocky Mountains Cooperative Ecosystem Studies Unit (RM-CESU)

February 6, 2013

DRAFT FINAL REPORT

Table of Contents

Executive summary

The report presented here is the final product of a cooperative agreement between the University of Montana (UM) and the U.S. Fish and Wildlife Service, in association with a multiagency partnership that includes the USFWS, the U.S. Bureau of Reclamation and the U.S. Army Corps of Engineers. A portion of the report was completed by researchers at Northern Arizona University and the University of Arizona under subcontract to UM. This project has included four components: (1) quantitative analysis of how Alamo Dam is affecting downstream sediment dynamics in the Bill Williams River, AZ; (2) a detailed hydro-acoustic survey of Alamo Lake and the Bill Williams Delta in Lake Havasu, to develop a bathymetric map of the lake bottoms, (3) the collection and analysis of sediment cores from Alamo Lake and the Bill Williams Delta in Lake Havasu, and (4) reporting on the linked geomorphic and vegetation responses of recent experimental flood releases. The goal of this project has been to develop a quantitative understanding of sediment dynamics along the Bill Williams River, Arizona, in a manner that will assist flow management and ecosystem restoration efforts.

Dam effects on flow and sediment regimes can be dramatic in dryland rivers. Flow regulation typically eliminates geomorphically significant, high-magnitude, low-frequency flood events in these systems. In dammed rivers, trapping of sediment behind dams can produce downstream coarsening and armoring, as well as incision. Interpreting the geomorphic effects of sediment supply reductions in dammed dryland rivers is important in the context of flow management and understanding ecosystem effects of dams.

One method of evaluating sediment supply dynamics is to calculate erosion rates for different contributing areas of a watershed. Cosmogenic nuclide analysis of beryllium-10 (^{10}Be) can yield long-term, catchment-wide erosion rates. Cosmogenic nuclide concentrations also provide a novel tracer to address the difficult problem of defining dam impacts on river sediment supply. Cosmogenic nuclide samples were collected in the BWR basin, including from the mainstem of the BWR upstream and downstream of the Alamo Dam and from tributaries downstream of the dam. Using cosmogenic nuclide analysis of ^{10}Be, we found that long-term erosion rates vary considerably in the BWR watershed between the upper catchment (136 t km^{-2} yr^{-1}) and tributaries downstream of Alamo Dam (61 t km^{-2} yr^{-1}).

Downstream adjustments of bed-material size can be one of the primary geomorphic responses to changes in flow and sediment regimes downstream of dams, but the downstream extent of grain-size adjustments can be mediated by valley confinement and tributary confluence effects. Grain size was coarsest immediately downstream of Alamo Dam (D_{50}= 41 mm) but fined exponentially downstream. Our analysis suggests that Alamo Dam causes grain size coarsening and sediment deficit conditions that extend to about 10 km downstream. Further downstream, however, the wide alluvial valleys in the BWR basin, which store substantial amounts of sediment, mitigate dam-induced supply reductions. Cosmogenic nuclide results along the mainstem BWR support this conclusion.

Seismic profiling, bathymetric mapping, and sediment coring were performed in Alamo Lake and the Bill Williams delta of Lake Havasu. Seismic profiling was successful in providing accurate bathymetric data, but had limited utility in providing a spatially resolved picture of sediment stratigraphy in the lakes. This was likely due to high concentrations of organic matter which obscured the seismic signal. The bathymetric mapping component of the study produced accurate digital elevation models of Alamo Lake for the years 1985 and 2009 and for the Bill Williams delta of Lake Havasu in 2009. The sediment coring component of the study produced a set of well-resolved high-resolution cores, which have been sampled and analyzed to produce a synoptic description of sedimentation in both lake systems.

Studies of a series of experimental floods on the BWR illustrate how interactions among flow, geomorphic processes, and riparian vegetation can strongly influence both channel form and vegetation communities. We found that floods produced geomorphic and vegetation responses that varied with

distance downstream of Alamo Dam, with scour and associated seedling mortality closer to the dam and aggradation and burial-induced mortality in a downstream reach. We also observed significantly greater mortality among nonnative tamarisk (*Tamarix*) seedlings than among native willow (*Salix gooddingii)* seedlings, reflecting the greater first-year growth of willow relative to tamarisk. When vegetation was small early in our study period, the effects of vegetation on flood hydraulics and on mediating flood-induced channel change were minimal. Vegetation growth in subsequent years resulted in stronger feedbacks, such that vegetation's stabilizing effect on bars and its drag effect on flow progressively increased, muting the geomorphic effects of a larger flood release. These observations suggest that the effectiveness of floods in producing geomorphic and ecological changes varies not only as a function of flood magnitude and duration, but also of antecedent vegetation density and size.

Introduction

Sediment dynamics are a key uncertainty in relation to management and restoration of many dammed rivers. The influence of sediment supply on fluvial processes is a fundamental tenet of fluvial geomorphology [Parker, 2004; Schmidt and Wilcock, 2008]. Manifestations of reduced supply in dammed rivers, such as coarsening of bed material and incision, are well documented [e.g., Williams and Wolman, 1984]. Most environmental flow plans, however, are designed without consideration of sediment supply and exclusively focus on the relationship between water discharge and ecosystem response. A notable exception is the environmental flow releases from Glen Canyon Dam to Grand Canyon on the Colorado River, which have attempted to rebuild downstream sandbars that have shrunk since dam construction [Hazel et al., 2006; Melis et al., 2012; Wright et al., 2008]. Studies of adaptively managed flow releases in Grand Canyon suggest that high flows can cause net sediment loss and that meeting objectives related to maintenance of sandbars and fan-eddy complexes requires increased sediment supply (Schmidt et al., 2001). Large releases from the dam have thus far failed to rebuild sandbars because insufficient sand is available in the system downstream of Glen Canyon Dam, and tributary supplies are inadequate to counteract dam-induced limitations. These results highlight the importance of understanding sediment supply for environmental flow management (Wright et al. 2008).

On the Bill Williams River (BWR) in western Arizona, improved understanding of how dams and reservoirs affect sediment storage, supply, and transport are needed in order to inform flow management, restoration of aquatic and riparian ecosystems, and management of sediment and turbidity delivery to Lake Havasu. The effects of flow alteration on riparian vegetation in this system are relatively well documented (Shafroth et al., 1998; Shafroth and Beauchamp, 2006), and recent flow experiments have provided insight into how flows affect ecosystems (Shafroth et al. 2010). Key questions remain, however, with respect to sediment dynamics, including reservoir sedimentation, tributary sediment supply, how high-flow releases from Alamo dam affect sediment dynamics, and ecosystem effects of changes in sediment supply. This study refines and quantifies our understanding of sediment dynamics in the Bill Williams River by quantifying erosion rates, assessing geomorphic signatures of altered sediment supply, reporting the results of reservoir hydroacoustic surveys and sediment coring, and documenting the geomorphic effects of recent high-flow releases on the BWR.

An open question in the BWR and other dammed rivers is how reductions in sediment supply influence vegetation and its feedbacks with morphodynamics. The effects of dam-induced reductions in sediment supply on vegetation are poorly understood. Dam-induced coarsening could influence vegetation both by altering the capacity of substrates to retain moisture and by increasing the critical shear stress of bed materials, thus reducing the frequency of bed (and seedling) scour. Vegetation, in turn, by altering drag and sediment deposition, can mediate relationships between sediment supply, flow, and bed material size.

The relative influence of dams on peak flows and sediment supply can be estimated using metrics proposed by Schmidt and Wilcock (2008). For example, Q^* is the ratio of the post-dam Q_2 to the pre-dam Q_2 and provides an indication of the extent to which a dam has reduced transport capacity (Magilligan and Nislow, 2005; Schmidt and Wilcock, 2008). For the BWR, $Q^* = 0.04$, based on Log Pearson III analysis of peak-flow data from the US Geological Survey BWR near Alamo gauge, a value that indicative of extreme peak flow reduction. Analogously to the Q^* metric, the reduction in sediment supply caused by a dam can be calculated as Q_s^* (Schmidt and Wilcock, 2008):

$$Q_S^* = \frac{Q_{S\ (post-dam)}}{Q_{S\ (pre-dam)}}$$

Back-of-the envelope methods to quantify the magnitude of sediment supply reduction to the BWR suggest that immediately downstream of Alamo Dam, $Q_s^* \approx 0.01$, and that in the lower BWR, below several tributaries, $Q_s^* \approx 0.1$. These calculations are based on pre-dam and post-dam contributing areas

for sediment to different study reaches, assumed unit sediment yields based on findings from nearby in the Mojave Desert (Griffiths et al., 2006), and the assumption that Alamo Dam currently blocks all sediment supply to downstream reaches.

One approach to understanding sediment dynamics is to develop a sediment budget, which is a quantitative statement of rates of production, transport, storage and discharge of sediment in a geomorphic system (e.g., Dietrich et al., 1982). A sediment budget has three components: input of sediment to some system of interest (*I*), output of sediment from that system (*O*), and the change in sediment storage within that system (ΔS), which can be expressed by the simple statement: $I-O=\Delta S$. A sediment budget can be used to quantify the magnitude and spatial pattern of sediment supply reduction below a dam and to provide information to managers about changes in sediment regimes. Complete sediment budgets that quantify all sediment input, output, and storage components of geomorphic systems are extremely difficult to develop, but "rapid sediment budgets" that synthesize data and / or develop new information on elements of a sediment budget can be extremely useful for increasing understanding and guiding management (e.g., Reid and Dunne, 1996). Development of a complete sediment budget was beyond the scope of this study, but we present several lines of analysis that clarify elements of the sediment balance of the BWR, particularly with respect to the effects of Alamo Dam. The primary data we use in this analysis are as follows:

- Measurement of spatially distributed long-term erosion rates in the upper BWR basin, along the BWR mainstem, and in tributaries to the BWR using isotopic methods
- Measurement of grain-size variations in the BWR basin, extending from upstream of Alamo Dam and down the mainstem BWR, including upstream and downstream of tributaries and in canyon and valley reaches, as a means of assessing one of the geomorphic expressions of changes in sediment supply in rivers.
- Hydroacoustic survey and sediment coring data from Alamo Reservoir and/or Lake Havasu
- Evaluation of geomorphic changes associated with recent (2006-2010) controlled flood releases from Alamo Dam.
- Sediment transport measurements from the BWR, including data from the March 2006 and March 2010 releases.

Side-scan sonar and seismic profiling are powerful tools for mapping the shape and stratigraphy of ocean and lake sediments. These instruments, linked with spatial analysis software, are capable of providing highly accurate maps of bathymetry, sediment thickness, and sediment deposition characteristics. This report presents the results of a detailed hydroacoustic survey and collection of sediment cores in Alamo Lake and Lake Havasu (in the vicinity of the delta of the BWR), including a depiction of sediment stratigraphy showing layering due to flood events and/or primary production, are presented. This work was performed by Dr. Paul Gremillion (Northern Arizona University) and Dr. David Walker (University of Arizona)

Sediment cores are useful only if the quality of the depositional record can be assessed. Cores collected from highly disturbed environments, for example, do not yield a systematic, chronological sequence of sediments. Sedimentation in reservoirs can be subject to highly dynamic conditions, particularly in arid lands where hydrologic events may be large in magnitude. Past work in the American Southwest has demonstrated that it is typical for these reservoirs to have large-magnitude hydrologic events deliver such massive pulses of sediment that these inputs tend to form distinct sediment strata that protect underlying sediment from disturbance. A major benefit of this work is to determine the amount of sedimentation since impoundment, and other depositional characteristics (for example, these data will enable the detection of deltas formed during high water and their subsequent erosion during low water levels).

The studies presented here provide insight into how sediment supply may influence erosional effects of floods, and whether and how design of pulse-flow releases should account for sediment dynamics. Our work also contributes more broadly to development of insights into feedbacks between sediment supply, flow, vegetation dynamics, and channel evolution.

Study area

The Bill Williams River (BWR) historically flowed 65 km from the confluence of the Santa Maria River and Big Sandy River into the Colorado River in western Arizona, USA (Figure 1), draining 13,800 km^2 and alternating between canyon and alluvial valley reaches (Figure 2). Because the hydrology of the BWR is influenced by wetter conditions in its mountainous headwaters, where average annual precipitation exceeds 40 cm yr^{-1}, and arid conditions in the lower basin (12 cm yr^{-1} precipitation) [Shafroth and Beauchamp, 2006], we characterize the river as "dryland" rather than arid or semiarid. Both the upstream and downstream limits of the BWR are currently submerged within reservoirs. Alamo Dam, a U.S. Army Corps of Engineers flood-control facility that was completed in 1968 (Figure 3) and impounds Alamo Lake, now forms the upstream limit of the BWR. At its downstream end, the BWR flows into Lake Havasu, an impoundment on the Colorado River that is the source for the Central Arizona Project Aqueduct and the Colorado River Aqueduct, which supply water to several large cities in the southwestern US.

Alamo Dam has substantially reduced peak flows in and sediment supply to the BWR (Figure 2). For example, the ratio of the post-dam two-year flood (Q_2) to the pre-dam Q_2 is 0.04, based on log Pearson III analysis of peak-flow data from the US Geological Survey BWR below Alamo Dam, AZ gauge (#09426000). This ratio, a metric known as Q* [Magilligan and Nislow, 2005; Schmidt and Wilcock, 2008], provides an indication of the extent to which a dam has reduced transport capacity; the 0.04 value for the BWR is indicative of extreme peak flow reduction. The upper 85 percent of the basin's drainage area is effectively disconnected from the BWR by Alamo Dam, blocking the supply of bed-material from the upper basin (Figure 1). Further, there are no perennial tributaries downstream of Alamo Dam (Figure 2). In the BWR, effects of supply limitation are evident immediately downstream of Alamo Dam, where the channel is coarse (gravel-cobble, compared to sand in upstream reaches) and incised several meters below its floodplain (Figure 3). The downstream extent of such changes are explored further in this report.

The BWR's alluvial valleys (Figure 2), the largest of which is the 13-km long Planet Valley, exert a strong control on the routing of both flow and sediment through the BWR, causing gains and losses of surface flow and storing large volumes of sediment. The alluvial aquiver in Planet Valley acts as a sponge, such that all of the river's baseflow typically infiltrates at the upstream end of the valley and emerges at the downstream end, where valley width and depth to bedrock decline [House et al., 2006; Jackson and Summers, 1988]. Planet Valley and its antecedent water-table elevation also influence routing of high flows down the BWR [Shafroth et al., 2010], as discussed further below.

The severe reduction of both transport capacity and sediment supply in the BWR has been accompanied by the spread of tamarisk and severe channel narrowing. Aerial photograph analysis indicates that since the 1950s channel width has declined dramatically, with corresponding expansion of floodplain vegetation [Shafroth et al., 2002]. This channel narrowing trend started even before Alamo Dam was built, likely as a result of regional climatic shifts [Sheppard et al., 2002] that reduced peak flows along many rivers in the southwestern US [Hereford, 1984].

Whereas many river corridors in the southwestern U.S. are dominated by nonnative tamarisk, the BWR has a diverse riparian flora that includes tamarisk but also Goodding's willow (*S. gooddingii*), Fremont cottonwood (*Populus fremontii*), seep willow (Baccharis salcifolia), arrowweed (Pluchea sericea), mesquite (*Prosopis* spp.), and cattail (*Typha* spp.). Plant species richness is lower in the BWR

than in its unregulated upstream tributary, the Santa Maria River, however, likely as a result of flood reduction [Stromberg et al., 2012]. In an effort to sustain the native riparian woodland habitat in the BWR, flow management at Alamo Dam has been guided in recent years by collaborative efforts between the Army Corps of Engineers and other stakeholders [Shafroth and Beauchamp, 2006; Shafroth et al., 2010] and have followed the Environmentally Sustainable Water Management (ESWM) framework [Konrad et al., 2012; Richter et al., 2003]. Environmental flow releases have included baseflows designed to provide summer and fall irrigation for cottonwoods and willows as well as flood releases as water availability allows. Dam reoperations for environmental purposes on the BWR are facilitated because competing water uses such as hydropower production or irrigation are absent or limited, because the downstream floodplain is sparsely populated, and because water released from Alamo Dam is delivered to and impounded by Lake Havasu. Communication among scientists and managers has allowed scientists to provide input into the design of flow releases and to mobilize for data collection during flood pulses. These factors combine to create a unique field laboratory.

A series of floods have been released from Alamo Dam into the BWR in the last decade. During the winter of 2004 and 2005, high runoff associated with El Niño caused multiple high-flow events in the range of the dam's maximum outlet capacity (approximately 200 m^3s^{-1}). These events scoured vegetation from low-elevation bars and created bare surfaces for seedling establishment, which was promoted by a managed drawdown of flows (approximately 0.5 $m^3s^{-1}day^{-1}$) in spring 2005. These floods subsequently resulted in the widespread establishment of riparian seedling patches initially co-dominated by tamarisk and willow. In March 2006, a controlled flood was released from Alamo Dam in which discharge was ramped up to an instantaneous peak of 69 m^3s^{-1}, maintained at that peak for 7.5 hours, and then dropped and held at 56 m^3s^{-1} for two days, followed by a gradual drawdown of approximately 1 $m^3s^{-1}day^{-1}$. Smaller pulse flow releases occurred in 2007 and 2008. In 2010, another El Niño year in which inflows to Alamo Lake were large, the highest-magnitude, longest-duration flood since 2005 was released.

Flows at the downstream end of the BWR were lower than those released from Alamo Dam during these floods as a result of infiltration and associated flow attenuation within Planet Valley and other alluvial valleys. Flows measured downstream of Planet, at the BWR near Parker, AZ gauge (# 09426620), were most similar to those measured at Alamo when antecedent water-table levels in Planet Valley were high and flood durations were longer (e.g., 2005, 2006, 2010). In contrast, when antecedent water levels were low and/or flood durations were short (2007 and 2008), flood peaks were substantially attenuated in downstream portions of the BWR. For example, peak flows measured at Parker were 19% and 2% of the upstream peaks in 2007 and 2008, respectively.

The magnitude and duration of the releases were constrained by water availability, dam release capacity, and concerns over potential impacts to other downstream land and water management interests. Consequently, the events were small compared to historic floods on the BWR. These events were substantial, however, when considered within the context of the post-dam hydrologic regime; the 2005 event was the largest since dam construction. The observed flood releases were timed to overlap with the seed release period of willow and cottonwood, although tamarisk also releases seed concurrently with willow on this river system [Shafroth et al., 1998].

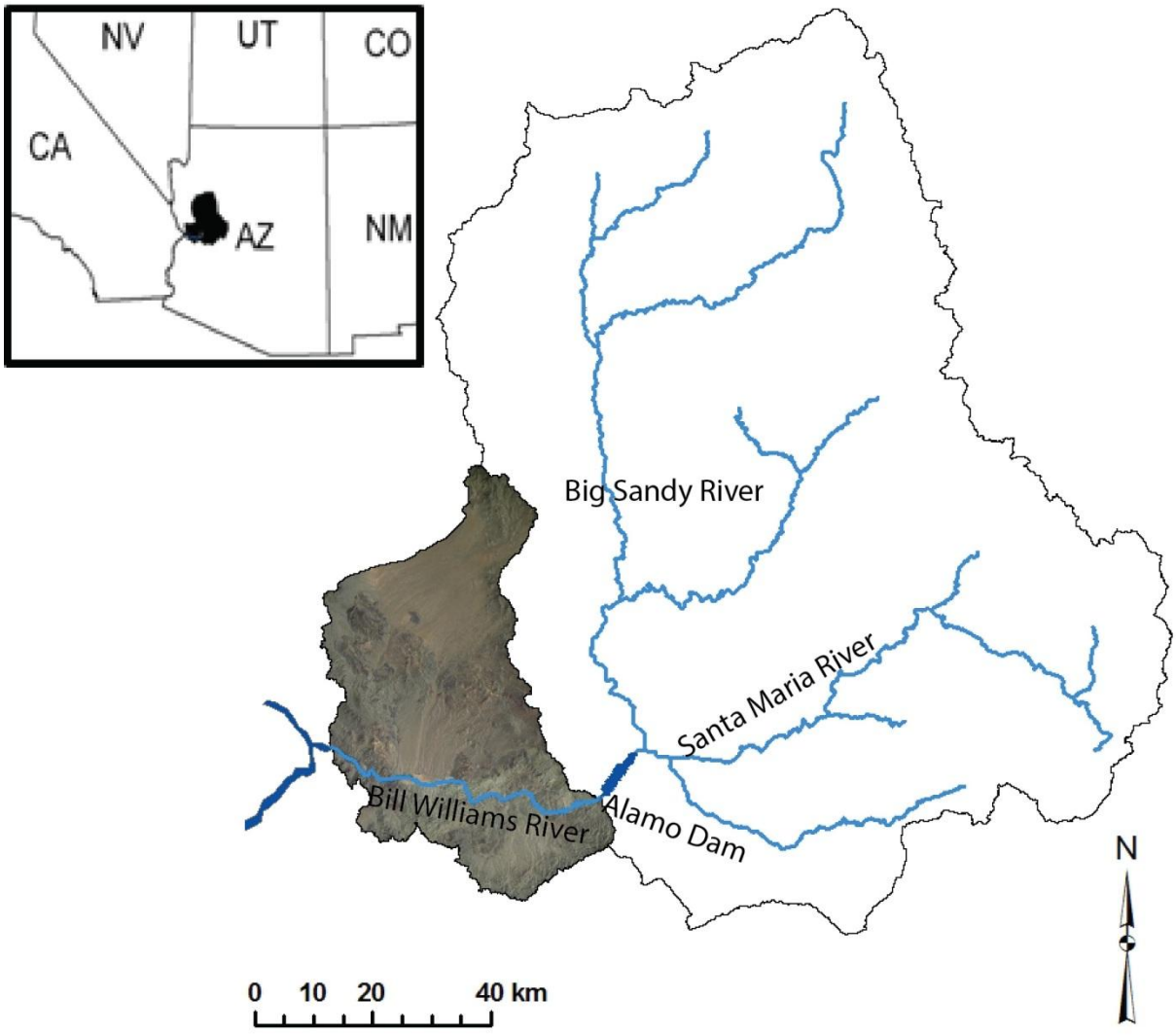

Figure 1. Bill Williams River basin. Inset map shows location in Arizona and southwestern United States. Large map shows BWR basin, with area downstream of Alamo Dam highlighted to show portion of basin that currently delivers sediment to mainstem BWR; supply from the upstream watershed area is cut off by the dam.

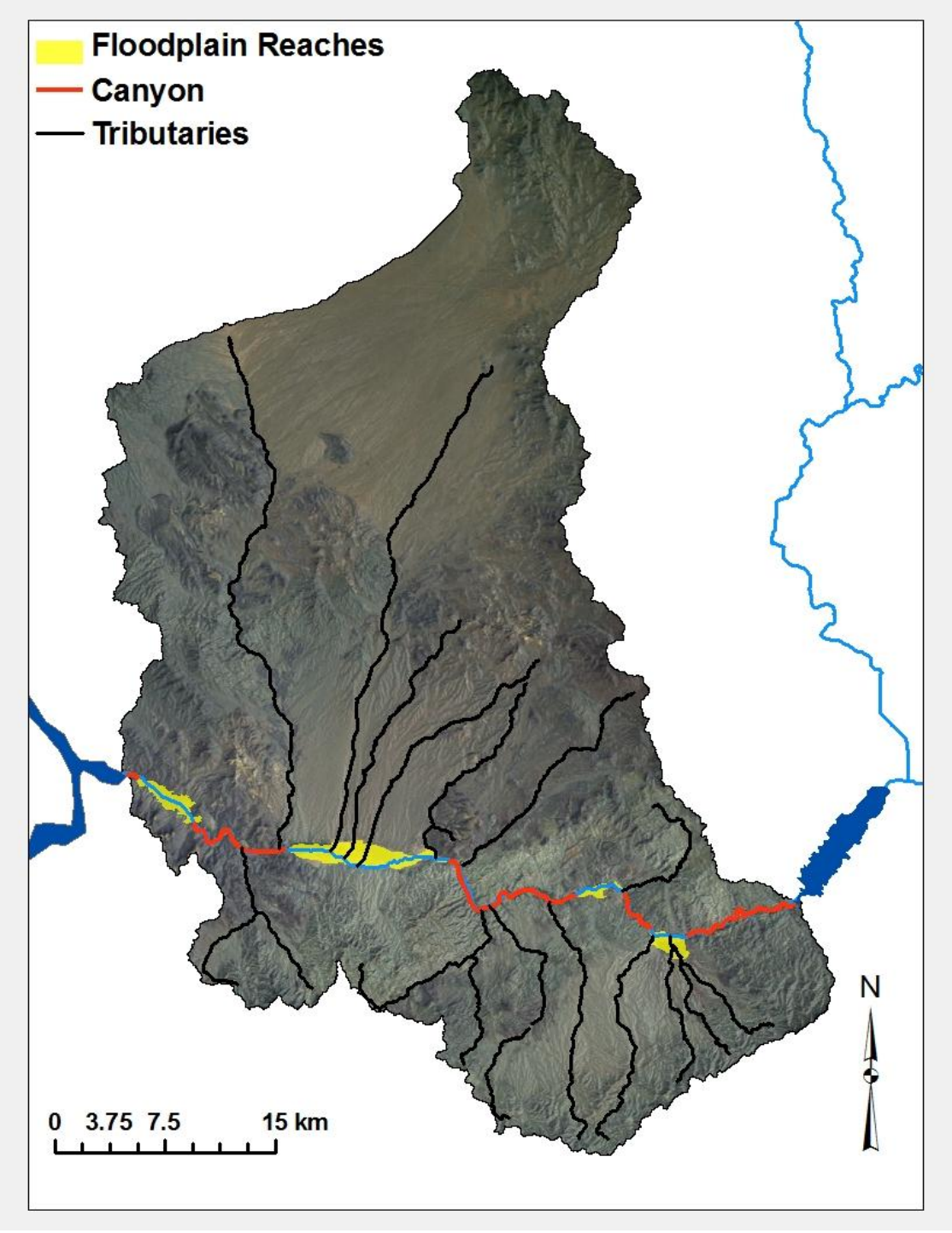

Figure 2. Bill Williams River basin downstream of Alamo Dam, showing tributaries to mainstem BWR and alternating canyon and valley (floodplain) reaches.

46. Alamo Dam; downstream side.

Figure 3. Alamo Dam and Bill Williams River. Left photo undated but possibly from Aug. 1968 at least before 1973 (publication date of report) ; right photo May 2011.

References

Dietrich, W.E., Dunne, T., Humphrey, N.F. and Reid, L.M., 1982. Construction of sediment budgets for drainage basins. In: F.J. Swanson, R.J. Janda, T. Dunne and D.N. Swanston (Editors), Sediment Budgets and Sediment Routing in Forested Drainage Basins, General Technical Report PNW-141. USDA Forest Service, pp. 5-23.

Griffiths, P.G., Hereford, R. and Webb, R.H., 2006. Sediment yield and runoff frequency of small drainage basins in the Mojave Desert, U.S.A. Geomorphology, 74(1-4): 232-244.

Magilligan, F.J. and Nislow, K.H., 2005. Changes in hydrologic regime by dams. Geomorphology, 71(1-2): 61-78.

Schmidt, J. C., R. A. Parnell, P. E. Grams, J. E. Hazel, M. A. Kaplinski, L. E. Stevens, and T. L. Hoffnagle (2001), The 1996 controlled flood in Grand Canyon: Flow, sediment transport, and geomorphic change, Ecological Applications, 11(3), 657-671.

Schmidt, J.C. and Wilcock, P.R., 2008. Metrics for assessing the downstream effects of dams. Water Resources Research, 44(4).

Shafroth, P.B., Auble, G.T., Stromberg, J.C. and Patten, D.T., 1998. Establishment of woody riparian vegetation in relation to annual patterns of streamflow, Bill Williams River, Arizona. Wetlands, 18(4): 577-590.

Shafroth, P.B. and Beauchamp, V.B. (Editors), 2006. Defining ecosystem flow requirements for the Bill Williams River, Arizona. Open-File Report, 2006-1314. U.S. Department of Interior, U.S. Geological Survey, Reston, VA, 135 pp.

Shafroth, P. B., A. C. Wilcox, D. A. Lytle, J. T. Hickey, D. C. Andersen, V. B. Beauchamp, A. Hautzinger, L. E. McMullen, and A. Warner (2010), Ecosystem effects of environmental flows: modelling and experimental floods in a dryland river, Freshwater Biology, 55, 68-85.

Vincent, K., J. Friedman, and E. Griffin (2009), Erosional consequence of saltcedar control, Environmental Management, 44(2), 218-227.

Wiele, S.M., Hart, R.J., Darling, H.L. and Hautzinger, A.B., 2009. Sediment transport in the Bill Williams River and turbidity in Lake Havasu during and following two high releases from Alamo Dam, Arizona, in 2005 and 2006. U.S. Geological Survey Scientific Investigations Report 2009-5195.

Reid, L.M. and T. Dunne. 1996. Rapid evaluation of sediment budgets. Catena Verlag, Reiskirchen.164 p.

Catchment Erosion Rates and Sediment Mixing in a Dammed Dryland River

Franklin J. Dekker[1], Andrew C. Wilcox[1], and Cliff Riebe[2]

[1]Department of Geosciences, University of Montana, Missoula, MT 59812, USA
[2]Department of Geology, University of Wyoming, Laramie, WY

This chapter is in preparation for submission to a peer-reviewed journal. We welcome feedback. Readers should contact Andrew Wilcox for information on the status of the manuscript and/or an updated version of the manuscript after it has been published.

Abstract

Cosmogenic nuclide analysis of beryllium-10 (^{10}Be) can yield long-term, catchment-wide erosion rates, but few such studies have been performed in dryland rivers. Cosmogenic nuclide concentrations also provide a novel tracer to address the difficult problem of defining dam impacts on river sediment supply. In this study, the following two questions are addressed: (1) Do large dryland rivers consistently mix riverbed sediments? (2) Can cosmogenic nuclide analysis be applied to determine the downstream extent of dam effects on sediment supply? Cosmogenic nuclide samples were collected in the Bill Williams River (BWR) basin in western Arizona, including from the mainstem of the BWR upstream and downstream of the Alamo Dam and from tributaries downstream of the dam. Riverbed sediment mixing calculations were used to address the main study questions by (1) determining if sediments from the BWR's large upstream catchment are well mixed to provide a valid ^{10}Be erosion rate and (2) testing if Alamo dam alters sediment mixing by increasing the proportion of tributary sediment to residual upstream sediment in mainstem samples downstream of Alamo Dam. Cosmogenic nuclide analysis shows that erosion rates vary considerably in the BWR watershed between the upper catchment (136 t km^{-2} yr^{-1}) and tributaries downstream of Alamo Dam (45.5 t km^{-2} yr^{-1}). Tributary catchments downstream of Alamo Dam erode at nearly one-third the rate of the Big Sandy and Santa Maria Rivers which form the BWR at their confluence 11 km upstream of Alamo Dam. The nuclide mixing at the confluence of the Big Sandy and Santa Maria Rivers supports the limited cosmogenics data previously reported that large arid catchments (>1,000 km^2) are well mixed despite their size and dryland river complexity.

Introduction

Analysis of the concentration of cosmogenic nuclides in fluvial sediments has emerged in recent years as a tool for determining catchment-wide erosion rates and addressing associated geomorphic questions (Brown et al., 1995; Bierman and Steig, 1996; Granger et al., 1996; Portenga et al., 2011). For example, long-term (10^3–10^5 years) erosion rates derived from cosmogenic nuclide analysis have been compared to short-term modern rates to gauge human impacts or landscape erosion cycles (Kirchner et al., 2001; Portenga et al., 2011). Comparison between outcrop erosion rates and catchment-wide rates has been used to test assumptions about steady-state conditions between sediment generation and sediment yield (Matmon et al., 2003; Schaller et al., 2001).

The most common method of cosmogenic nuclide analysis uses the steady accumulation of beryllium-10 (^{10}Be) isotopes from secondary cosmic radiation in the top 1 m of rock or soil. The accumulated ^{10}Be isotopes are reliably measured in quartz (SiO_2), because it contains no beryllium atoms naturally and quartz is resistant to chemical alteration. The secondary cosmic rays convert oxygen atoms (^{16}O) within quartz to ^{10}Be (Granger and Riebe, 2007), a process referred to as *in situ* produced, as opposed to meteoric produced ^{10}Be, which will not be discussed or applied here. *In situ* ^{10}Be is the preferred nuclide for catchment erosion rate studies because it has a long half life (1.36 Myr) and low analytical background uncertainty (Dunai, 2010).

Repeated chemical dissolution is required to purify quartz and remove adsorbed meteoric ^{10}Be. Precise isotope measurements are taken with an accelerator mass spectrometer (AMS) to determine the ratio between a known ^{9}Be spike and the in-situ produced ^{10}Be (^{9}Be/^{10}Be). ^{10}Be nuclide concentrations are calculated from this ratio (Dunai, 2010). Nuclide concentrations are converted to erosion rate by applying models of nuclide production (Bierman and Steig, 1996; Brown et al., 1995; Granger et al., 1996). Erosion rates are averaged over 1,000 – 30,000 years depending on the time required to erode approximately 1 m (Von Blanckenburg, 2005). Faster-eroding catchments have lower nuclide concentrations while slower-eroding catchments have a greater concentration due to longer near-surface residence times (Granger and Riebe, 2007).

Cosmogenic nuclide analysis can also be used to determine the source and mixing of fluvial sediment. This approach requires the assumption that a fluvial sediment sample is an aggregate of all sediment that originates upstream of that sample, and that all sources of sediment are mixed proportional to each source area and erosion rate (Von Blanckenburg, 2005; Granger et al., 1996). Because sediment is being mixed, so are nuclides, such that the fluvial sample will be a spatial average of nuclide concentration for the catchment. Nuclide concentrations have been used to track sediment sources and the extent of sediment mixing (e.g. Clapp et al., 2002; Fruchter et al., 2011; Matmon et al., 2003; Schaller et al., 2001). This application of cosmogenic nuclides requires multiple samples within a watershed and simple sediment mixing calculations. A mixing calculation is an average of two or more cosmogenic nuclide concentrations weighted according to erosion rate and contributing area to create a new mixed nuclide concentration (Granger et al. 1996). The mixing equation for two sampled catchments (1 and 2) is written as:

$$\langle N_{12} \rangle = \frac{N_1 E_1 A_1 + N_2 E_2 A_2}{E_1 A_1 + E_2 A_2} \qquad (1)$$

where (N_x) is the nuclide concentration in atoms per gram of quartz (at g^{-1}), (E_x) the erosion rate in tons per square kilometer per year (t km^{-2} yr^{-1}) and (A_x) the area in square kilometers (km^2) of the two or more catchments being mixed. The mixing equation result is ($\langle N_{12} \rangle$) for nuclide concentration. The calculated nuclide concentration can then be compared to actual cosmogenic samples taken downstream of the samples used in the mixing calculation. Differences between these values could

indicate additional sources of sediment, such as unaccounted for basin storage or fluvial terraces (Clapp et al., 2002), or dam effects on sediment mixing, as we hypothesize here.

Catchment-wide erosion rate calculations from cosmogenic nuclides have been applied to rivers in many climatic settings (Portenga et al., 2011), and this method holds promise for advancing the understanding of dryland river sediment dynamics (Tooth, 2007). Cosmogenics analysis has been applied to many small catchments (< 300km^2) in dryland regions (Clapp et al., 2000, 2001, 2002; Fruchter et al., 2011) but to fewer larger catchments (>1,000 km^2) (Bierman et al., 2005). Bierman et al. (2005) found that nuclide concentrations from large complex catchments mixed as expected by simple mixing equations. This result was previously only found in small homogeneous catchments (Clapp et al., 2000; Granger et al., 1996). Well-mixed nuclide concentrations were also found in intermittent or ephemeral drainages (Bierman et al., 2005). This lends confidence that cosmogenic samples from any dryland stream, perennial or ephemeral, are representative of the entire source area over short distances (Bierman et al., 2005). The study question investigated here is: do all drainages in a large dryland river system yield consistent sediment mixing results?

Cosmogenic nuclide analysis provides a novel approach to the difficult problem of defining dam impacts on river sediment supply. The downstream extent of dam effects on sediment supply varies among dammed rivers as a function of the severity of flow and sediment supply reduction and the volume and spatial distribution of sediment inputs from tributaries (Schmidt and Wilcock, 2008; Williams and Wolman, 1984). Schaller et al. (2001) noted that the locks on the Neckar River in southern Germany resulted in a greater signal from local nuclide concentration sources. However, we know of no applications of cosmogenics to address how a dam alters sediment mixing. Nuclide concentrations will theoretically show the severity and downstream extent to which a dam has altered sediment supply from pre-dam conditions. Determining the extent of dam impacts are typically hindered by a lack of pre-dam observations (Williams and Wolman, 1984). Moreover, sediment budgets applied to determine dam effects are time-consuming to construct and can have high uncertainty (Grams and Schmidt, 2005; Schmidt and Wilcock, 2008). *In situ* cosmogenic nuclide analysis is an alternative that does not require sampling prior to dam construction. The research question stemming from this is, can sediment mixing equations be applied to determine the downstream extent of dam effects on sediment supply and if so, what is that extent? To structure our inquiries into this question, we pose the following hypotheses:

1) Sediment from large dryland rivers watersheds is well mixed despite discontinuous dryland river processes. Questions remain whether dryland fluvial sediment is well mixed with sediment from all parts of a dryland watershed, because dryland rivers tend to move the most sediment during large floods at infrequent intervals, and sometimes with active flow occurring only in isolated parts of a watershed.
2) Dams alter sediment mixing by increasing the proportion of tributary sediment to residual upstream sediment. Nuclide concentrations in the mainstem of a dammed river are most similar to tributary nuclide concentrations immediately downstream of a dam due to stripping of pre-dam sediment. Further downstream, tributary nuclide concentrations mix with more and more residual pre-dam sediment adjusting nuclide concentrations.

Here we present nuclide concentrations and erosion rates found in the mainstem and tributaries of a dammed dryland river. Sample collection was designed to make each hypothesis testable with mixing calculations. The discussion compares long-term ^{10}Be erosion rates to modern rates, but mainly focuses on mixing calculation results and implications for cosmogenic nuclide analysis of dammed and dryland rivers.

Methods

Field Site

The Bill Williams River (BWR) in western Arizona is at the transition between the Mojave and Sonoran Deserts, and it was dammed in 1968 by Alamo Dam. The BWR originates at the confluence of the Big Sandy and Santa Maria Rivers and flows 63 km west to Lake Havasu, a dammed section of the Colorado River (Shafroth et al., 2010). Alamo Dam is located 58 km upstream from Lake Havasu. The catchment area of the BWR includes 12,000 km^2 upstream of Alamo Dam and 1,900 km^2 downstream. Alamo Dam traps all bed-load sediment in Alamo Lake (Shafroth and Beauchamp, 2006).

To assess sediment mixing, samples were collected from three distinct groups: upstream of Alamo Dam, downstream of Alamo Dam and tributaries entering the BWR downstream of Alamo Dam (Figure 1). Upstream samples included three samples, one from the Big Sandy River (BS), one from the Santa Maria River (SM) and a sample 1 km downstream from their confluence at the beginning of the BWR (BWR_C). The nuclide concentrations found in the upstream samples were required to test hypothesis (1) but were also used to characterize upper catchment sediment contribution needed to address hypothesis (2).

Five samples were collected from the mainstem of the BWR downstream of Alamo Dam. These samples were taken at 10, 18, 28, 32, and 48 km downstream from the dam and are referred to as DS1 through DS5. Mainstem samples downstream of the dam area were used to determine the extent Alamo Dam has affected sediment mixing to address hypothesis (2).

Tributary sediments downstream of the dam were sampled because tributary nuclide concentrations were needed to determine if Alamo Dam has altered the ratio of tributary and upper catchment sediment in the mainstem samples. Twelve samples were collected from tributaries to the BWR downstream of Alamo Dam. They are labeled T1 through T12, with T1 closest to Alamo Dam while T12 is furthest downstream. The combined area of all 12 tributaries samples is equal to 74% of the total area of the BWR watershed downstream of Alamo Dam.

Sample Preparation, Erosion Rate Calculation, and Analysis

Quartz purification, beryllium precipitation and target packing were conducted at the University of Wyoming Cosmogenic Nuclide Laboratory with methods similar to Kohl and Nishiizumi (1992). However, unlike Kohl and Nishiizumi (1992) samples were sieved by phi class, weighed and then separately disk-milled to between 0.25 and 0.5 mm. Milled phi classes were homogenized according to the percent weight of each size before milling to prevent any grain-size-dependent effects on nuclide concentration. Other cosmogenic studies in arid or semi-arid watersheds have found minimal variation in nuclide concentration across grain size (Clapp et al., 2000, 2001, 2002; Fruchter et al., 2011; Granger et al., 1996). This is attributed to slow sediment transport processes in semiarid drainages that move sediment independent of grain size, such as soil creep and surface wash (Clapp et al., 2001). Packed

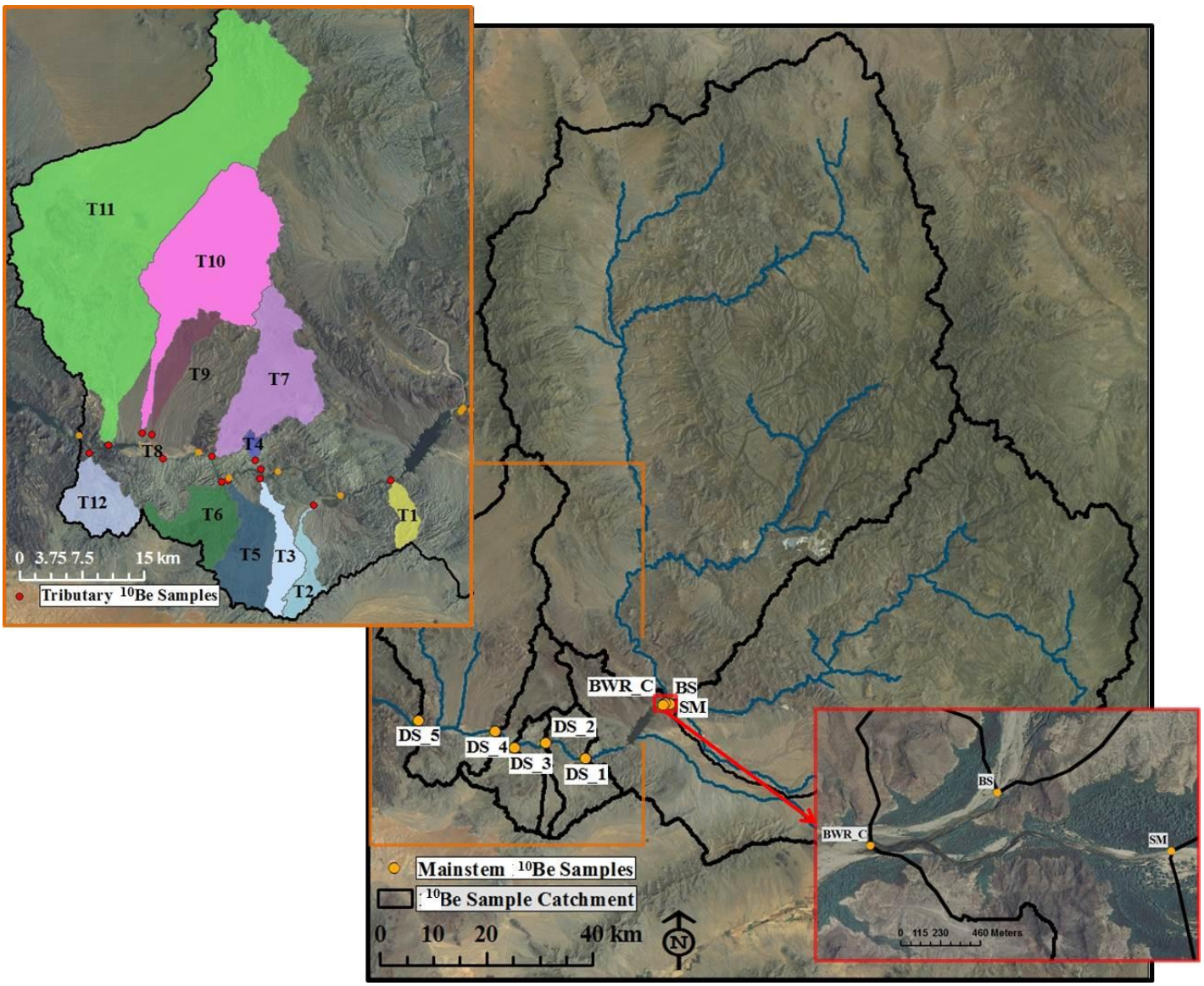

Figure 1. Sample locations for cosmogenic nuclide analysis in the BWR watershed. Samples BS, SM, and BWR_C (lower right inset) were upstream of Alamo Dam. All other samples were from downstream of the dam, including DS_1 – 5 (mainstem BWR) and T1 – 12 (tributaries; upper left inset).

targets were sent to the PRIME Lab (Purdue University) for AMS isotope analysis. Nuclide concentration uncertainty was determined from AMS instrument error provided by PRIME Lab.

Erosion rate calculations were conducted with MatLab and included scaling and shielding corrections. Nuclide production rates were scaled to air pressure and latitude according to Stone and Vasconcelos (2000). A US Geological Survey (USGS) 30 m digital elevation model (DEM) was used to determine altitude of each sample catchment (Dunai, 2000). Fast and slow muon nuclide production rates were calculated with equations by Heisinger et al. (2002a, 2002b) and adjusted for atmospheric attenuation (Rossi, 1948). Adjustments for slope shielding were made from slope data collected with ArcHydro toolbox in ArcGIS from the above-mentioned 30 m DEM (Binnie et al., 2006; Dunne et al., 1999). A chemical erosion factor (CEF) was calculated to address potential loss of nuclide concentration due to chemical erosion (Riebe and Granger, 2011). To calculate the CEF, average precipitation for each catchment was determined from PRISM 30-year average annual precipitation data (PRISM Climate

Group, 2006). PRISM 30-year averages are similar to averages reported for three locations in the BWR watershed by Shafroth et al. (2010). PRISM precipitation data uncertainty has minimal effect on CEF calculation. The very small average precipitation rate for the BWR samples mean the CEF has marginal effects on erosion rate calculation. Overall erosion rate uncertainty was calculated by including a 9% factor of uncertainty in nuclide production rates.

Linear regressions were used to determine the relationship between ^{10}Be erosion rates and catchment characteristics including altitude, relief, slope, area and precipitation. SPSS software was used to run linear regressions with R^2 and p-values to assess the strength and significance of correlation results. Altitude and relief data came from the above-mentioned USGS 30 m DEM. The expression for relief was as follows (from Schaller et al., 2001):

$$\text{Relief} = (\text{mean catchment altitude} - \text{minimum catchment altitude}) \quad (2)$$

Slope and area were both determined using the ArcHydro toolbox in ArcGIS. PRISM precipitation data was clipped and averaged according to sample catchment areas.

Sediment Mixing Equations

Sediment mixing calculations are commonly applied to determine if upstream or tributary samples contribute sediment downstream in expected proportions relative to their contributing areas (Clapp et al., 2002; Fruchter et al., 2011; Granger et al., 1996; Matmon et al., 2003). Mixing calculation results were compared to nuclide concentrations sampled downstream. Mixing calculations have been shown to agree with downstream samples in most settings, except small, rapidly eroding, high-relief catchments (Binnie et al., 2006).

We wrote mixing equations for the BWR to determine if sediment upstream of Alamo Dam is well mixed in both (A) nuclide concentration and (B) erosion rate, and to (C) calculate a theoretical pre-Alamo Dam nuclide concentration for sediment at the mouth of the BWR to compare to samples downstream of Alamo Dam. Units for nuclide concentration are reported in atoms per gram (at g^{-1}), and erosion rates are in tonnes per square kilometer per year (t km^{-2} yr^{-1}). The uncertainty in each equation result was determined by propagating uncertainty in nuclide concentrations and erosion rates. An example of a sediment mixing calculation with work shown can be found in appendix section A. Equations and definitions of terms are as follows.

(A) Nuclide concentration upstream of Alamo Dam:

$$\langle \mathrm{N_{Confluence}} \rangle = \frac{(\mathrm{N_{BS}E_{BS}A_{BS}} + \mathrm{N_{SM}E_{SM}A_{SM}})}{(\mathrm{E_{BS}A_{BS}} + \mathrm{E_{SM}A_{SM}})} \quad (3)$$

(B) Erosion rate upstream of Alamo Dam:

$$\langle \mathrm{E_{Confluence}} \rangle = \frac{(\mathrm{E_{BS}A_{BS}} + \mathrm{E_{SM}A_{SM}})}{(\mathrm{A_{BS}} + \mathrm{A_{SM}})} \quad (4)$$

$\langle N_{confluence} \rangle$ = Mixing calculation result for nuclide concentration at BWR confluence (at g^{-1})
$\langle E_{confluence} \rangle$ = Mixing calculation result for erosion rate at BWR confluence (at g^{-1})
N_{BS} = BS (*Big Sandy River*) nuclide concentration (at g^{-1})
E_{BS} = BS erosion rate (t km^{-2} yr^{-1})
A_{BS} = BS catchment area (km^2)
N_{SM} = SM (*Santa Maria River*) nuclide concentration (at g^{-1})
E_{SM} = SM erosion rate (t km^{-2} yr^{-1})
A_{SM} = SM catchment area (km^2)

(C) Theoretical pre-dam nuclide concentration at the mouth of the BWR:

$$\langle \mathrm{N} \rangle = \frac{(\mathrm{N_U E_U A_U} + \mathrm{N_L E_L A_L})}{(\mathrm{E_U A_U} + \mathrm{E_L A_L})} \quad (5)$$

$\langle N \rangle$ = Mixing Calculation Result for Nuclide Concentration at Mouth (at g^{-1})
N_U = Upper catchment nuclide concentration from BWR_C (*BS and SM confluence*) (at g^{-1})
E_U = Upper catchment erosion rate from BWR_C (t km^{-2} yr^{-1})
A_U = Upper catchment area – upstream of BWR_C (km^2)
N_L = Lower catchment nuclide concentration from mean of tributaries (at g^{-1})
E_L = Lower catchment erosion rate from mean of tributaries (t km^{-2} yr^{-1})
A_L = Lower catchment area – downstream of BWR_C (km^2)

Modern Erosion Rates

To place long-term ^{10}Be erosion rates in context, modern erosion rates for the BWR were collected from three sources. (1) Two erosion rates for the mouth of the BWR were reported by the Bureau of Reclamation (Bureau of Reclamation, 1970). One of these rates was determined based on the growth rate of the BWR sediment delta in Lake Havasu, and the other was determined from average literature rates for the US southwest. (2) The US Army Corp of Engineers determined an erosion rate for the catchment upstream of Alamo Dam (US Army Corp of Engineers - Los Angeles District, 2003). This rate is based on stream gauge data and reservoir filling rates for streams and reservoirs within and in the vicinity of the BWR watershed. (3) A final rate was obtained by calculating the volume change between Alamo Lake bathymetric survey DEMs in 1963 and 1985. This rate is likely the most reliable of the modern BWR erosion rates because it did not include regional averages or any agency erosion formulas. Survey data came from the US Army Corp of Engineers. The 1963 data were part of a pre-dam land survey that mapped the reservoir site with 25 ft (7.6 m) contour intervals. The 1985 survey was made with bathymetric soundings at a 1 ft (0.3 m) interval. The two DEMs were differenced in MatLab and uncertainty was determined according to Wheaton et al. (2010).

All rates were converted to t km^{-2} yr^{-1}. Catchment areas were quantified in ArcHydro. A sediment density of 1.8 g cm^{-3} was used to convert to tonnes. The bulk density of BWR channel deposits was measured in the field by weighing known volumes of dried sediment. It provided results similar to bulk density assumptions used elsewhere (Phillips et al., 2004).

Results

Nuclide Concentration and Erosion Rates

Nuclide concentrations varied between mainstem samples and tributary samples (Figure 2). The average of all tributary nuclide concentrations (2.24×10^5 at g^{-1}) was greater than the average concentration of BWR_C and the mainstem samples downstream of Alamo Dam (1.53×10^5 at g^{-1}) (Table 2). However several tributary samples had similar nuclide concentrations to the mainstem samples (T4, T6, T7, T8, T12; Figure 2). In terms of erosion rates, the upper catchment erosion rate, represented by BWR_C (135 t km^{-2} yr^{-1}), was more than double the average tributary erosion rate (61 t km^{-2} yr^{-1}). Relief, altitude and precipitation are all greater in the upper catchment samples (BWR_C, SM and BS) than in the tributary samples (Table 1). Linear regressions for controls on erosion rates showed significant correlation ($p < 0.05$) for altitude and relief with R^2 value of 0.94 and 0.89, respectively. Mainstem samples downstream of Alamo Dam (DS_1 – 5) were not included in regression statistics because the sediment capture by Alamo Dam may have altered the source area of sediment in the mainstem BWR. An erosion rate for a mainstem sample calculated with the entire upstream BWR catchment would be erroneous if degradation caused by Alamo Dam has altered the ratio of upper-catchment-sourced sediment to lower-catchment sediment.

Mixing calculations confirmed that the BWR_C sample was representative of the upper catchment; the results of equations (3) and (4) estimated very similar erosion rate and nuclide concentrations to those of BWR_C (Figure 3). The results from the mixing calculation and the actual BWR_C sample differed by 6.5% in nuclide concentration and 6.3% in erosion rate.

Complete analysis of the cosmogenic nuclide results for tributaries downstream of Alamo Dam are still in progress because of delays in receiving the AMS results from PRIME Lab. Summary data are shown in Figure 2 and Table 2. Mixing results and additional analysis are in progress.

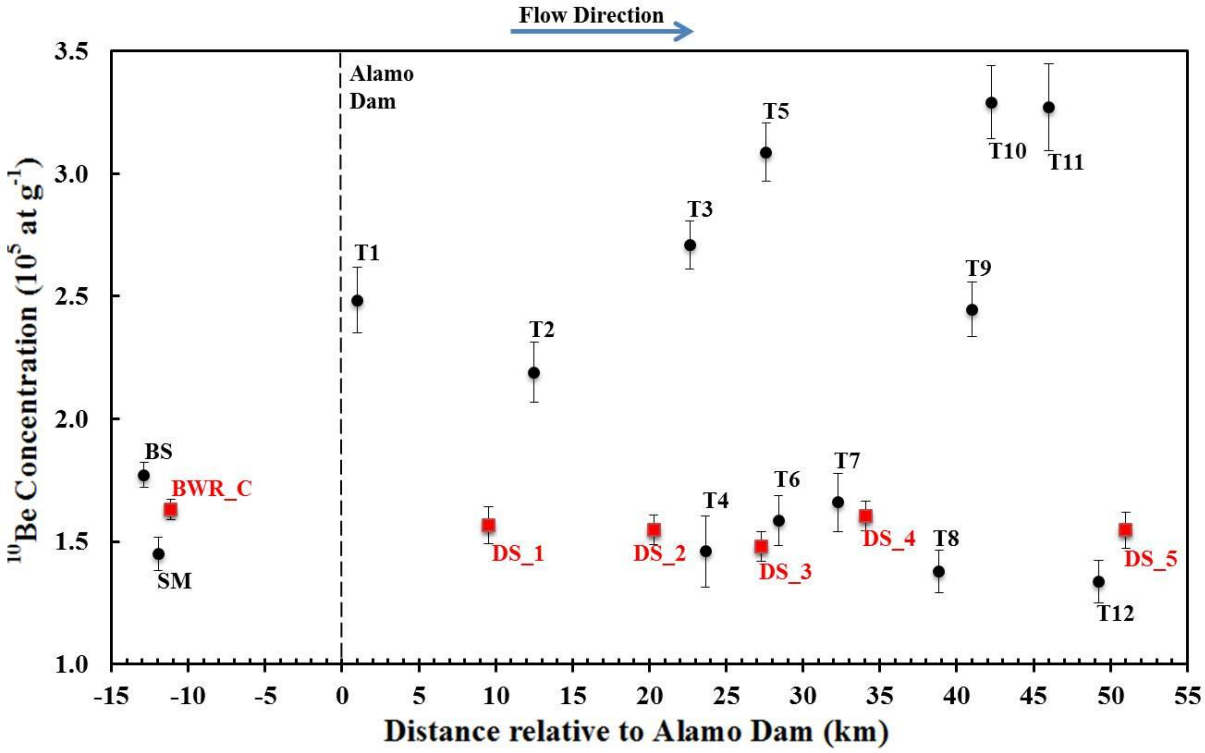

Figure 2. Nuclide concentration results versus distance relative to Alamo Dam. Error bars are from analytical error to determine ^{10}Be concentration. Below-dam mainstem concentrations were similar to above-dam samples; tributaries show variable nuclide concentration.

Table 1. Characteristics of sampled catchments.

	Mainstem Sample	Tributaries Contributing	Catchment Area (km^2)	Mean Altitude (m)	Latitude (decimal °)	Slope (°)	Annual Precipitation (m)	Relief (m)
Upstream of Alamo Dam		BS	7428	1314	34.90	11.0	0.40	940
		SM	3707	1136	34.44	10.7	0.40	760
	BWR_C		11139	1255	34.74	10.9	0.40	880
Downstream of Alamo Dam		T1	20	681	34.23	21.7	0.22	379
	DS_1		56	561	34.21	21.2	0.25	290
		T2	27	588	34.20	14.0	0.14	299
	DS_2		246	507	34.20	15.7	0.24	276
		T3	39	497	34.14	9.5	0.23	255
		T4	6	398	34.25	13.6	0.14	120
	DS_3		326	484	34.20	14.5	0.23	264
		T5	69	476	34.22	10.1	0.10	257
		T6	62	450	34.22	12.9	0.13	232
		T7	133	587	34.25	8.7	0.09	372
	DS_4		604	499	34.22	12.6	0.25	290
		T8	0.1	232	34.25	13.5	0.13	34
		T9	39	452	34.27	8.2	0.08	243
		T10	236	678	34.46	6.5	0.34	468
		T11	692	714	34.26	6.8	0.07	542
		T12	58	418	34.25	15.1	0.15	242
	DS_5		1861	581	34.37	9.4	0.27	426

Table 2. Cosmogenic nuclide concentrations and erosion rates.

	Mainstem Sample	Tributaries Contributing	^{10}Be Concentration (10^5 at/g)	^{10}Be Concentration Uncertainty (10^5 at/g)	Erosion Rate (t km^{-2} yr^{-1})	Rate Uncertainty (t km^{-2} yr^{-1})
Upstream of Alamo Dam		BS	1.45	0.07	159.5	10.7
		SM	1.77	0.05	114.9	6.5
	BWR_C		1.63	0.04	135.9	7.4
Downstream of Alamo Dam		T1	2.48	0.13	53.5	3.9
	DS_1		1.56	0.08	78.7	5.4
		T2	2.19	0.12	59.6	4.4
	DS_2		1.55	0.06	79.9	4.9
		T3	2.71	0.10	46.8	2.8
		T4	1.46	0.14	78.1	8.6
	DS_3		1.48	0.06	82.8	5.2
		T5	3.09	0.12	39.6	2.4
		T6	1.59	0.10	74.9	6.1
		T7	1.66	0.12	80.0	6.9
	DS_4		1.60	0.06	78.2	4.8
		T8	1.38	0.09	73.1	5.7
		T9	2.45	0.11	49.3	3.3
		T10	3.29	0.15	45.2	3.0
		T11	3.27	0.18	44.6	3.2
		T12	1.33	0.09	86.0	7.0
	DS_5		1.55	0.07	87.8	5.9

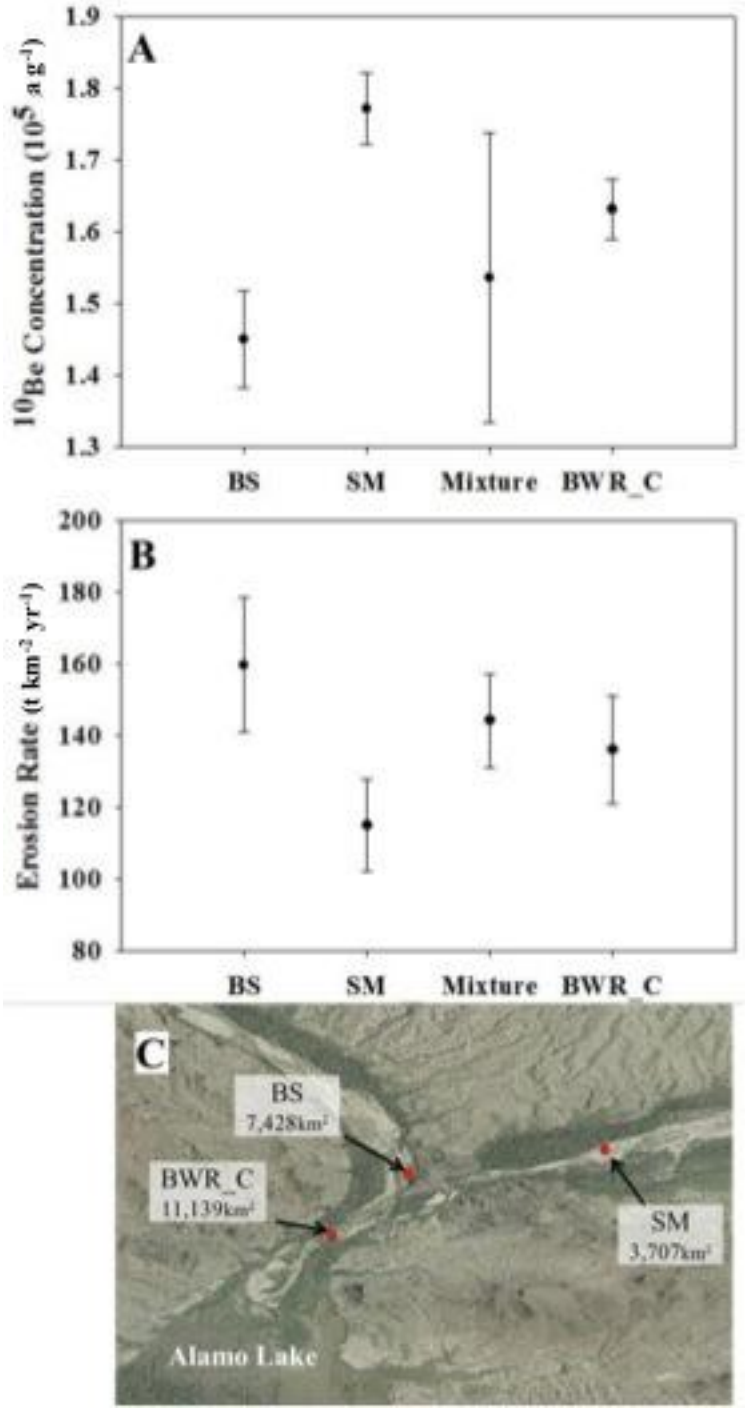

Figure 3. Comparison of results from measured samples in Big Sandy (BS), Santa Maria (SM) and BWR_C with results of calculations of BS and SM sediment mixing (Mixture), expressed in terms of ^{10}Be concentrations (A) and erosion rate (B). Locations of BS, SM and BWR_C samples are shown in (C) and in Figure 1. Mixture results are near the BWR_C values, which indicates BS and SM are well mixed in the BWR_C sample. Error bars show value uncertainty, and the mixing calculation result is a propagated uncertainty.

Modern Erosion Rates

Modern erosion rates from the Bureau of Reclamation and Army Corp of Engineers varied considerably (Table 3). The Army Corp of Engineers rate was 2.7 times greater than the long-term rate from BWR_C. Modern rates cited by the Bureau of Reclamation in 1973 were within ± 39 t km^{-2} yr^{-1} of BWR_C.

Table 3. Modern erosion rates for the BWR.

Source	Modern Rate ($t\ km^{-2}\ yr^{-1}$)	Method
1973 BoR (a)	113	Lake Havasu reservoir record at BWR mouth
1973 BoR (b)	174	Reported southwest regional erosion rate
2003 US ACoE	366	Nearby gauged streams and other area reservoirs
Alamo Lake Sediment Record	270 ± 20	Bathymetric DEM differencing 1963 - 1985

Discussion

The ^{10}Be erosion rates from the BWR are similar to rates found by previous ^{10}Be studies in the US Southwest and other arid settings. Granger et al. (1996) reported an erosion rate of 162 ± 38 t km^{-2} yr^{-1} in the Fort Sage Mountains, California, which is comparable to mainstem BWR rates. Two studies of small catchments with ephemeral streams, the Nahal Yael, Israel and Yuma Wash, Arizona both found erosion rates greater than BWR tributaries but less than BWR mainstream samples. The Nahal Yael rate was 78 ± 16 t km^{-2} $yr^{-1}$and Yuma Wash was 81 ± 5 t km^{-2} yr^{-1}(Clapp et al., 2000, 2002). Bierman et al. (2005) collected 42 samples from large and small catchment sizes in the arroyo-impacted Rio Puerco watershed in New Mexico and found rates greater than and less than BWR rates.

The agreement between mixing results from equation (i.a) and (i.b) with the BWR_C sample results (Figure 3) indicates that our first hypothesis is supported. Sediment at the confluence of the Big Sandy and Santa Maria Rivers is well mixed despite the large contributing watersheds and intermittent dryland stream flow patterns. Bierman et al. (2005) also found that large semi-arid catchments in New Mexico were similarly well mixed. The consistency in the mixing result for the BS and SM allows for two further assumptions (1) that sediment throughout the BWR is well mixed so the second hypothesis on dam effects can be tested and (2) the BWR_C sample nuclide concentration is representative of the upper BWR catchment and can be used for mixing calculation in equation (5).

^{10}Be analysis shows that erosion rates are generally higher in the upper catchment than in the lower basin, although a few of the tributaries to the lower BWR show similar erosion rates to the upper catchment. Erosion rates from the mainstem are markedly lower than in the upper catchment, however. Regression analysis found that relief and altitude were both significantly correlated with erosion rate. Bierman et al. (2005) found that ^{10}Be erosion rates were well explained by a model that considered relief and vegetation. However, several others have found that ^{10}Be erosion rates in arid settings are best explained by colluvium cover (Clapp et al., 2000, 2001, 2002; Fruchter et al., 2011). Further analysis of BWR samples with colluvium and vegetation cover information would likely be useful.

The even distribution of quartz in a sampled catchment is another assumption necessary for confidence in catchment-wide erosion rates. A sample's nuclide concentration will be biased toward the part of the watershed where quartz is more abundant (Granger and Riebe, 2007). Considering the distribution of mafic rock, which is low in quartz, within a catchment is one way to determine if this assumption is valid. The catchment for the BS sample had the highest percentage of mafic rock near

20%, which may slightly skew its nuclide concentration (See Appendix B). However, if the mafic rock is well distributed in a catchment in may be less of an issue since erosion rates will likely be well averaged (Granger and Riebe, 2007).

The ^{10}Be concentrations in samples DS_1 – 5 are lower than the upstream BWR_C sample, contrary to our expectations. This finding is inconsistent with hypothesis 2, because on average tributaries downstream of BWR_C contribute sediment with greater ^{10}Be concentrations, which in turn was expected to cause mainstem concentrations to at least be greater than BWR_C. These results are ambiguous with respect to how Alamo Dam affects sediment mixing. Additional tributary mixing calculations could clarify these ambiguities, because some tributaries contribute sediment with low nuclide concentrations. Additional testing of Alamo Dam's effects on sediment mixing could include separate mixing calculations for all downstream mainstem samples (DS_1 – 5).

Clapp et al. (2002) also found a pattern of downstream decreasing ^{10}Be concentrations on Yuma Wash, which is south of the BWR in western Arizona. They observed that basin fill sediment was activated by erosion of terrace deposits. They suspected two reasons why the basin fill could be contributing the smaller nuclide concentration:

1) *Buried basin fill sediment was older than 3 to 4 Ma.* If this were the case ^{10}Be would have decayed, decreasing its concentration. Activation of these sediments downstream would lower the overall nuclide concentration.
2) *The basin fill was deposited during a time of faster erosion, such as the Late-Pleistocene.* Faster erosion means smaller ^{10}Be concentration. Reworked Late-Pleistocene sediment would lower the expected ^{10}Be concentration.

Although parts of the BWR flow through terraced areas where basin fill might be reactivated, both explanations from Clapp et al. (2001) seem unlikely for the BWR:

1) *Lower BWR terrace deposits are not older than 3 to 4 Ma.* The sediment history of the BWR is tied to base-level changes in the Colorado River. All BWR valley sediment was stripped from the BWR in the mid-Pleistocene due to a base-level fall (Wilson and Owen-Joyce, 2002). Sediment was then redeposited up to current levels during the late-Pleistocene, suggesting that sediment could have been in the BWR valley bottom for 11,000 years at most (Wilson and Owen-Joyce, 2002).
2) *Although faster erosion may have occurred in the Late-Pleistocene, the entire BWR valley bottom was active with modern sediment transport prior to damming.* Historic air photos show that before damming the BWR regularly activated the entire valley bottom (House et al., 1999), so all sediment is likely modern. OSL dating of valley bottom terrace sediments could be used to confirm this assumption.

Modern Erosion Rates

Modern erosion rates for the mouth of BWR determined by the Bureau of Reclamation were both less than and greater than the long-term ^{10}Be mainstem erosion rates (Table 3). The modern erosion rates for the BWR's upper catchment found by the US Army Corp of Engineers and by measuring the difference between 1965 and 1985 bathymetric surveys of Alamo Lake were larger than ^{10}Be mainstem erosion rates. Bureau of Reclamation (1970) rates for the mouth of the BWR support the idea that the wide valleys in the lower BWR are locations of sediment storage. Additional analysis of recent reservoir bathymetry and coring (Gremillion and Walker 2011) could yield a more reliable modern erosion rate.

Long-term ^{10}Be erosion rates that are differ from modern rates have been found in multiple studies, depending on human land use, natural erosion cycles and the time span of modern erosion records. In the Rio Puerco, NM modern rates were greater than ^{10}Be rates by a factor of two (Bierman et al., 2005). This was attributed to the current phase of arroyo growth in the Rio Puerco watershed.

Arroyo erosion processes were not observed in the BWR watershed. On four rivers in Europe, Schaller et al. (2001) found that long-term nuclide erosion rates were 1.5 to 4 times greater than rates found from river bed-load measurements. The brief record of bed-load measurements likely contributed to the smaller modern rates on the European rivers. Erosion rates based on only a few decades of sediment transport measurements failed to capture high magnitude transport events that occur at low frequencies. Kirchner et al. (2001) also found a similar result on rivers in Idaho.

The BWR records are similarly limited in the modern record length. The Alamo Lake bathymetric survey comparison provides an erosion rate averaged over only 17 years. In contrast to the modern records for the European rivers and those in Idaho, the bathymetric surveys provide a rate greater than the ^{10}Be long-term. Further investigation of flood events on the Big Sandy and Santa Maria Rivers during those 17 years could show that a large-magnitude, low-frequency flood event was responsible for a large amount of the reservoir deposition. Also, human land use and arroyo processes in the upper BWR watershed might provide explanations for the larger modern rate.

Although the 1 ka – 100 ka ^{10}Be rates of erosion are on a much longer time scale than the decadal time scale of Alamo Dam's influence on the BWR, they still yield important information. The ^{10}Be erosion rates shows a long-time scale sediment budget where the sediment inputs to the BWR vary considerably between the upper catchment and the lower catchment. However, the use of ^{10}Be concentration and mixing equations is effectively a kind of tracer that is expected to show the decadal timescale effects of Alamo Dam on sediment mixing. Alamo Dam's effects should be observable where dam-related degradation has occurred. According to grain size and stream cross section observation this degradation extends at least 10 km downstream (Jackson and Summers, 1988). Mainstem sample DS_1 was collected in this degradation zone; sediment mixing for samples further downstream may also be affected.

Conclusion

Cosmogenic nuclide analysis has revealed that erosion rates vary considerably in the BWR watershed between the upper catchment and tributaries downstream of Alamo Dam. The Big Sandy River erodes faster than the Santa Maria River and has a larger area, such that a large proportion of sediment in the BWR historically came from the Big Sandy. Tributary catchments downstream of Alamo Dam erode at three quarters the rate of the Big Sandy and Santa Maria Rivers. Higher altitude, relief and precipitation might contribute to the difference. The mixing calculation for the Big Sandy and Santa Maria confluence determined that the upper catchment of the BWR is well mixed, which validated hypothesis (1). The nuclide mixing result for the BWR confluence supports the conclusion that large arid catchments (>1,000 km^2) are well mixed despite their size and complexity. Nuclide concentrations in the mainstem of the BWR do not allow testing of hypothesis (2) until further analysis of recently received nuclide results can be completed. Beyond dam effects and the field of cosmogenic nuclide analysis, the long-term erosion rates found for the BWR are useful for Quaternary geology study of the lower Colorado River basin.

Acknowledgements

This work was funded by a Geological Society of America Graduate Student Research grant to FJD, a PRIME Lab grant, and by grants from the US Fish & Wildlife Service and National Science Foundation (EAR-1025076).

References Cited

Bierman, P. R., J. M. Reuter, M. Pavich, A. C. Gellis, M. W. Caffee, and J. Larsen (2005), Using cosmogenic nuclides to contrast rates of erosion and sediment yield in a semi-arid, arroyo-dominated landscape, Rio Puerco Basin, New Mexico, Earth Surface Processes and Landforms, 30(8), 935–953.

Bierman, P., and E. J. Steig (1996), Estimating rates of denudation using cosmogenic isotope abundances in sediment, Earth surface processes and landforms, 21(2), 125–139.

Binnie, S. A., W. M. Phillips, M. A. Summerfield, and L. Keith Fifield (2006), Sediment mixing and basin-wide cosmogenic nuclide analysis in rapidly eroding mountainous environments, Quaternary Geochronology, 1(1), 4–14.

Von Blanckenburg, F. (2005), The control mechanisms of erosion and weathering at basin scale from cosmogenic nuclides in river sediment, Earth and Planetary Science Letters, 237(3), 462–479.

Brown, E. T., R. F. Stallard, M. C. Larsen, G. M. Raisbeck, and F. Yiou (1995), Denudation rates determined from the accumulation of in situ-produced 10Be in the Luquillo Experimental Forest, Puerto Rico, Earth and Planetary Science Letters, 129(1-4), 193–202.

Bureau of Reclamation (1970), Final Design Sediment Deposition Study, Bill Williams River Arm of Lake Havasu, Central Arizona Project, Arizona., Sedimentation Section, Division of Planning Coordination in Collaboration with the Phoenix Development Office, Phoenix, Arizona. In The Papers of Whitney M. Borland, Colorado State University.

Clapp, E. M., P. R. Bierman, and M. Caffee (2002), Using< sup> 10</sup> Be and< sup> 26</sup> Al to determine sediment generation rates and identify sediment source areas in an arid region drainage basin, Geomorphology, 45(1), 89–104.

Clapp, E. M., P. R. Bierman, K. K. Nichols, M. Pavich, and M. Caffee (2001), Rates of sediment supply to arroyos from upland erosion determined using in situ produced cosmogenic 10Be and 26Al, Quaternary Research, 55(2), 235–245.

Clapp, E. M., P. R. Bierman, A. P. Schick, J. Lekach, Y. Enzel, and M. Caffee (2000), Sediment yield exceeds sediment production in arid region drainage basins, Geology, 28(11), 995.

Dunai, T. J. (2000), Scaling factors for production rates of in situ produced cosmogenic nuclides: a critical reevaluation, Earth and Planetary Science Letters, 176(1), 157–169.

Dunai, T. J. (2010), Cosmogenic nuclides : principles, concepts and applications in the earth surface sciences, Cambridge University Press, Cambridge, UK; New York.

Dunne, J., D. Elmore, and P. Muzikar (1999), Scaling factors for the rates of production of cosmogenic nuclides for geometric shielding and attenuation at depth on sloped surfaces, Geomorphology, 27(1), 3–11.

Fruchter, N., A. Matmon, Y. Avni, and D. Fink (2011), Revealing sediment sources, mixing, and transport during erosional crater evolution in the hyperarid Negev Desert, Israel, Geomorphology, 134(3-4), 363-377.

Grams, P. E., and J. C. Schmidt (2005), Equilibrium or indeterminate? Where sediment budgets fail: Sediment mass balance and adjustment of channel form, Green River downstream from Flaming Gorge Dam, Utah and Colorado, Geomorphology, 71(1-2), 156–181.

Granger, D. E., J. W. Kirchner, and R. Finkel (1996), Spatially averaged long-term erosion rates measured from in situ-produced cosmogenic nuclides in alluvial sediment, The Journal of Geology, 249–257.

Granger, D. E., and C. S. Riebe (2007), Cosmogenic nuclides in weathering and erosion, Treatise on Geochemistry: Oxford, Pergamon, 1–42.

Heisinger, B., D. Lal, A. J. T. Jull, P. Kubik, S. Ivy-Ochs, K. Knie, and E. Nolte (2002a), Production of selected cosmogenic radionuclides by muons: 2. Capture of negative muons, Earth and Planetary Science Letters, 200(3), 357–369.

Heisinger, B., D. Lal, A. J. T. Jull, P. Kubik, S. Ivy-Ochs, S. Neumaier, K. Knie, V. Lazarev, and E. Nolte (2002b), Production of selected cosmogenic radionuclides by muons 1. Fast muons, Earth and Planetary Science Letters, 200(3-4), 345–355, doi:10.1016/S0012-821X(02)00640-4.

House, P. K., M. L. Wood, P. A. Pearthree, and Arizona Geological Survey (1999), Hydrologic and geomorphic characteristics of the Bill Williams River, Arizona, Arizona Geological Survey, Tucson, AZ.

Jackson, W. L., and P. Summers (1988), Bill Williams River field assessment: hydrology, hydrogeology, and geomorphology, Bureau of Land Management, Denver, CO.

Kirchner, J. W., R. C. Finkel, C. S. Riebe, D. E. Granger, J. L. Clayton, J. G. King, and W. F. Megahan (2001), Mountain erosion over 10 yr, 10 ky, and 10 my time scales, Geology, 29(7), 591.

Kohl, C. P., and K. Nishiizumi (1992), Chemical isolation of quartz for measurement of in-situ-produced cosmogenic nuclides, Geochimica et Cosmochimica Acta, 56(9), 3583–3587.

Matmon, A., P. R. Bierman, J. Larsen, S. Southworth, M. Pavich, and M. Caffee (2003), Temporally and spatially uniform rates of erosion in the southern Appalachian Great Smoky Mountains, Geology, 31(2), 155–158.

Phillips, J. D., M. C. Slattery, and Z. A. Musselman (2004), Dam-to-delta sediment inputs and storage in the lower Trinity River, Texas, Geomorphology, 62(1), 17–34.

Portenga, E. W., P. R. Bierman, J. Libarkin, E. Ward, S. Anderson, G. Kortemeyer, and S. Raeburn (2011), Understanding Earth's eroding surface with 10 Be, GSA Today, 21(8).

PRISM Climate Group (2006), United States Average Monthly or Annual Precipitation, 1971 - 2000, The PRISM Climate Group at Oregon State University, Corvallis, Oregon, USA. [online] Available from: http://www.prism.oregonstate.edu/docs/meta/ppt_30s_meta.htm

Riebe, C. S., and D. E. Granger (2011), Effects of Chemical Erosion on Cosmogenic Nuclide Buildup in Soils, Saprolite and Sediment.

Rossi, B. (1948), Interpretation of cosmic-ray phenomena, Reviews of Modern Physics, 20(3), 537.

Schaller, M., F. Von Blanckenburg, N. Hovius, and P. W. Kubik (2001), Large-scale erosion rates from in situ-produced cosmogenic nuclides in European river sediments, Earth and Planetary Science Letters, 188(3), 441–458.

Schmidt, J. C., and P. R. Wilcock (2008), Metrics for assessing the downstream effects of dams, Water Resources Research, 44(4), W04404.

Shafroth, P. B., and V. B. Beauchamp (2006), Defining ecosystem flow requirements for the Bill Williams River, Arizona, US Geological Survey.

Shafroth, P. B., A. C. Wilcox, D. A. Lytle, J. T. Hickey, D. C. Andersen, V. B. Beauchamp, A. Hautzinger, L. E. McMullen, and A. Warner (2010), Ecosystem effects of environmental flows: modelling and experimental floods in a dryland river, Freshwater Biology, 55(1), 68–85, doi:10.1111/j.1365-2427.2009.02271.x.

Stone, J., and P. Vasconcelos (2000), Studies of geomorphic rates and processes with cosmogenic isotopes—examples from Australia, Journal of Conference Abstracts, p. 961. [online] Available from: http://www.the-conference.com/JConfAbs/5/961.pdf (Accessed 4 July 2012)

Tooth, S. (2007), Arid geomorphology: investigating past, present and future changes, Progress in Physical Geography, 31(3), 319.

US Army Corp of Engineers - Los Angeles District (2003), Water Control Manual: ALamo Dam and LAke Colorado River Basin Bill Williams River, Arizona, US Army Corp of Engineers, Los Angeles District.

Wheaton, J. M., J. Brasington, S. E. Darby, and D. A. Sear (2010), Accounting for uncertainty in DEMs from repeat topographic surveys: improved sediment budgets, Earth surface processes and landforms : the journal of the British Geomorphological Research Group., 35(2), 136–156.

Williams, G. P., and M. G. Wolman (1984), Downstream effects of dams on alluvial rivers, US Government Printing Office Washington, DC. [online] Available from: http://relicensing.pcwa.net/documents/Library/PCWA-L-307.pdf (Accessed 19 May 2012)
Wilson, R. P., and S. J. Owen-Joyce (2002), Hydrologic Conditions in the Bill Williams River National Wildlife Refuge and Planet Valley, Arizona, 2000, United States Geological Survey.

Dryland River Grain-Size Variation due to Damming, Tributary Confluences, and Valley Confinement

Franklin J. Dekker and Andrew C. Wilcox
Department of Geosciences, University of Montana, Missoula, MT 59812, USA

This chapter is in preparation for submission to a peer-reviewed journal. We welcome feedback. Readers should contact Andrew Wilcox for information on the status of the manuscript and/or an updated version of the manuscript after it has been published.

Abstract

Dam effects on flow and sediment regimes can be dramatic in dryland rivers. Downstream adjustments of bed-material size can be one of the primary geomorphic responses to such changes, but the downstream extent of grain-size adjustments can be mediated by valley confinement and tributary confluence effects. Determining the extent of dam effects is important for designing successful environmental flow management plans. Here, two questions are addressed: (1) *what is the pattern of grain size in a dryland river, downstream of a dam*, and (2) *how do valley confinement and tributaries control that pattern?* Grain size data were collected downstream and upstream of Alamo Dam on the Bill Williams River (BWR) in western Arizona to address these questions. The average D_{50} upstream of Alamo Dam was 0.65 mm. Grain size was coarsest immediately downstream of Alamo Dam (D_{50}= 41 mm) but fined exponentially downstream. Our analysis suggests that sediment deficit conditions extend from Alamo Dam to about 10 km downstream. Multiple regressions show that distance from the dam is the most important control variable in the first 10 km, however it is not a significant control variable further downstream. No control variable was a strong predictor further than 10 km downstream. Yet, a pattern of fining grain size was apparent in wide valley reaches. Tributary confluence effects on mainstem grain sizes did not yield a statistically significant pattern. The ephemeral tributary flow pattern may not provide enough sediment to noticeable effect grain size. Considerable flow reduction on the BWR and the mix of valley and canyon reaches appears to have confined the extent of dam effects on grain size to only the upper reaches.

Short Title (up to 70 characters): *Dryland river grain-size variation*

Introduction

Downstream variations in the bed-material size of alluvial rivers reflect variations in transport capacity (e.g., as a function of slope and valley confinement), sediment input from tributaries, and abrasion (e.g., Hoey and Ferguson, 1994; Paola et al., 1992). Grain size adjustments can also be one of the primary geomorphic expressions in response to changes in sediment supply. In dammed rivers, trapping of sediment behind dams can produce downstream coarsening and armoring, as well as incision, and the downstream pattern of grain size can be indicative of the extent of dam effects on sediment supply (Lagasse, 1994; Ligon et al., 1995; Williams and Wolman, 1984; Schmidt and Wilcock, 2008). Here we investigate the effects of damming, tributary confluences, and valley confinement on grain size in a dryland river.

Interpreting the extent to which grain size variations are indicative of dam effects versus geomorphic controls on grain size is especially challenging in dryland rivers. In these systems, large infrequent floods often set channel form and sediment grain size patterns for long periods of time (Reid and Frostick, 1994; Tooth, 2000). Moreover, inputs of flow and sediment from tributaries can also disrupt downstream grain size trends (Benda et al., 2004; Heitmuller and Hudson, 2009), although these inputs may be asynchronous with mainstem high-flow events. On the one hand, tributaries can have limited effects on mainstem grain size patterns, as a result of their ephemeral nature and infrequent activation (Tooth, 2000; Thornes, 2009). On the other hand, asynchronous activation of ephemeral tributaries while the mainstem is at low flow (e.g., as a result of small convective thunderstorms) can produce large alluvial fans that alter mainstem grain size patterns (Bourke and Pickup, 1999). Dryland rivers can also be losing rivers as a result of infiltration of surface water to groundwater, which can enhance bed-material size sorting by decreasing stream power downstream (Dunkerley, 1992). Valley confinement changes (e.g., transitions to unconfined valleys) can also cause abrupt changes in stream power that influence selective transport and local grain size adjustments (Topping et al., 2000; Ralph and Hesse, 2010). As a result of these factors, dryland rivers can be in an apparent state of disequilibrium between flow and morphology (Reid and Frostick, 1994), although in general less is known about dryland rivers compared to rivers in more humid regions (Tooth, 2000).

Dryland rivers are particularly susceptible to dam-induced changes in flow and sediment supply. Flow regulation typically eliminates geomorphically significant, high-magnitude, low-frequency flood events (Graf, 2006; Davies et al., 1994). Interpreting the geomorphic effects of sediment supply reductions and understanding grain size patterns in dammed dryland rivers is important in the context of flow management (Topping et al., 2000) and understanding ecosystem effects of dams (Shafroth et al., 2010). Experimental flood releases from Glen Canyon Dam on the Colorado River have highlighted the importance of sediment supply in achieving downstream objectives such as rebuilding sand bars (Wright et al., 2008). On the Bill Williams River (BWR), Arizona, experimental floods in recent years have been designed to maintain native riparian vegetation communities, but a key uncertainty is the extent to which dam-induced reductions in sediment supply need to be factored into flow management (Shafroth et al., 2010; Wilcox and Shafroth, 2013). Determining grain size patterns and controls in a dammed dryland river is therefore relevant to understanding dam-induced sediment supply effects and implications for the design and assessment of environmental flows.

Conceptual models can assist interpretation of the downstream extent of dam-induced versus natural grain size effects in dryland rivers. The *process domain concept* (PDC) characterizes spatial divisions along a river by delineating zones of distinct geomorphic processes that are dominated by particular disturbance regimes (Montgomery, 1999). For example, narrow canyons and wide floodplain valleys can be defined as distinct *process domains*. A process domain defined by a confined channel in a canyon with steep and narrow valley walls will have enhanced disturbance by floods and coarser grain size compared to an unconfined channel with adjacent floodplains. A second conceptual model, the *network dynamics hypothesis* predicts that tributary inputs of sediment and flow will result in a

response in mainstem rivers, where (1) sediment coarsens and gradient increases downstream of the confluence, and (2) gradient decreases and grain size fines upstream (Benda et al., 2004).

Downstream propagation of dam-induced grain-size effects has a spatial component, as a function of the valley-confinement and tributary effects discussed above, and a temporal component, as a function of the time since damming and the history of flow releases (Williams and Wolman, 1984). As a result, downstream systems may either maintain states of disequilibrium between flow, sediment supply, and morphology or adjust to new equilibrium states, at spatial scales of a few kilometers or hundreds of kilometers (Williams and Wolman, 1984; Schmidt and Wilcock, 2008) and temporal scales of years to centuries (Brandt, 2000; Phillips et al., 2004).

In this study we address the following questions: (1) what is the pattern of grain size in a dammed dryland river, (2) how do valley confinement and tributaries control that pattern, and (3) what is the net effect of dam-induced reductions in sediment supply on downstream grain size? We investigate these questions in the context of two hypotheses: (1) a dam will disrupt and reset downstream fining, and (2) the downstream distance to which dam effects on grain size have propagated will depend on (a) tributaries, as a result of their effects on sediment supply, and (b) valley confinement, as a result of effects on stream power. In a dryland river, valley confinement is hypothesized to be more important because ephemeral tributaries may rarely activate and contribute sediment. We frame our investigation in the context of two proposed process domains. In the *dam-effect domain*, dam-induced supply limitation governs geomorphic processes and grain size. The *valley-confinement process domain* combines the wide-valley and narrow-canyon process domains discussed above and is governed by transport capacity rather than sediment supply limitations.

Study Area

The Bill Williams River (BWR) is a dammed dryland tributary of the Colorado River in western Arizona (Figure 1). The BWR originates at the confluence of the Big Sandy and Santa Maria Rivers and flows 63 km west to Lake Havasu, a dammed section of the Colorado River (Shafroth et al., 2010). In 1968, Alamo Dam was constructed on the BWR 11 km downstream from the Big Sandy and Santa Maria confluence, 58 km upstream from Lake Havasu. Alamo Dam is an 86 m high earthen structure with a maximum capacity of 1.6 billion m^3 (Bowles et al., 2000). Rainfall averages 45 cm annually in the eastern highlands region of the watershed and 13 cm annually at Lake Havasu (Shafroth et al., 1998).

Flow regulation has reduced the magnitude and frequency of floods. Alamo Dam is structurally limited to a maximum release discharge of 200 $m^3 s^{-1}$ (Wilson and Owen-Joyce, 2002), which corresponds to a Q_2 in the context of the pre-dam flow regime, and a Q_{20} in the post-dam period. Since dam closure, discharge has reached the maximum release three times, most recently in 2005. Since 2005, other high-flow releases have occurred in 2006 (58 $m^3 s^{-1}$), 2008 (65 $m^3 s^{-1}$) and 2010 (87 $m^3 s^{-1}$), as measured by the USGS Bill Williams River below Alamo Dam stream gauge (09426000). Alamo Dam has also reduced sediment supply to the BWR, blocking supply from the upper 85% of the basin's drainage area.

Downstream of Alamo Dam, the BWR flows through a series of canyon and floodplain reaches that likely influence the pattern of sediment supply and transport capacity (Figure 1). Alamo Dam is located in a canyon reach and the river remains confined for 8 km downstream. In four reaches the BWR flows through wide alluvial valleys with widths greater than 500 m: Reid, Rankin, Pipeline, and Planet Valleys, which begin 8, 18, 23, and 33 km downstream, respectively (Figure 2). Planet Valley is 10 km long and 2 km wide, with thick alluvial deposits that dissipate high flows and produce discontinuous baseflow conditions (Shafroth et al., 1998). Downstream of Alamo Dam all tributaries to the BWR are dry washes with unknown flow frequency; 13 of these have catchments greater than 20 km^2 (Figure 1).

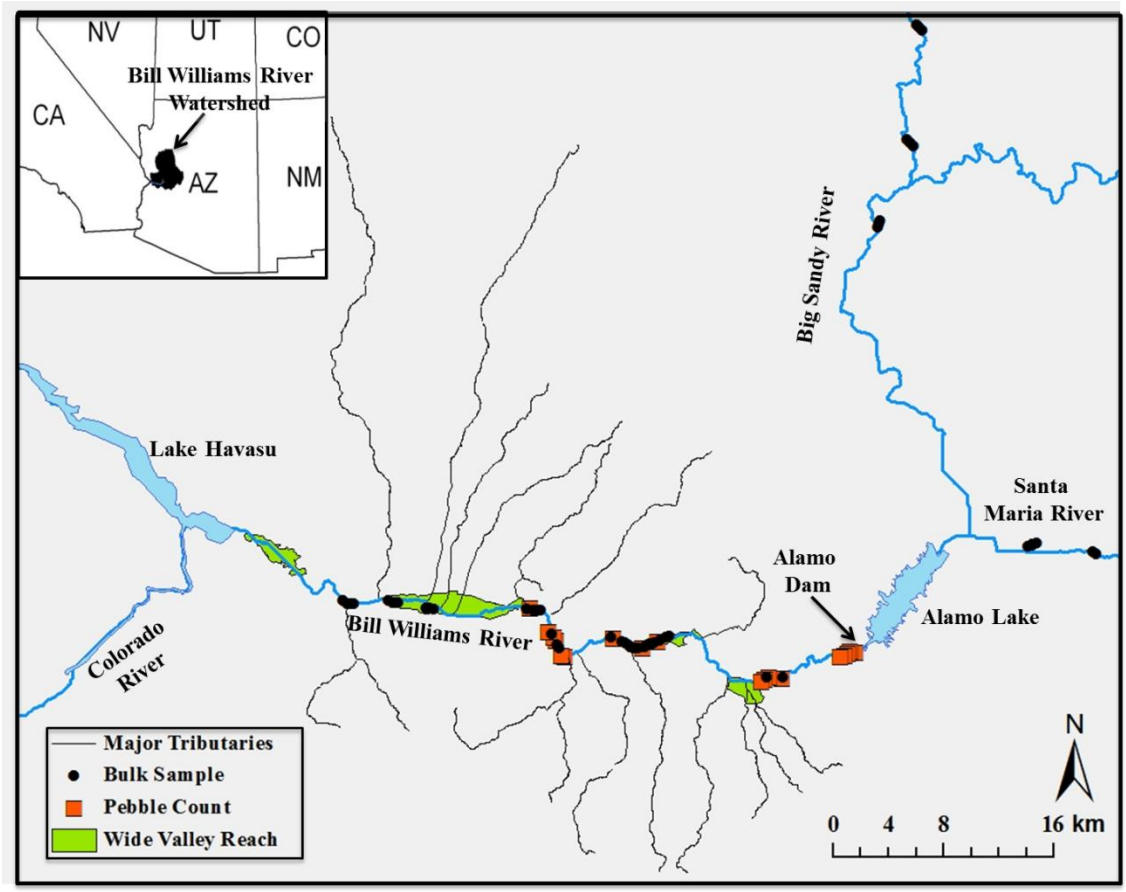

Figure 1. The Bill Williams River watershed in Arizona, USA (upper left) and sediment sample locations. Photo grain size locations overlap with the bulk samples and pebble counts at 30m intervals, but are not shown. Valley reaches with widths >500m are shown in green. Tributaries downstream of Alamo Dam with greater than >20km^2 catchment areas are marked with black lines.

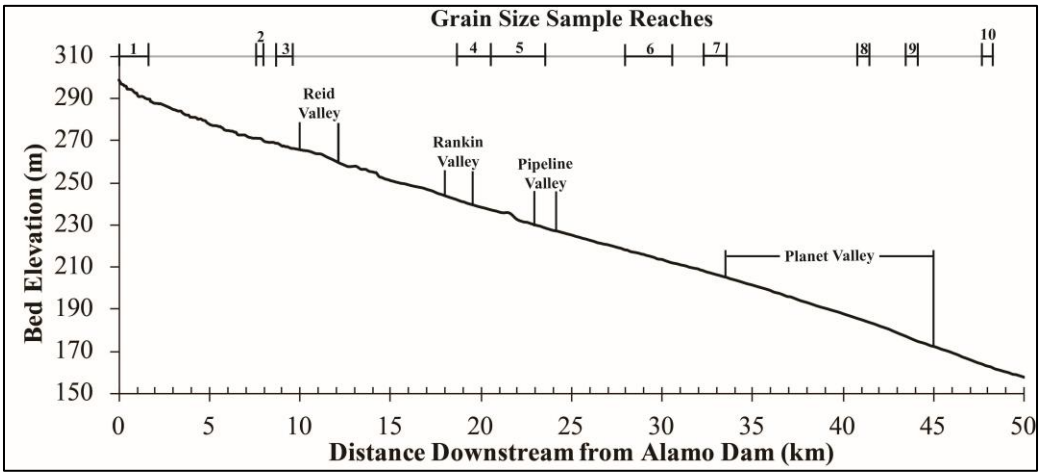

Figure 2. Longitudinal profile of the BWR downstream of Alamo Dam from US Army Corps of Engineers HEC-RAS modeling from 2006 3 m LIDAR data. Valleys >500 m wide and10 reaches where grain size was sampled are labeled.

Methods

Grain Size Data Collection and Analysis

To assess the relative effects of Alamo Dam versus antecedent geomorphology on grain size, we combine extensive field sampling of grain size with GIS and statistical methods. In January 2011, we collected grain size samples longitudinally in the BWR basin, upstream from Alamo Dam in the unregulated Big Sandy and Santa Maria Rivers and downstream from the dam in the BWR. Grain size data were collected along unvegetated secondary channels that are dry at baseflow but active during floods, including during the most recent dam release in 2010. We used bulk samples, collected with a USGS RBMH-80 sampler, pebble counts (Wolman, 1954) and digital photos. Bulk samples or pebble counts (for coarser materials) were collected every 300 m and a digital photo was taken every 30 m; all samples were georeferenced. As described below, we analyzed grain size samples in the context of reach averages, for which the even-interval sampling applied here is well suited (Kondolf and Piégay, 2003). Facies-specific sampling, as is commonly applied to gravel bed rivers with well-defined patches (Seal and Paola, 1995), was unfeasible in this setting as a result of both less distinct patches and dense vegetation made this approach unfeasible.

In the BWR downstream of Alamo Dam, 18 pebble counts, 55 bulk samples and 328 sediment digital photos were collected across 10 different reaches covering a total of 12 km, or about 20% of the 58 km long BWR (Figure 2; Table 1). In the Big Sandy River 9 bulk samples and 56 digital photo samples were collected in three reaches. In the Santa Maria River, 6 bulk samples and 27 digital photo samples were collected in two reaches.

Table 1. Grain size sampling reaches with distance downstream or upstream (denoted by negative number) from Alamo Dam.

Reach	Distance From Alamo Dam (km)	Reach Length (m)	Geographic names
Big Sandy River	-42	1800 (in 3 sub-reaches)	Signal Rd. Crossings
Santa Maria River	-63	1100 (in 2 sub-reaches)	Grey Wash area
1	0.3	1300	Canyon downstream of Alamo Dam
2	7.7	100	Right bank meander bend upstream of Reid Valley
3	8.8	800	Immediately upstream of Reid Valley
4	18.7	1700	Rankin Ranch Area
5	20.5	3000	Pipeline Crossing Area
6	28	2500	Downstream of Swansea Wash
7	32.3	1200	Upstream of Planet Valley
8	40.8	600	Mid Planet Valley
9	43.6	700	Lower Planet Valley
10	47.1	1100	Upstream and downstream of Mineral Wash

Digital photo grain size characterization, a rapid alternative to traditional sediment sieve analysis that has been applied successfully in the Colorado River (Rubin et al., 2010) and elsewhere, was applied here to increase the quantity of samples collected. Digital photo samples were taken with a 12.1 megapixel Canon PowerShot D10. Depending on grain size, one of three possible camera mounts was used for sampling. A "small" photo mount was used on sand-sized photos, a "medium" mount was used for pebble-sized grains, and for gravel-sized sediment an "overview" photo was taken from chest height. Each chest height photo had a tape measure in view for calibration. The focal distance from lens to sediment for the small mount was 2 cm and the light source was a ring of LEDs as in Rubin et al. (2007). The medium mount was a rectangular box with a constant 50 cm focal length, similar to (Buscombe and Masselink, 2009). The camera flash was used as the light source. The overview photos had variable focal length around 1.5 m. A calibration factor from pixels to millimeters was found for each overview photo. A constant calibration factor was found for the small and medium mounts and applied to each photo because focal length was constant. For sand-sized sediments, the top 1 cm of sediment was removed prior to taking a photo (after (Rubin et al., 2007)). The two different camera mounts and overview photos were used to ensure each grain had at least 2 pixels and each field of view had greater than 1000 grains.

The b-axis of 100 grains in each photo was measured in MatLab using a code from the Grain Size Toolbox written by D. Buscombe (Buscombe et al., 2010). The code produced 100 randomly placed dots on the image, then the grain beneath each dot was measured. Measurements in pixels were converted to millimeters using a conversion factor generated by MatLab code from the Grain Size Toolbox. This 100-point manual photo grain size measurement method (Sime and Ferguson, 2003) was used as an alternative to autocorrelation digital photo grain size analysis methods (Rubin, 2004)(Buscombe and Masselink, 2009)

Uncertainty for each photo mount was determined by comparing photo grain size results of samples that also had a corresponding bulk sample or pebble count. The average uncertainty in D_{16}, D_{50}, and D_{84} was found for those samples and then applied to the rest of photo grain size results according to the mount used (Table 2). Thirty-five small mount photos and 17 medium mount photos were compared to sieved bulk sample results. Ten overview photos were compared to corresponding pebble counts. Small mount photos had a 20% uncertainty in D_{50}, medium mount photos had a 40% uncertainty and overview photos showed 50% uncertainty. The medium photo mount displayed systematic error in D_{16} and D_{50}. Results were consistently larger than sieved samples. The other photo mount results showed random error around either side of the mean. The relative error in D_{50} and D_{84} was fairly consistent between mount and overview photos. The medium mount and overview photos poorly measured D_{16}, with 90 and 100% relative error, respectfully.

Grain size parameters (D_{16}, D_{50}, D_{84}) obtained for all sample types were grouped into reaches 1 – 10 (Figure 2), and log averages of these parameters were calculated for each reach. Reaches 4, 5, and 6 were longer than the other reaches, so each were split into two halves and log averaged separately. Log averages, also called geometric means, provide equal weight to each sample and therefore limit the effect of individual outliers (e.g. a single gravel-sized sample in an otherwise sand-bed reach) on reach averages. Geometric mean and sorting were also calculated to further describe grain size distributions and analyze grain size trends (Kondolf and Piégay, 2003). Geometric mean grain size (D_g) was calculated according to (Kondolf and Wolman, 1993):

$$D_g = \sqrt{D_{84} \times D_{16}}$$

Sorting (S_g) was calculated to determine how uniform a sample was (Simons and Sentürk, 1992):

$$S_g = \sqrt{\frac{D_{84}}{D_{16}}}.$$

Table 2. The mean absolute and relative error and standard deviation of each photo mount compared to bulk sample or pebble count results.

		Mean Difference in Phi Size
Small Mount	D_{16}	-0.01 ± 0.65
	D_{50}	0.20 ± 0.57
	D_{84}	-0.29 ± 0.62
Medium Mount	D_{16}	-0.82 ± 0.53
	D_{50}	-0.35 ±0.55
	D_{84}	0.09 ± 0.89
Overview Photo	D_{16}	-0.50 ± 1.67
	D_{50}	0.25 ± 1.14
	D_{84}	0.30 ± 0.89

To describe the strength and significance of correlations between reach-averaged grain size and sample position downstream of Alamo Dam, we determined exponential decay fits with R^2 and p-values in SigmaPlot. The strength of the fining pattern downstream of Alamo Dam and the grain size observed upstream of Alamo Dam was used to examine hypothesis (1).

Multiple Regression Analysis

The process domain concept (Montgomery, 1999) was used to interpret grain size results and inform the statistical analysis of the downstream extent of dam effects on grain size. To address each aspect of hypothesis (2), we used forward selection multiple regression to identify the relative influence of the distance from the dam, valley width and the cumulative number of upstream tributaries on D_{50} grain size. We conducted three independent analyses using (1) all samples downstream of Alamo Dam; (2) samples in the *dam-effect process domain* (0 - 10 km downstream); and (3) samples in *the valley-confinement process domain* (>10 km downstream). The domains were independently analyzed to observe how controls on grain size change downstream.

In each regression, D_{50} was the response variable and distance from dam (km), valley width (m) and the cumulative number of upstream tributaries were control variables. The cumulative number of tributaries upstream was a count of upstream tributaries greater than 5 km^2 at each grain size sample point. Initial bivariate correlations showed that the cumulative number of tributaries upstream was most significantly correlated to grain size. Other tributary variables, such as cumulative upstream tributary area, had weaker correlations with grain size. We used SPSS software for all regression analyses. Valley width was manually measured every 500 m in ArcGIS based on air photography and a 3 m 2006 LiDAR digital elevation model (DEM). Valley width was assigned to each grain size sample by linearly extrapolating between 500m valley width data.

We used effect-size calculations to test the relative influence of the dam, tributaries, and valley confinement on grain size (hypothesis 2) (Arnqvist and Wooster, 1995). The *dam effect-size* was calculated as a log response ratio (Hedges et al., 1999) of mean grain size upstream of Alamo Dam versus the mean grain size in each of 13 reaches downstream (reaches 4, 5, and 6 were split in half to make 3 additional reaches since they were larger than other reaches). A large dam effect-size was expected to mean more influence by Alamo Dam.

The hypothesis of tributary controls on grain size was also tested with calculations of effect-size for two separate responses: mainstem grain size and slope upstream and downstream of tributary confluences. The *network dynamics hypothesis* predicted that geomorphically significant tributaries

affect mainstem grain size and slope as discussed above. Tributary effect-size was calculated by (1) *tributary grain size effect size*: the log response ratio of mean grain size upstream versus mean grain size downstream for each individual tributary; and (2) *tributary slope effect size*: the log response ratio of mean slope upstream verses mean slope downstream. A large positive tributary effect-size for either the grain size or slope effect-size was expected to mean that a particular tributary affected mainstem grain size per the *network dynamics hypothesis*, with coarsening grain size and steepening slope from upstream to downstream. For *tributary grain size effect size*, only five tributaries had grain size data available upstream and downstream of their confluences. *Tributary slope effect size* was calculated for 25 tributaries.

ArcHydro tools in ArcGIS and a USGS 30m DEM were used to locate tributary confluences in terms of distance downstream from Alamo Dam (in km) and calculate catchment areas (in km^2). Slope data was collected from a 2006 LiDAR DEM at 100 m intervals beginning 150 m downstream of Alamo Dam. The average slope 300 m upstream and 300 m downstream from a tributary were used for slope effect-size calculations. For the grain size effect-size, the average D_{50} of between 3 and 15 samples upstream and downstream of a tributary was used depending on sample availability. Multiple regression analysis was conducted on effect-size results with the same methods listed above, but with tributary grain size and slope effect-sizes as dependent variables and tributary catchment area, distance downstream from Alamo Dam and valley width as control variables.

Historical Grain Size Data

To further assess dam impacts on grain size, we compared our grain size results to grain size information in USACE (1973), which presents surface and sub-surface grain size for the BWR channel where Alamo Dam would be located, and Bureau of Reclamation (1970), which provides reach-by-reach general observations of grain size shortly after Alamo Dam was completed. These grain size data were used to evaluate changes in grain size immediately downstream of Alamo Dam (USACE 1973) and to determine the timing and downstream propagation of grain size changes (USBR 1970). Bureau of Reclamation (1970) results are reported as size descriptors from the Wentworth scale, so they were translated to a D_{50} in mm for comparison (Krumbein and Sloss, 1963).

Results

Bed material observed upstream of Alamo Dam, in the Big Sandy River and Santa Maria Rivers, was in the coarse sand range (log-average D_{50} = 0.53 mm and 0.77 mm, respectively; Table 3, Figure 3). Bed material coarsens substantially between the upstream reaches and immediately downstream of the dam (log-average D_{50} in Reach 1 was 41 mm; Table 3, Figure 3). From Reach 1 to Reach 10 (i.e., from Alamo Dam toward the mouth of the BWR), reach log-averaged grain size fined exponentially downstream ($p=0.0001$, $R^2= 0.90$; Figure 4). The finest sediments, and those most similar to the Santa Maria River, were collected in the lower Planet Valley Reach 9 (Figure 4, Table 3). Despite the overall exponential decrease in grain size downstream, among several reaches the reach average coarsened relative to the reach that preceded it upstream (Figure 4). Moreover, when samples were not averaged by reach, the pattern of downstream fining was poorly explained by an exponential decay trend (R^2 = 0.24) as a result of large within-reach grain size variability (Figure 4).

The average sorting coefficient was fairly uniform (approximately 2) for all reaches (Table 3). Sorting coefficient values in the range of 2 indicate that BWR sediments are transitional between poor and very poor sorting, according to the classification of (Folk and Ward 1957).

Valley confinement changes considerably at the four major valleys, Reid, Rankin, Pipeline and Planet. Grain sizes coarsened at transitions from wide valleys to canyons, including between Rankin and Pipeline valleys and downstream of Planet Valley. However, within Reid, Rankin and Pipeline valleys, the effect of valley width on grain size was unclear because there was considerable variation between both

sand and gravel present. Planet Valley had the clearest pattern of fining grain size from upstream to downstream in the valley. Median grain size fined and became predominantly sandy downstream in Planet Valley. Sorting was still poor but was the most sorted of any site (Table 3).

Table 3. Bed-material size classes (in mm) log-averaged by reach, including the geometric mean (D_g) and sorting (S_g, with standard deviation).

Reach	D_5 (mm)	D_{16} (mm)	D_{50} (mm)	D_{84} (mm)	D_{95} (mm)	D_g (mm)	S_g
Big Sandy	0.2	0.3	0.5	1.0	1.6	0.5	2.0 ± 0.6
Santa Maria	0.3	0.4	0.8	1.7	2.6	0.9	2. ± 2
1	6.4	14.9	41.2	83.2	104.5	35.2	2.4 ± 0.4
2	0.6	1.2	3.2	7.3	6.4	3.0	2. ± 1
3	2.4	4.4	10.0	21.0	31.6	9.6	2. ± 1
4	0.9	1.3	2.6	5.1	7.9	2.6	2.0 ± 0.6
5	1.0	1.6	3.4	7.1	11.3	3.3	2. ± 1
6	1.3	2.2	4.5	8.8	12.4	4.4	2.1 ± 0.7
7	0.7	1.0	1.9	3.5	5.7	1.9	2.0 ± 0.9
8	0.5	0.7	1.2	2.1	3.1	1.2	1.7 ± 0.2
9	0.3	0.4	0.7	1.2	1.8	0.7	2. ± 1
10	0.3	0.4	0.8	1.6	2.4	0.8	2 ± 1

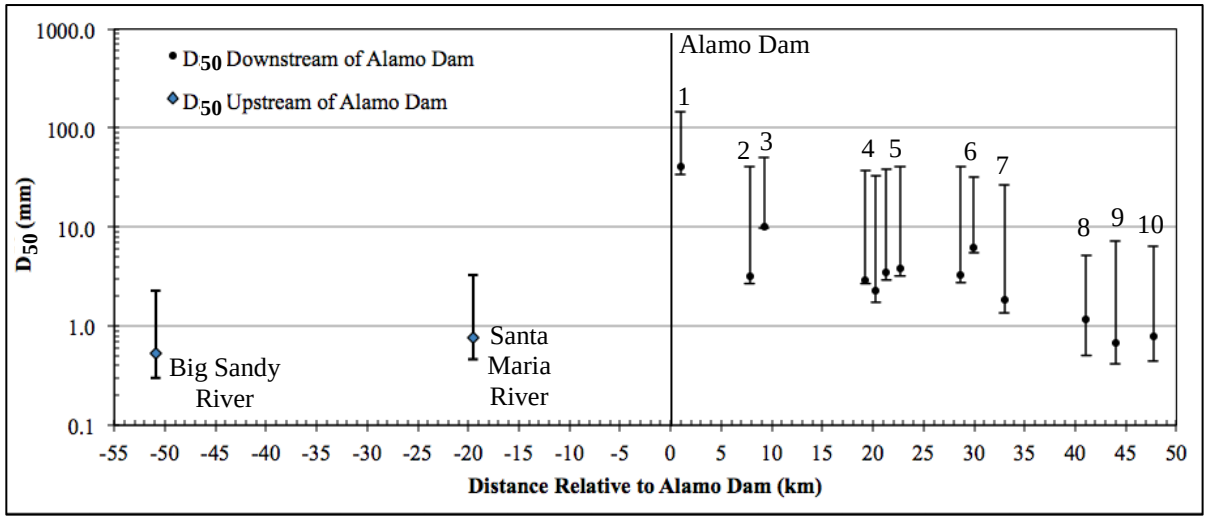

Figure 3. Log-average D_{50} for each reach, with error bars showing the maximum and minimum D_{50} in each reach. Comparison of reaches upstream and downstream of Alamo Dam shows a large increase in grain size, with downstream fining below the dam.

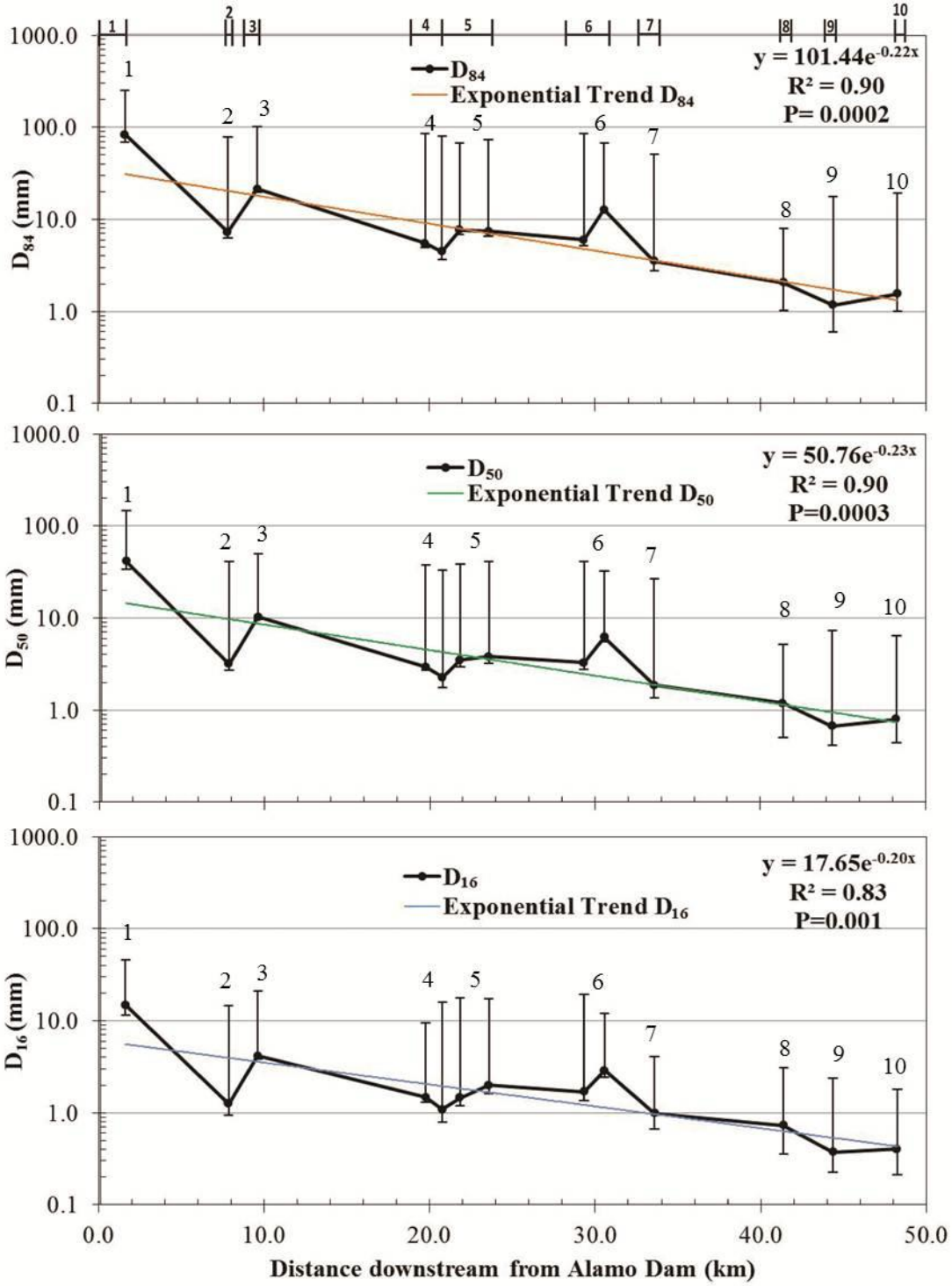

Figure 4. Log-average D_{16}, D_{50} and D_{84}, by reach, against distance downstream of Alamo Dam. The downstream trend is fit with an exponential equation for each size class. Vertical bars show the maximum and minimum D_{16}, D_{50} and D_{84} values within each reach.

Effect-Size and Multiple Regression Statistical Analysis

Our statistical analysis of controls on grain size found that, for the entire BWR below Alamo Dam, the best model for D_{50} grain size includes all three control variables: distance from Alamo Dam, cumulative number of tributaries and valley width ($p=0.048$, $R^2 = 0.33$). Distance from dam was the dominant control variable ($p<0.001$, $R^2 = 0.24$) (Table 4). In the dam-effect process domain (the first 10 km downstream of Alamo Dam), distance from dam is the only significant control on D_{50} ($p<0.001$, $R^2 = 0.43$). In contrast, in the valley-confinement domain (downstream of 10 km), distance from dam is no longer a significant control and only the cumulative number of tributaries upstream is significantly correlated to grain size ($p<0.001$, $R^2 = 0.065$).

The *dam effect size* decreases with distance downstream from Alamo Dam (Figure 5). The dam effect is small in reaches greater than 40 km downstream of Alamo Dam, because in those reaches, grain size was most similar to grain size upstream of Alamo Dam. For *tributary grain size effect size*, two of the five tributaries tested had a positive effect size, where grain size coarsened downstream of the confluence, and three had negative effect sizes, with grain size fining downstream. *Tributary slope effect size* likewise showed no discernable pattern. The *tributary slope* or *grain size effect size* both had no significant correlation to tributary area, distance from Alamo Dam or mainstem valley width.

Table 4. Forward regression results for controls on D_{50} (mm).

Data Group	Step	Added Variables	Coefficient (B)	p	Model R^2
All Samples Downstream of Alamo Dam	1	Distance from dam (km)	-3.233	<0.001	0.244
	2	Cumulative # of tributaries upstream	4.937	<0.001	0.326
	3	Valley Width (m)	-0.002	0.048	0.333
Dam Effect Domain (0 - 10 km) [a]	1	Distance from dam (km)	-4.032	<0.001	0.426
Valley Confinement Domain (>10 km)[b]	1	Cumulative # of tributaries upstream	-0.341	<0.001	0.065

a. Cumulative # of tributaries upstream and Valley Width (m) not significantly correlated to D50 in model, excluded from regression

b. Distance from dam (km) and Valley Width (m) not significantly correlated to D50 in model, excluded from regression

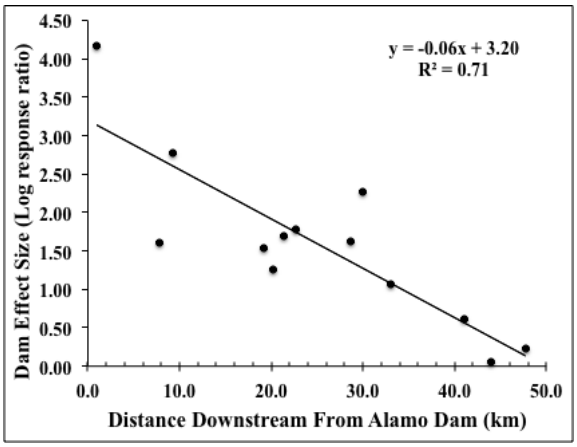

Figure 5. Dam effect size as a log response ratio with distance downstream from Alamo Dam. The dam effect size is greatest near Alamo Dam and decreases linearly downstream.

Historical Grain Size Data

Comparison of our field samples to data from near the time Alamo Dam was constructed suggests that coarsening has occurred since then. Cores from the bed of the BWR collected before Alamo Dam construction show sand or silty-sand was the dominant grain size from the surface to depths of at least 1.5 m (United States. Army. Corps of Engineers. Los Angeles District, 1973). Compared to grain size observations from (Bureau of Reclamation, 1970), current bed materials in Reach 2 and 3 are considerably coarser than the "sand" grain size observed in 1968 (Figure 6). Downstream of those reaches, however, current grain size patterns are similar to those observed in 1968. The report also showed that degradation was observed below Alamo Dam only a few months after dam completion. Dam effects on grain size had propagated 3 km downstream of Alamo Dam in 1968, but not 10 km downstream to Reach 3 where the grain size was still sandy.

Discussion

The downstream pattern of bed-material sizes in the BWR basin supports our hypothesis regarding dam-induced disruption and resetting of downstream fining (hypothesis 1). Sand-sized bed materials predominate upstream of Alamo Dam, sediment coarsens dramatically immediately downstream of the dam, and then fines downstream following an exponential pattern. These findings are consistent with other work (Williams and Wolman, 1984; Kira, 1972).

To evaluate our hypothesis regarding the downstream extent of dam effects on grain size, we framed our analysis in the context of *dam-effect* and *valley-confinement* process domains (Figure 6). In the *dam-effect* process domain, sediment supply reduction by Alamo Dam has caused incision and grain size coarsening. Reach 3 has coarsened considerably since the Bureau of Reclamation's 1968 survey, suggesting that *dam-effect* process domain extends to Reach 3. In Reach 4 and further downstream, there has been minimal change compared to the 1968 survey. The historical grain size comparison therefore suggests that dam effects on grain size extend to between 10 and 18 km downstream from Alamo Dam. Reach 3 is also situated near the entrance to the first wide alluvial valley downstream of the dam (Reid Valley), which could halt the propagation of dam-effects by a dramatic reduction in stream power. These findings are consistent with Jackson and Summers (1988), who estimated that degradation caused by Alamo Dam extended 12 km downstream.

The considerable flow reduction in the BWR also supports the conclusion that Alamo Dam effects on grain size are limited to only the 10 km near the dam. The ratio of the post-dam to pre-dam Q_2, a measure of flood reduction in dammed rivers (Schmidt and Wilcock 2008), is 0.04 in the BWR, suggesting extreme flood reduction compared to other dammed rivers assessed by Schmidt and Wilcock (2008). The magnitude of flow reduction can be compared to changes in grain size and sediment supply to assess whether rivers are in sediment surplus or deficit downstream of dams and whether incision is expected (Schmidt and Wilcock 2008). Our observations suggest that the BWR is in sediment deficit in the dam-effect process domain, but that this deficit is mitigated by extensive sediment storage within alluvial valleys further downstream.

Long-term ^{10}Be erosion rates show that at the top of Reid Valley the ratio of post-dam supply from tributaries to the supply pre-dam is 0.02 (Dekker, 2012). According to the long-term rates, the sediment supply reduction near Reid Valley is of the same order of magnitude as the flow reduction (0.04). Activation of sediment stored in Reid Valley might be sufficient for the regulated BWR to reach a new equilibrium, judging from the grain size pattern and the similar magnitude of reduction in supply and flow near the upstream end of the valley. The Trinity River, had a 0.15 flow reduction value and 0.01 sediment supply ratio, and dam effects extended 52 km downstream of Livingston Dam, until the supply ratio was shifted by floodplain sediment storage (Phillips et al., 2004; Schmidt and Wilcock, 2008).

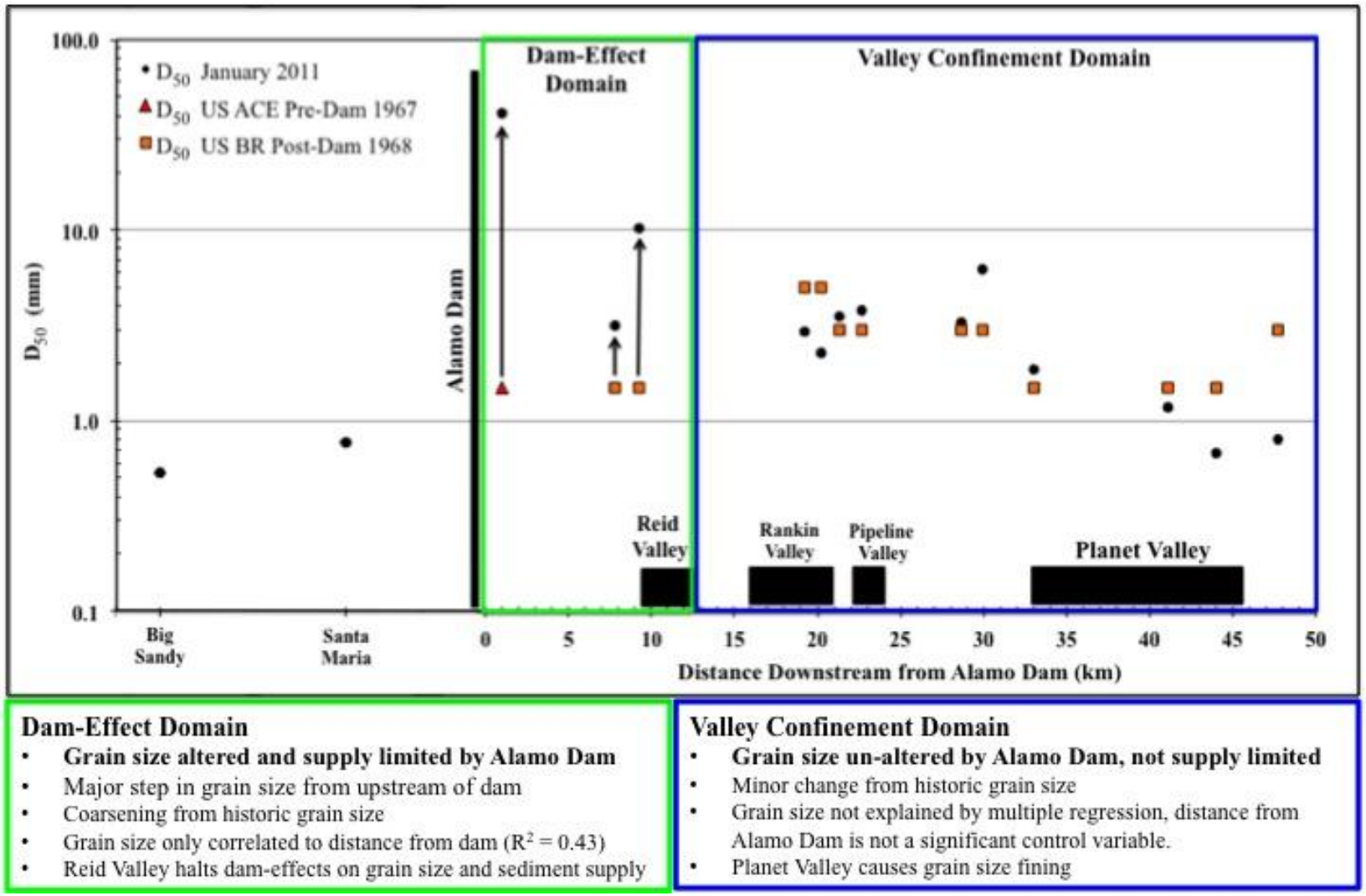

Figure 6. Modern and historical grain size results, valleys wider than 500 m, and BWR process domains. Historical grain size results are from United States. Army. Corps of Engineers. Los Angeles District (1973) and Bureau of Reclamation (1970).

The *valley-confinement* process domain begins at Reach 4 where grain size becomes sandier, but still quite variable (Figure 6). Alamo Dam likely does not affect Reach 4 since it has changed little since the 1968 grain size survey (Figure 6). After Reid Valley the multiple regression analysis showed that distance from Alamo Dam was no longer significantly correlated to grain size. Valley width was also not significantly correlated to grain size downstream of Reid Valley, however this may be due to increased grain size scatter. There was a pattern of grain size fining in Planet Valley, 33 km downstream (Figure 6). The grain size coarsening in the canyon reach near 30 km downstream is also an example where valley confinement affects grain size despite the lack of statistical significance.

Tributaries merit their own process domain governed by the *network dynamic hypothesis*. However, their effects are at a smaller spatial scale than either the *dam-effect* or *valley-confinement* domains. As discussed above, the *network dynamic hypothesis* suggests that tributaries influence mainstem slope and grain size (Benda et al., 2004). Tributaries on the BWR do not appear to alter the mainstem as predicted by the *network dynamics hypothesis*, however, suggesting that this conceptual model may be less applicable to dryland rivers. The multiple regression models for grain size downstream of Alamo Dam were only slightly improved by the number of tributaries upstream variable (Table 4). *Tributary grain size effect size* and *slope effect size*, calculated with a log response ratio, showed no significant pattern with distance from Alamo Dam, tributary catchment area, or valley width.

Ephemeral rivers may display very high rates of sediment transport (Laronne and Reid, 1993), while others have found that tributaries cause no change in the pattern of downstream fining (Singer, 2008; Frings, 2008). The magnitude of tributary effects may depend on the relative volume of sediment a tributary contributes compared to the volume of sediment in the mainstem (Knighton, 1982; Benda et al., 2004). The recent history of timing of tributary flows and mainstem flows is likely also important to understand tributary effects for dryland rivers with infrequent flow and sediment transport.

Dryland River Disequilibrium

Prior to Alamo Dam, dryland geomorphic processes defined the BWR. Large floods set channel form. The 1891 flood on the BWR is the largest recorded event from a basin of its size along the Lower Colorado River (House et al., 1999). Historic aerial photographs show much wider channels, with less valley-bottom vegetation than under current conditions. The regulated BWR no longer activates its pre-dam, valley-spanning floodplains in wide reaches, and vegetation has increased dramatically. Shafroth et al. (1998) found reaches on the BWR with such well-established vegetation that not even the largest dam release could cause geomorphic change.

Despite these changes, the modern river shows evidence of having reached a Alamo Dam-related equilibrium between regulated flow and supply limitation. The grain size pattern shows that dam effects have propagated to Reach 3, where Reid Valley appears to impede downstream propagation of sediment deficit. If the BWR can maintain access to historic floodplain sediment in Reid Valley then it is unlikely for Alamo Dam to cause further downstream degradation. In a sense, the natural dryland river disequilibrium that transported large quantities of sediment to the floodplains of the BWR during historic large floods may effectively insulate the river from the extensive sediment degradation common to dammed rivers.

Repeat grain size studies in the future would provide further insights into the propagation rate of dam effects in the BWR. Increased channelization in some reaches due to vegetation growth could limit access to historic floodplain sediment and lead to incision and grain size adjustment further downstream in the future.

Other Controls on Grain Size

Grain size at a local scale (30 m) showed considerable scatter, and many samples collected just 30 m apart showed abrupt shifts in grain size. When the BWR floods and transports the most sediment

the river becomes braided with numerous bifurcations around vegetated islands. Vegetation in dryland river valley bottoms causes uneven bed elevations, increased channel roughness and variable flow velocities that cause local grain size variation (Dunkerley, 2008). Bifurcations cause grain size variation because multiple channels have differing slopes, sediment loads and confluence effects (Frings, 2008). The scatter observed is not likely caused by the uncertainty found in digital photo grain size methods. At most, the percent uncertainty in digital photo D_{50} grain size was 50%. This is likely not a significant error for the scale of this study, because the percent difference in size between medium sand and medium gravel is 500% (Table 2).

Variable discharge due to losses to groundwater could be another factor contributing to the scattered grain size pattern within and between reaches (Wiele et al., 2009). The BWR has a complicated history tied to base-level changes of the Colorado River. According to Wilson and Owen-Joyce (2002), during the early Pleistocene the Planet Valley floodplain was 27 m above modern levels. Later in the Pleistocene the Colorado River base level dropped and caused the BWR floodplain in Planet Valley to erode 36 m below modern levels. This suggests the BWR would have been incised to bedrock in some reaches. Since the late Pleistocene the BWR has aggraded to its modern floodplain elevation. All reaches are above bedrock levels today. The alluvium deposited since the late Pleistocene low stand is highly permeable (Wilson and Owen-Joyce, 2002). The depth to bedrock is not uniform and discharge loss or gain from groundwater varies in canyon and floodplain reaches (House et al., 1999). The discharge loss pattern might correlate well with slope changes and affect grain size similarly. The discharge pattern may also vary more complexly due to unpredictable depth to bedrock. The effect of discharge loss and gain on grain size would require further study of alluvium depths along the entire BWR.

Conclusions

Alamo Dam has had the effect of grain size coarsening until about 10 km downstream where the river meets a wide floodplain valley. The *dam-effect* process domain, dominant in the first 10 km, is defined by coarse grain size that is significantly correlated to distance from Alamo Dam. Downstream of 10 km, a *valley-confinement* process domain controls grain size according to valley confinement and grain size is not significantly correlated to distance from Alamo Dam. In the downstream reaches grain size results resemble observations from 1968. Gravel in the lower reaches could be due to tributary inputs, although only certain tributaries in canyon reaches display patterns predicted by the *network dynamic hypothesis*. Narrow canyon reaches cause brief increases in average grain size, but do not alter the overall downstream fining trend. Planet Valley strongly affects grain size and average sorting coefficient increases. The extreme flow reduction on the BWR and the mix of valley and canyon reaches appears to have confined the extent of dam effects on grain size to only the upper reaches near Alamo Dam.

This study shows the application of grain size analysis to better understand dam management effects on a river. Our work indicates that sediment supply reductions and grain-size coarsening as a result of Alamo Dam are marked in the 10 km downstream of the dam, but further downstream, these effects dissipate as a result of the influence of large, sediment-rich alluvial valleys. These results suggest that high-flow releases from Alamo Dam will likely not cause widespread sediment degradation on the BWR.

Acknowledgements

We thank Robert Livesay for field assistance and Laurie Marczak for guidance. This work was funded by a Geological Society of America Graduate Student Research grant to FJD, and by grants from the US Fish & Wildlife Service and National Science Foundation (EAR-1025076).

References Cited

Arnqvist, G., and Wooster, D., 1995, Meta-analysis: synthesizing research findings in ecology and evolution: Trends in Ecology & Evolution, v. 10, no. 6, p. 236–240.

Benda, L., Poff, N.L., Miller, D., Dunne, T., Reeves, G., Pess, G., and Pollock, M., 2004, The network dynamics hypothesis: how channel networks structure riverine habitats: BioScience, v. 54, no. 5, p. 413–427.

Bourke, M.C., and Pickup, G., 1999, Fluvial form variability in arid central Australia, *in* Miller, A. J. and Gupta, A. eds., Varieties of Fluvial Forms, J. Wiley, p. 248–271.

Bowles, D.S., Anderson, L.R., Evelyn, J.B., Glover, T.F., and Van Dorpe, D.M., 2000, Alamo dam demonstration risk assessment: Ancold Bulletin, p. 113–128.

Brandt, S.A., 2000, Classification of geomorphological effects downstream of dams: Catena, v. 40, no. 4, p. 375–401.

Bureau of Reclamation, 1970, Final Design Sediment Deposition Study, Bill Williams River Arm of Lake Havasu, Central Arizona Project, Arizona: Sedimentation Section, Division of Planning Coordination in Collaboration with the Phoenix Development Office, Phoenix, Arizona. In The Papers of Whitney M. Borland, Colorado State University.

Buscombe, D., and Masselink, G., 2009, Grain-size information from the statistical properties of digital images of sediment: Sedimentology, v. 56, no. 2, p. 421–438.

Buscombe, D., Rubin, D.M., and Warrick, J.A., 2010, A universal approximation of grain size from images of noncohesive sediment: Journal of Geophysical Research, v. 115, no. F2, p. F02015.

Davies, B.R., Thoms, M.C., Walker, K.F., O'keeffe, J.H., and Gore, J.A., 1994, Dryland rivers: their ecology, conservation and management: The rivers handbook, p. 484–511.

Dekker, F., 2012, 10-Beryllium Catchment Erosion Rates and Sediment Mixing in a Dammed Dryland River: M.S. Thesis, Chapter 3.

Dunkerley, D.L., 1992, Channel geometry, bed material, and inferred flow conditions in ephemeral stream systems, Barrier Range, western NSW Australia: Hydrological Processes, v. 6, no. 4, p. 417–433.

Dunkerley, D., 2008, Flow chutes in Fowlers Creek, arid western New South Wales, Australia: Evidence for diversity in the influence of trees on ephemeral channel form and process: Geomorphology, v. 102, no. 2, p. 232–241.

Frings, R.M., 2008, Downstream fining in large sand-bed rivers: Earth-Science Reviews, v. 87, no. 1-2, p. 39–60.

Graf, W.L., 2006, Downstream hydrologic and geomorphic effects of large dams on American rivers: Geomorphology, v. 79, no. 3-4, p. 336–360.

Hedges, L.V., Gurevitch, J., and Curtis, P.S., 1999, The meta-analysis of response ratios in experimental ecology: Ecology, v. 80, no. 4, p. 1150–1156.

Heitmuller, F.T., and Hudson, P.F., 2009, Downstream trends in sediment size and composition of channel-bed, bar, and bank deposits related to hydrologic and lithologic controls in the Llano River watershed, central Texas, USA: Geomorphology, v. 112, no. 3-4, p. 246–260.

Hoey, T.B., and Ferguson, R., 1994, Numerical simulation of downstream fining by selective transport in gravel bed rivers: Model development and illustration: Water Resources Research, v. 30, no. 7, p. 2251–2260.

House, P.K., Wood, M.L., Pearthree, P.A., and Arizona Geological Survey, 1999, Hydrologic and geomorphic characteristics of the Bill Williams River, Arizona: Arizona Geological Survey, Tucson, AZ.

Jackson, W.L., and Summers, P., 1988, Bill Williams River field assessment: hydrology, hydrogeology, and geomorphology: Bureau of Land Management, Denver, CO.

Kira, H., 1972, Factors influencing the river behavior—river-bed variation due to dam construction and gravel gathering: Transactions of the 8th International Committee on Irrigation and Drainage, v. 5.

Knighton, A.D., 1982, Longitudinal changes in the size and shape of stream bed material: evidence of variable transport conditions: Catena, v. 9, no. 1-2, p. 25–34.

Kondolf, G.M., and Piégay, H. (Eds.), 2003, Tools in fluvial geomorphology: John Wiley & Sons Ltd., San Francisco.

Kondolf, G.M., and Wolman, M.G., 1993, The sizes of salmonid spawning gravels: Water Resources Research, v. 29, no. 7, p. 2275–2285.

Krumbein, W.C., and Sloss, L.L., 1963, Stratigraphy and sedimentation: W.H. Freeman, San Francisco.

Lagasse, P.F., 1994, Variable response of the Rio Grande to dam construction: New York, NY: American Society of Civil Engineers Press.

Laronne, J.B., and Reid, I., 1993, Very high rates of bedload sediment transport by ephemeral desert rivers: Nature, v. 366, p. 148–150.

Ligon, F.K., Dietrich, W.E., and Trush, W.J., 1995, Downstream ecological effects of dams: BioScience, v. 45, no. 3, p. 183–192.

Montgomery, D.R., 1999, Process Domains and the River Continuum: Journal of the American Water Resources Association, v. 35, no. 2, p. 397–410.

Paola, C., Parker, G., Seal, R., Sinha, S.K., Southard, J.B., and Wilcock, P.R., 1992, Downstream fining by selective deposition in a laboratory flume: Science, v. 258, no. 5089, p. 1757 - 1760.

Phillips, J.D., Slattery, M.C., and Musselman, Z.A., 2004, Dam-to-delta sediment inputs and storage in the lower Trinity River, Texas: Geomorphology, v. 62, no. 1, p. 17–34.

Ralph, T.J., and Hesse, P.P., 2010, Downstream hydrogeomorphic changes along the Macquarie River, southeastern Australia, leading to channel breakdown and floodplain wetlands: Geomorphology, v. 118, no. 1-2, p. 48–64.

Reid, I., and Frostick, L.E., 1994, Fluvial sediment transport and deposition: Sediment transport and depositional processes, p. 89–155.

Rubin, D.M., 2004, A simple autocorrelation algorithm for determining grain size from digital images of sediment: Journal of Sedimentary Research, v. 74, no. 1, p. 160-165.

Rubin, D.M., Chezar, H., Harney, J.N., Topping, D.J., Melis, T.S., and Sherwood, C.R., 2007, Underwater microscope for measuring spatial and temporal changes in bed-sediment grain size: Sedimentary Geology, v. 202, no. 3, p. 402–408.

Rubin, D.M., United States. Interagency Advisory Committee on Water Data. Hydrology Subcommittee, United States. Inter-agency Committee on Water Resources. Subcommittee on Sedimentation, Federal Interagency Hydrologic Modeling Conference, and Federal Inter-agency Sedimentation Conference, 2010, 20,000 grain-size observations from the bed of the Colorado River, and implications for sediment transport through Grand Canyon.

Schmidt, J.C., and Wilcock, P.R., 2008, Metrics for assessing the downstream effects of dams: Water Resources Research, v. 44, no. 4, p. W04404.

Seal, R., and Paola, C., 1995, Observations of downstream fining on the North Fork Toutle River near Mount St. Helens, Washington: Water Resources Research, v. 31, no. 5, p. 1409.

Shafroth, P.B., Auble, G.T., Stromberg, J.C., and Patten, D.T., 1998, Establishment of woody riparian vegetation in relation to annual patterns of streamflow, Bill Williams River, Arizona: Wetlands, v. 18, no. 4, p. 577–590.

Shafroth, P.B., Wilcox, A.C., Lytle, D.A., Hickey, J.T., Andersen, D.C., Beauchamp, V.B., Hautzinger, A., McMullen, L.E., and Warner, A., 2010, Ecosystem effects of environmental flows: modelling and experimental floods in a dryland river: Freshwater Biology, v. 55, no. 1, p. 68–85.

Sime, L.C., and Ferguson, R.I., 2003, Information on grain sizes in gravel-bed rivers by automated image analysis: Journal of Sedimentary Research, v. 73, no. 4, p. 630–636.
Simons, D.B., and Sentürk, F., 1992, Sediment transport technology : water and sediment dynamics: Water Resources Publications, Littleton, CO.
Singer, M.B., 2008, Downstream patterns of bed material grain size in a large, lowland alluvial river subject to low sediment supply: Water Resources Research, v. 44, no. 12, p. W12202.
Thornes, J.B., 2009, Catchment and channel hydrology, *In* Parsons, A.J. and Abrahams, A.D. eds., Geomorphology of Desert environments, Springer, Netherlands, p. 303–332.
Tooth, S., 2000, Process, form and change in dryland rivers: a review of recent research: Earth-Science Reviews, v. 51, no. 1-4, p. 67–107.
Topping, D.J., Rubin, D.M., and Vierra Jr, L.E., 2000, Colorado River sediment transport 1. Natural sediment supply limitation and the influence of Glen Canyon Dam: Water Resources Research, v. 36, no. 2, p. 515–542.
United States. Army. Corps of Engineers. Los Angeles District, 1973, Foundation report for Alamo Lake : Colorado River Basin, Bill Williams River, Arizona, flood control: Army Engineer District, Los Angeles, Los Angeles.
Wiele, S.M., Hart, R.J., Darling, H.L., and Hautzinger, A.B., 2009, Sediment transport in the Bill Williams River and turbidity in Lake Havasu during and following two high releases from Alamo Dam, Arizona, in 2005 and 2006: US Geological Survey Scientific Investigations Report, v. 5195.
Wilcox, A.C., and Shafroth, P.B., 2013, Coupled hydrogeomorphic and woody-seedling responses to controlled flood releases in a dryland river: Water Resources Research, In review.
Williams, G.P., and Wolman, M.G., 1984, Downstream effects of dams on alluvial rivers: US Geological Survey, Professional Paper, v. 1286.
Wilson, R.P., and Owen-Joyce, S.J., 2002, Hydrologic Conditions in the Bill Williams River National Wildlife Refuge and Planet Valley, Arizona, 2000: US Geological Survey, Water-Resources Investigation 02-4214.
Wolman, M.G., 1954, A method of sampling coarse river-bed material: Transactions of the American Geophysical Union, v. 35, no. 6, p. 951–956.
Wright, S.A., Schmidt, J.C., Melis, T.S., Topping, D.J., and Rubin, D.M., 2008, Is there enough sand? Evaluating the fate of Grand Canyon sandbars: GSA Today, v. 18, no. 8, p. 4–10.

Analysis of Sediment Dynamics in the Bill Williams River, Arizona: Hydroacoustic Surveys and Sediment Coring

Authors: Paul Gremillion (Northern Arizona University) and David Walker (University of Arizona)

(attached)

Coupled Hydrogeomorphic and Woody-Seedling Responses to Controlled Flood Releases in a Dryland River

Andrew C. Wilcox[1] and Patrick B. Shafroth[2]

[1]*Department of Geosciences, University of Montana, Missoula, MT 59812, USA*
[2]*US Geological Survey, Fort Collins Science Center, 2150 Center Avenue, Building C, Fort Collins, CO 80526-8118, USA*

This chapter has been submitted to the journal *Water Resources Research* and is currently in revision. Readers should consult the journal's website or contact Andrew Wilcox for an updated version of the manuscript after it has been published.

ABSTRACT
Interactions among flow, geomorphic processes, and riparian vegetation can strongly influence both channel form and vegetation communities. To investigate such interactions, we took advantage of a series of dam-managed flood releases that were designed in part to maintain a native riparian woodland system on a sand-bed, dryland river, the Bill Williams River, Arizona, USA. Our resulting multi-year flow experiment examined differential mortality among native and nonnative riparian seedlings, associated flood hydraulics and geomorphic changes, and the temporal evolution of feedbacks among vegetation, channel form, and hydraulics. We found that floods produced geomorphic and vegetation responses that varied with distance downstream of a dam, with scour and associated seedling mortality closer to the dam and aggradation and burial-induced mortality in a downstream reach. We also observed significantly greater mortality among nonnative tamarisk (*Tamarix*) seedlings than among native willow (*Salix gooddingii)* seedlings, reflecting the greater first-year growth of willow relative to tamarisk. When vegetation was small early in our study period, the effects of vegetation on flood hydraulics and on mediating flood-induced channel change were minimal. Vegetation growth in subsequent years resulted in stronger feedbacks, such that vegetation's stabilizing effect on bars and its drag effect on flow progressively increased, muting the geomorphic effects of a larger flood release. These observations suggest that the effectiveness of floods in producing geomorphic and ecological changes varies not only as a function of flood magnitude and duration, but also of antecedent vegetation density and size.

Running title: Coupled hydrogeomorphic and vegetation responses to floods

Keywords: tamarisk, willow, riparian vegetation, dams, feedbacks, ecogeomorphology

INTRODUCTION

Riparian vegetation and morphodynamics can be tightly coupled along river corridors. Vegetation produces both below-ground and above-ground effects that strengthen banks, stabilize bars, trap sediment, and alter local hydraulics [*Petryk and Bosmajian*, 1975; *Hey and Thorne*, 1986; *Nepf*, 1999; *Micheli and Kirchner*, 2002; *Green*, 2005; *Corenblit et al.*, 2007; *Schnauder and Moggridge*, 2009; *Rominger et al.*, 2010; *Sandercock and Hooke*, 2010; *Dean and Schmidt*, 2011; *Edmaier et al.*, 2011]. These effects can in turn influence channel pattern by, for example, promoting the evolution of anabranching [*Tooth and Nanson*, 2000] or single-thread, meandering channels instead of braided channels [*Williams*, 1978; *Gran and Paola*, 2001; *Tal and Paola*, 2007; *Braudrick et al.*, 2009; *N S Davies and Gibling*, 2011]. Flow and sediment regimes, water availability, and channel morphology can strongly influence distribution patterns and population dynamics of woody riparian vegetation [*Hupp and Osterkamp*, 1996; *Scott et al.*, 1996; *Cooper et al.*, 2003; *Stella et al.*, 2011]. Many investigations into hydrogeomorphic effects on riparian vegetation have focused on the establishment of pioneer riparian trees and the role of site creation, soil moisture, and the timing of floods compared to seed-dispersal timing [*Scott et al.*, 1996; *Mahoney and Rood*, 1998; *Cooper et al.*, 1999; *Stella et al.*, 2006; *Asaeda et al.*, 2011]. A more limited number of studies have examined how the subsequent fate of seedlings established within or near the active channel is affected by flood-induced scour, burial, or breakage [*Stromberg et al.*, 1993; *Johnson*, 1994; *Auble and Scott*, 1998; *Friedman and Auble*, 1999; *Johnson*, 2000; *Levine and Stromberg*, 2001; *Dixon et al.*, 2002; *Polzin and Rood*, 2006; *Asaeda and Rajapakse*, 2008].

Feedbacks between morphodynamics and vegetation may be strongly time-dependent, as a result of changes in vegetation characteristics, flow variability, and other factors. As vegetation grows with time since establishment, plants both exert a greater influence on physical processes and become more resilient to them. Increases in plant diameter and height produce greater vegetation drag [*Freeman et al.*, 2000], reducing the proportion of total shear stress applied to grains on the bed and thereby reducing the erosional effects of floods of a given magnitude. Time since establishment can also influence the strength of roots, their cohesive effect, and their resilience to scour [*Edmaier et al.*, 2011]. The shifting strength and direction of feedbacks once vegetation becomes well established produces a "ratchet effect" whereby such vegetation becomes progressively more difficult to remove as it grows [*Tal et al.*, 2004]. Seasonal variations (presence or absence of leaves) may also alter vegetation drag by increasing or reducing frontal area [*Freeman et al.*, 2000]. A conceptual model proposed by *Corenblit et al.* [2007] suggests four stages in the temporal evolution of feedbacks: an initial period following a channel-setting flood in which geomorphic processes dominate; a second stage in which pioneer vegetation is recruited on bare surfaces; a third stage in which ecogeomorphic feedbacks are strongest, and a fourth stage in which vegetation is mature and dense enough that it strongly controls channel planform and is insensitive to all but the largest floods.

Efforts to restore riparian zones and manage non-native riparian vegetation would benefit from improved understanding of hydrogeomorphic effects on vegetation. Multiple species and hybrids of tamarisk (*Tamarix* spp., aka saltcedar), shrubs and small trees native to Eurasia, have become the dominant riparian vegetation along many rivers in the southwestern United States, often replacing native cottonwood-willow (*Populus-Salix*) woodlands [*Friedman et al.*, 2005; *Nagler et al.*, 2011]. Tamarisk invasions have altered riparian habitat [*Shafroth et al.*, 2005] and contributed to reductions in channel width, increased sediment storage, and other geomorphic changes along western rivers [*Graf*, 1978; *Hereford*, 1984; *Allred and Schmidt*, 1999; *Grams and Schmidt*, 2002; *Birken and Cooper*, 2006; *Dean and Schmidt*, 2011]. Millions of dollars have been spent on controlling tamarisk by chemical, mechanical, and biological control methods [*Shafroth et al.*, 2005], sometimes with unintended geomorphic consequences such as increased erosion [*Vincent et al.*, 2009].

Shifts in the magnitude and timing of peak flows and other anthropogenic alterations of flow regimes can favor tamarisk over native pioneer species [*Stromberg*, 2001; *Stromberg et al.*, 2007; *Merritt and Poff*, 2010]. Comparisons of tamarisk and native pioneer trees (cottonwood and/or willow) at the seedling stage have found that tamarisk is more vulnerable to the effects of burial [*Levine and Stromberg*, 2001] and inundation [*Gladwin and Roelle*, 1998] and that cottonwood seedlings can outcompete tamarisk seedlings when grown in mixtures [*Sher et al.*, 2000; 2002]. Tamarisk recolonizes rapidly following floods [*Shafroth et al.*, 2005], however, and beyond the seedling stage, tamarisk becomes highly resilient to hydrogeomorphic forces as well as to drought [*Everitt*, 1980; *Cleverly et al.*, 1997]. Identification of flows and fluvial processes that adversely affect tamarisk relative to native taxa could assist efforts to prescribe flows downstream of dams for managing tamarisk.

Although to our knowledge, managed flood releases have not been used as an explicit tool for tamarisk control, manipulation of flow releases from dams by mimicking natural flows has been implemented to achieve other ecosystem objectives [*Poff et al.*, 1997; *Arthington et al.*, 2006; *Merritt et al.*, 2010; *Konrad et al.*, 2012]. Tools are lacking, however, for providing managers with site-specific, quantitative information about the magnitude, duration, frequency, rate of change, and timing of flows sufficient to achieve such objectives [*Rood et al.*, 2005; *Palmer and Bernhardt*, 2006]. One avenue for developing the information to address these questions, and more generally to develop new insights into relationships between hydrogeomorphic processes and ecosystem functions, is conducting large-scale flow experiments [*Konrad et al.*, 2011].

Here, we report on a series of dam-managed flood releases on a dryland river that we used as a multi-year flow experiment to investigate geomorphic changes, flood hydraulics, woody seedlings, and their interactions. At the outset of our study, we used a planned flood release to test the hypothesis that this event would cause greater mortality among a cohort of small (1-year old) nonnative tamarisk seedlings than among native willow (*Salix gooddingii*) seedlings, as well as to evaluate associated flood hydraulics and geomorphic changes. Our study evolved and broadened in subsequent years, as additional managed floods that varied in magnitude and duration were released in our study system, into an investigation of the evolving nature and strength of vegetation-hydrogeomorphic feedbacks as a result of spatial and temporal variations in coupled geomorphic and vegetation responses to controlled floods. We apply these inquiries to develop guidance regarding the effectiveness of flow prescriptions in dammed rivers, where high-flow releases are small compared to pre-dam floods, in achieving downstream geomorphic and ecological objectives.

STUDY AREA

The Bill Williams River (BWR) historically flowed 65 km from the confluence of the Santa Maria River and Big Sandy River into the Colorado River in western Arizona, USA (Figure 1), draining 13,800 km^2 and alternating between canyon and alluvial valley reaches. Because the hydrology of the BWR is influenced by wetter conditions in its mountainous headwaters, where average annual precipitation exceeds 40 cm yr^{-1}, and arid conditions in the lower basin (12 cm yr^{-1} precipitation) [*Shafroth and Beauchamp*, 2006], we characterize the river as “dryland” rather than arid or semiarid. Both the upstream and downstream limits of the BWR are currently submerged within reservoirs. Alamo Dam, a U.S. Army Corps of Engineers flood-control facility that was completed in 1968 and impounds Alamo Lake, now forms the upstream limit of the BWR. At its downstream end, the BWR flows into Lake Havasu, an impoundment on the Colorado River that is the source for the Central Arizona Project Aqueduct and the Colorado River Aqueduct, which supply water to several large cities in the southwestern US.

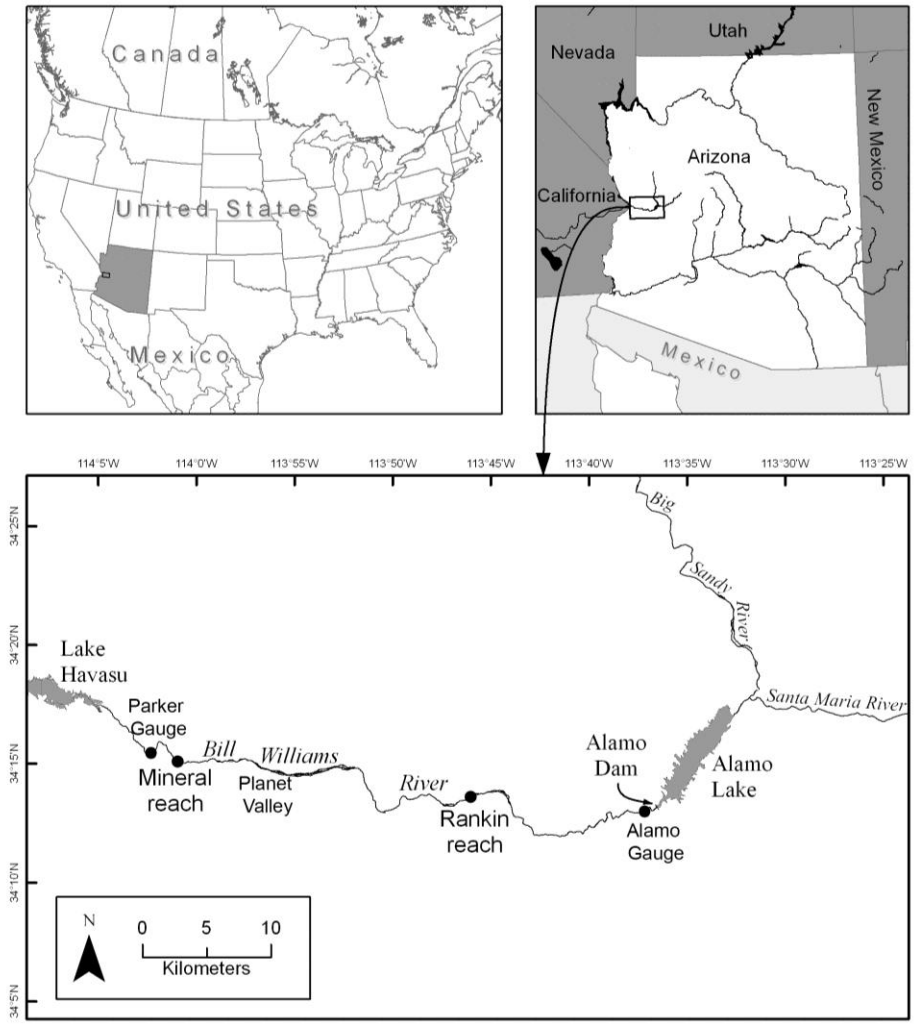

Figure 1. Bill Williams River in western Arizona, USA. The two study reaches identified in the bottom panel, Rankin and Mineral Wash, are 18 and 48 km downstream of Alamo Dam, respectively (flow is from right to left).

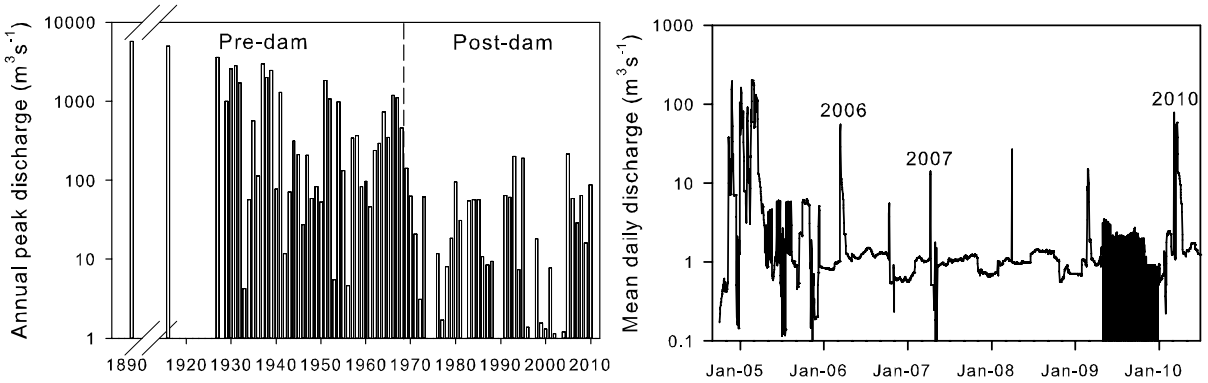

Figure 2. Flow data for the Bill Williams River below Alamo Dam gauge. Left panel shows annual peak discharges for the period of record and illustrates the post-dam reduction of high flows. Right panel shows mean daily flows from late 2004 to mid-2010, with annotations of flood events around which our data collection was completed; note difference in y-axis scale compared to left panel.

Alamo Dam has substantially reduced peak flows in and sediment supply to the BWR (Figure 2). For example, the ratio of the post-dam two-year flood (Q_2) to the pre-dam Q_2 is 0.04, based on Log Pearson III analysis of peak-flow data from the US Geological Survey BWR below Alamo Dam, AZ gauge (#09426000). This ratio, a metric known as *Q** [*Magilligan and Nislow*, 2005; *Schmidt and Wilcock*, 2008], provides an indication of the extent to which a dam has reduced transport capacity; the 0.04 value for the BWR is indicative of extreme peak flow reduction. The upper 85 percent of the basin's drainage area is effectively disconnected from the BWR by Alamo Dam, blocking the supply of bed-material from the upper basin. Further, there are no perennial tributaries downstream of Alamo Dam.

The BWR's alluvial valleys, the largest of which is the 13-km long Planet Valley, exert a strong control on the routing of both flow and sediment through the BWR, causing gains and losses of surface flow and storing large volumes of sediment. The alluvial aquifer in Planet Valley (Figure 1) acts as a sponge, such that all of the river's base flow typically infiltrates at the upstream end of the valley and emerges at the downstream end, where valley width and depth to bedrock decline [*Jackson and Summers*, 1988; *House et al.*, 2006]. Planet Valley and its antecedent water-table elevation also influence routing of high flows down the BWR [*Shafroth et al.*, 2010], as discussed further below.

The severe reduction of both transport capacity and sediment supply in the BWR has been accompanied by the spread of tamarisk and severe channel narrowing. Aerial photograph analysis indicates that since the 1950s channel width has declined dramatically, with corresponding expansion of floodplain vegetation [*Shafroth et al.*, 2002]. This channel narrowing trend started even before Alamo Dam was built, likely as a result of regional climatic shifts [*Sheppard et al.*, 2002] that reduced peak flows along many rivers in the southwestern US [*Hereford*, 1984].

Whereas many river corridors in the southwestern U.S. are dominated by nonnative tamarisk, the BWR has a diverse riparian flora that includes tamarisk but also Goodding's willow (*S. gooddingii*), Fremont cottonwood (*Populus fremontii*), seep willow (*Baccharis salcifolia*), arrowweed (*Pluchea sericea*), mesquite (*Prosopis* spp.), and cattail (*Typha* spp.). Plant species richness is lower in the BWR than in its unregulated upstream tributary, the Santa Maria River, however, likely as a result of flood reduction [*Stromberg et al.*, 2012]. In an effort to sustain the native riparian woodland habitat in the BWR, flow management at Alamo Dam has been guided in recent years by collaborative efforts between the Army Corps of Engineers and other stakeholders [*Shafroth and Beauchamp*, 2006; *Shafroth et al.*, 2010] and has followed the Environmentally Sustainable Water Management (ESWM) framework [*Richter et al.*, 2003; *Konrad et al.*, 2012]. Environmental flow releases have included base flows designed to provide summer and fall irrigation for cottonwoods and willows as well as flood releases, as water availability allows, to promote cottonwood and willow recruitment. Dam reoperations for environmental purposes on the BWR are facilitated because competing water uses such as hydropower production or irrigation are absent or limited, because the downstream floodplain is sparsely populated, and because water released from Alamo Dam is delivered to and impounded by Lake Havasu (Figure 1). Communication among scientists and managers has allowed scientists to provide input into the design of flow releases and to capitalize on planned flood releases for data collection. These factors combine to create a unique field laboratory.

This study investigates a series of floods released from Alamo Dam into the BWR (Table 1, Figure 2). During the winter of 2004 and 2005, high runoff associated with El Niño caused multiple high-flow events in the range of the dam's maximum outlet capacity (approximately 200 m^3s^{-1}). These events, although they occurred before the data collection effort described below, were significant to our study because they scoured vegetation from low-elevation bars and created bare surfaces for seedling establishment. The falling limb of the last of these events, in spring 2005, was managed to promote seedling recruitment by drawing down flow releases from Alamo Dam at a rate of approximately 0.5 $m^3s^{-1}day^{-1}$, subsequently resulting in the widespread establishment of riparian seedling patches initially

co-dominated by tamarisk and willow, some of which we subsequently monitored. In March 2006, a controlled flood was released from Alamo Dam in which discharge was ramped up to an instantaneous peak of 69 m^3s^{-1}, maintained at that peak for 7.5 hours, and then dropped and held at 56 m^3s^{-1} for two days, followed by a gradual drawdown of approximately 1 $m^3s^{-1}day^{-1}$. Smaller pulse flow releases occurred in 2007 and 2008 (Table 1). In 2010, another El Niño year in which inflows to Alamo Lake were large, the highest-magnitude, longest-duration flood since 2005 was released (Table 1).

Flows at the downstream end of the BWR were lower than those released from Alamo Dam during these floods as a result of infiltration and associated flow attenuation within Planet Valley and other alluvial valleys. Flows measured downstream of Planet, at the BWR near Parker, AZ gauge (# 09426620), were most similar to those measured at Alamo when antecedent water-table levels in Planet Valley were high and flood durations were longer (e.g., 2005, 2006, 2010). In contrast, when antecedent water levels were low and/or flood durations were short (2007 and 2008), flood peaks were substantially attenuated in downstream portions of the BWR. For example, peak flows measured at Parker were 19% and 2% of the upstream peaks in 2007 and 2008, respectively (Table 1).

The magnitude and duration of the releases were constrained by water availability, dam release capacity, and concerns over potential impacts to other downstream land and water management interests. Consequently, the events were small compared to historic floods on the BWR (Figure 2). These events were substantial, however, when considered within the context of the post-dam hydrologic regime; the 2005 event was the largest since dam construction. The observed flood releases were timed to overlap with the seed-release period of willow and cottonwood, although tamarisk also releases seed concurrently with willow on this river system [*Shafroth et al.*, 1998].

Table 1. Summary of high-flow characteristics for 2005 - 2010 flood releases from Alamo Dam on Bill Williams River, AZ, based on measurements at the Alamo gauge, immediately downstream of Alamo Dam (USGS #09426000), and the Parker gauge, 50 km downstream (BWR near Parker, AZ, # 09426620)

Date[a]	USGS Gauge	Peak magnitude (m^3s^{-1})	Duration (hrs)
21 February 2005	Alamo	205	Multi-day[b]
	Parker	208	
14 March 2006	Alamo	69	7.5[c]
	Parker	66	
9 April 2007	Alamo	29	16
	Parker	5.1	
31 March 2008	Alamo	65	8
	Parker	1.6	
7 March 2010	Alamo	85	36[d]
	Parker	63	

a. Date of initial flood release from Alamo Dam, passage of peak at Parker gauge may differ
b. The peak magnitude reported for this event is a daily average. Flows remained > 100 m^3s^{-1} for approximately 3 weeks during this event
c. 69 m^3s^{-1} maintained for 7.5 hours, followed by 2 days at 56 m^3s^{-1}
d. 85 m^3s^{-1} maintained for 36 hours, followed by 56 m^3s^{-1} for 5 days

METHODS

We conducted a multi-year field campaign that combined measurements of vegetation, topography, bed sediment, and flood hydraulics in two study reaches (Figure 1, 3). The first reach is 18 km downstream from Alamo Dam and is referred to hereafter as the Rankin reach (after a nearby ranch). The second reach is 48 km downstream from the dam and is referred to as the Mineral reach (after a nearby ephemeral tributary, Mineral Wash). These reaches were selected for detailed study

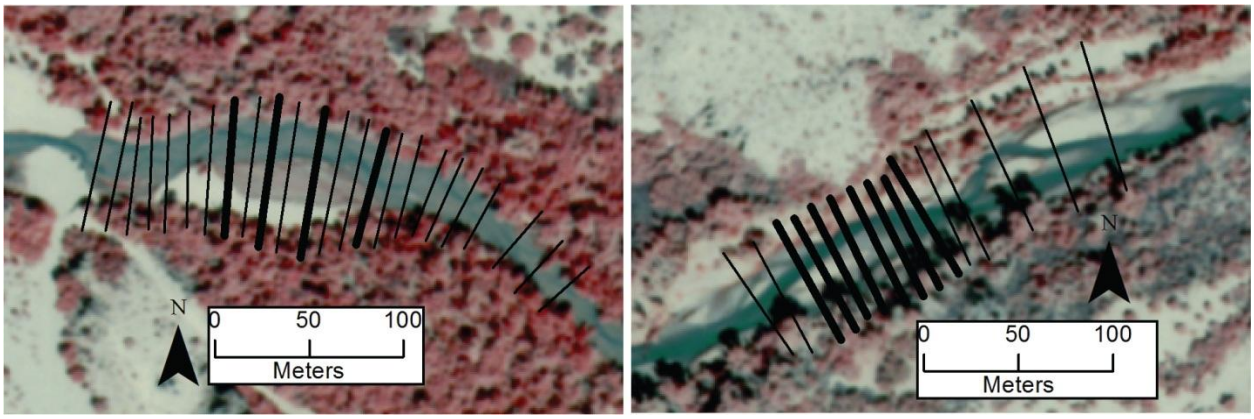

Figure 3. Mineral (left) and Rankin (right) study reaches (September 2005 aerial photographs), showing data collection transects. Topography was measured along all transects; grain size and vegetation data were collected along transects denoted with thicker line (grain size was also measured at upstream- and downstream-most transects). Flow is from right to left.

because of (1) the presence of bars with cohorts of seedlings that established on bare surfaces in 2005, as indicated by our observations during multiple field visits between November 2004 and February 2006, (2) differences in flow, sediment supply, and bed-material size, as a result of relative positions downstream from Alamo Dam, allowing assessment of spatial variations in ecogeomorphic interactions, and (3) access; these are among a small number of reaches of the BWR with road access.

Our field measurements focused on the 2006, 2007, and 2010 flood releases and their effects. Data collection among years varied as a function of the amount of advance notice we had for floods, personnel and equipment availability, and study objectives. Our most intensive data collection effort surrounded the 2006 event, which we used to investigate (1) differential seedling mortality among willow and tamarisk (the most frequently occurring species in our study plots) and associated changes in the size distribution of seedlings, (2) spatial variability in flood-induced changes in channel morphology and grain size, in relation both to the presence of vegetation and proximity of study reaches to Alamo Dam, (3) flood hydraulics. Elements of these analyses were continued for the 2007 and 2010 event, which, in combination with the 2006 flood, were used to study the evolution of vegetation-hydrogeomorphic feedbacks over a multi-year, multi-flood period. Whereas the 2006 and 2007 flood releases were planned well enough in advance to permit detailed pre-flood measurements, the 2010 flood was an El Niño-driven event with minimal advance notice.

Vegetation sampling

Starting in late February 2006, we sampled woody seedlings in 1 m^2 plots within belt transects aligned perpendicularly to the long axis of the sample bars. These transects align with the geomorphic surveys of cross-section topography and bed-material texture described below. At Mineral the plots were arrayed along four transects, spaced 20 to 30 m apart, ranging in width from 10 to 24 m, and distributed along one vegetated bar with a surface area of approximately 1500 m^2, as measured in ArcGIS (Figure 3). At Rankin the plots were arrayed along eight transects, spaced 10 m apart, ranging in width from 2 to 14 m, and distributed along two vegetated bars with surface areas of approximately 500 m^2 and 300 m^2 (Figure 3).

At the time of our first vegetation sampling effort, all woody plants in our study plots were less than one-year-old seedlings that established in association with the 2005 floods. Ninety percent of all measured woody seedlings were tamarisk, 9% were Goodding's willow, and < 1% were arrowweed or seep willow. Herbaceous vegetation cover in our plots was 5.9±9.8% at Mineral and 16.0±18.3% at

Rankin (mean±standard deviation). Sixty and 38 plots at Mineral and Rankin, respectively, contained seedlings of either tamarisk or willow at the beginning of our field study; approximately half of the study plots included both species. Within each plot, the diameter at the ground surface, total height, and species identity of every woody seedling were recorded, and stem density (# of woody plants per square meter). The same variables were measured in all plots ten weeks later (in early May 2006) following the March 2006 pulse flood.

In April 2007, we re-measured the same variables in all plots immediately before that year's flood release. Several days later, after the 2007 flood recession, we resurveyed stem density in all plots at Rankin; plant size was not resurveyed because the short time since the previous surveys precluded likely plant growth. At Mineral, because of flood attenuation and the previous year's aggradation, the vegetated study plots were not inundated by the 2007 event, so we did not complete post-flood vegetation surveys. Field measurements associated with the 2010 event (described below) did not include vegetation surveys because of time and personnel limitations.

We calculated seedling mortality as the change in the number of live stems in each plot (post-flood minus pre-flood stem density) associated with the 2006 and 2007 events. We equate stem-density reductions to mortality based the associated geomorphic mechanisms, as discussed below, and the absence of standing dead stems in our plots. We then completed several tests of the significance of these changes as a function of species (tamarisk versus willow), reach (Rankin versus Mineral), year (2006 versus 2007), and antecedent plant conditions. First, we completed a two-way ANOVA on species and reach for the 2006 data only (the test on differences between reaches was restricted to 2006 because we did not measure density changes in 2007 at Mineral). Second, using the Rankin data only, we completed a two-way ANOVA with species and year as factors. Third, to test the effects of drag associated with seedlings on observed stem-density differences, we added antecedent vegetation density [*Nepf*, 1999] as a covariate. Vegetation density, the projected plant area per unit volume (m^{-1}), can be approximated, treating plants as cylinders, as stem density times average stem diameter. In our case we calculated vegetation density as, for each plot: $(\text{stem density})_{\text{tamarisk}}*(\text{average diameter})_{\text{tamarisk}} + (\text{stem density})_{\text{willow}}*(\text{average diameter})_{\text{willow}}$. For plots with other woody seedlings (e.g., seep willow, arrowweed), this equation was modified accordingly. This approach neglects details of how plant architecture and flexibility influence drag but provides a reasonable approximation of vegetation drag [*Nepf*, 1999; also see *Kean and Smith*, 2005].

Stem-density-difference values included zeros (no change in density) and negative values, where stem density increased as a result of addition of flood-trained stems from upstream of the plot and/or burial of the main stem, leaving multiple secondary stems protruding from the ground surface. Because these negative values resulted from our methods rather than from real increases in the numbers of plants, we set them to zero for statistical tests. We applied a $\log_{10}(x+1)$ transformation to the density-difference values to better satisfy normality and homoscedasticity assumptions.

To compare the size distribution of seedlings before and after the 2006 flood and to test for significant differences, we performed two-sample Kolmogorov-Smirnov (K-S) tests on diameter and height. The K-S test is suited to comparing distributions and, as a non-parametric test, does not require normally distributed data. Quantile-quantile plots (not shown here) confirmed that seedling size for the stems sampled was not normally distributed.

Geomorphic change surveys

Topographic surveys of the Mineral and Rankin reaches were completed in 2006, 2007, and 2010 to measure flood-induced topographic changes and channel evolution. At the outset of our field campaign, in February 2006, we surveyed 23 and 15 cross sections in the Mineral and Rankin reaches, respectively, a subset of which contained the plots in which vegetation was sampled, as well as thalweg profiles. In May 2006, both reaches were resurveyed. We used Trimble Real Time Kinematic (RTK) GPS

units for these surveys. To characterize topographic change associated with the March 2006 event, we calculated differences in the average May (post-flood) versus February (pre-flood) bed elevation for each cross section. Calculations of elevation differences were performed for all portions of the bed inundated by the 2006 event (according to water surface elevation surveys at the flood peak) and for subsets of transects along our vegetated study bars. To gain additional insight into scour and fill dynamics, we deployed scour chains longitudinally along vegetation study bars in the two study reaches in February 2006 [see for example *Powell et al.*, 2006, for details on methods of interpreting scour chains].

We resurveyed topography along varying subsets of our cross sections, as well as longitudinal profiles, in subsequent years. Following the 2007 high-flow release, we resurveyed six cross sections in the Rankin reach using a Pentax PCS300 total station. Because of the substantial attenuation of the 2007 flood (Table 1), we did not resurvey topography at Mineral after this event. Before and after the 2010 flood, 13 and 15 cross sections were resurveyed in the Mineral and Rankin reaches, respectively, using RTK-GPS.

Bed sediment samples were collected before and after the 2006 flood to measure flood-induced changes in grain size, inter-reach differences, and the mediating effect of vegetation on grain size changes. We used a "can-on-a-stick" bulk sampler [*Edwards and Glysson*, 1999], which was suitable for the sand- and fine-gravel-dominated sediments in our study reaches, that penetrated to a depth of 7 cm and collected 0.4–1 kg of sediment per sample. Between 80 and 93 samples were collected in each reach during each sampling period at evenly spaced intervals along selected cross sections, some of which overlapped with our vegetation transects. All samples were dried and sieved at 1/2–ϕ intervals (from 0.063 mm to 32 mm) to determine grain size distributions.

For statistical comparisons, we composited grain size samples either by cross section, for unvegetated cross sections, or into unvegetated and vegetated portions of those cross sections that contained vegetation plots. This resulted in 56 composite samples (10 in Mineral, 18 in Rankin, measured both before and after the 2006 event). For each of these, we calculated the D_{50} and the fraction of the composited sample mass within five grain size categories: >8mm ($\phi<-3$), 2–8 mm ($-3<\phi<-1$), 1–2 mm ($-1<\phi<0$), 0.5–1 mm ($0<\phi<1$), and 0.0625–0.5 mm ($1<\phi<4$); the categories that encompass a smaller range of ϕ classes are those in which bed materials are most prevalent on the BWR. We first tested whether the 2006 flood produced a change in grain size distributions using two-way ANOVAs, with D_{50} and fraction of sample mass within grain-size categories as response variables and time (pre- versus post-flood) and reach (Rankin versus Mineral) as factors. We then calculated the post-flood minus pre-flood difference in grain size (for D_{50} and within each of the size categories), and using these differences as response variables, we applied a linear model with reach and vegetation (vegetation versus no vegetation along transects) as factors. We also represented vegetation as a continuous variable, using the average pre-flood stem density along the transect (0 for unvegetated transects) as a covariate, but this did not change results compared to using vegetation as a categorical variable. Tests for autocorrelation of grain size responses among transects, using the acf function in R, showed that autocorrelation was not significant for lag=1 (i.e. among adjacent transects) and therefore did not need to be accounted for in subsequent significance testing.

Flood hydraulics measurements

In addition to the surveys described above of pre- and post-flood ecogeomorphic characteristics, we also measured several components of high-flow hydraulics during our study floods. To determine the arrival time of floods released from Alamo Dam at Rankin, we deployed pressure transducers (in 2006 and 2010); in 2007 we visually recorded the arrival of the flood pulse at Rankin. These data were used to calculate the reach-average velocity for the 18 km between Alamo Dam and Rankin. Flood timing and duration at Mineral were largely inferred from the BWR near Parker gauge (<2 km downstream).

We also measured local velocities during the 2006 and 2007 floods along our study transects, including measurements within vegetation patches, at positions near (2 m from) the edge of patches, and at positions further away from (>4 m) patches. In 2006, we completed 15 velocity measurements (n=7 within, 4 near, 4 away from vegetation patches) at Mineral and Rankin, and in 2007, we completed 18 velocity measurement, 6 in each location type, at Rankin. We used a SonTek FlowTracker acoustic Doppler velocimeter, at 0.4 times the flow depth and recording for 40 seconds. Velocity samples were limited to wadeable areas; depths at measurement positions were 0.50±0.27 m (range of 0.2 to 1.2 m). Velocities did not vary significantly with the flow depth of the measurement position (p=0.09). To evaluate the effects of measurement proximity to vegetation patches on velocity, we performed two-way analysis of variance, where year (2006 and 2007) and location (in, near, and away from vegetation patches) were factors, and a Tukey HSD multiple comparison test was applied.

RESULTS

We observed differences in vegetation and geomorphic responses to flood releases both temporally, between the 2006, 2007, and 2010 events, and spatially, between our upstream (Rankin) and downstream (Mineral) study reaches. Evolution of vegetation and morphology are evident in repeat photographs of the study reaches (e.g., Figures 4 and 5) and are illustrated by the data presented below on seedling mortality, shifts in seedling size distributions, topographic and textural changes, and flood hydraulics.

Vegetation responses to controlled floods

Both the 2006 and 2007 floods caused substantial seedling mortality. Stem density reductions associated with the 2006 flood differed significantly between species (Figure 6) and reaches (Table 2). Pre-flood stem densities of tamarisk seedlings exceeded willow densities in both study reaches (Figure 6; $F_{1,143}$=96, p<0.001), but tamarisk experienced significantly greater flood mortality. The 2006 event produced 85% reductions in tamarisk density in both reaches, compared to reductions of 26% and 64%

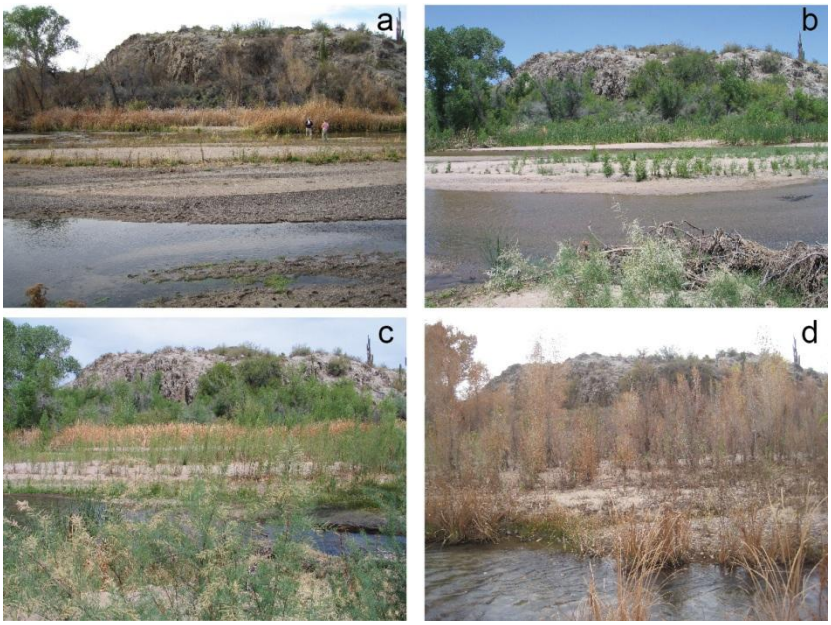

Figure 4. Repeat photographs of central portion of Rankin study reach, from left bank looking to north: (a) February 2006, (b) May 2006, (c) April 2007, (d) December 2010. Sequence illustrates lateral movement of bars, growth of seedlings that have survived floods, resilience of larger woody plants to floods, and presence of cattail (along far bank).

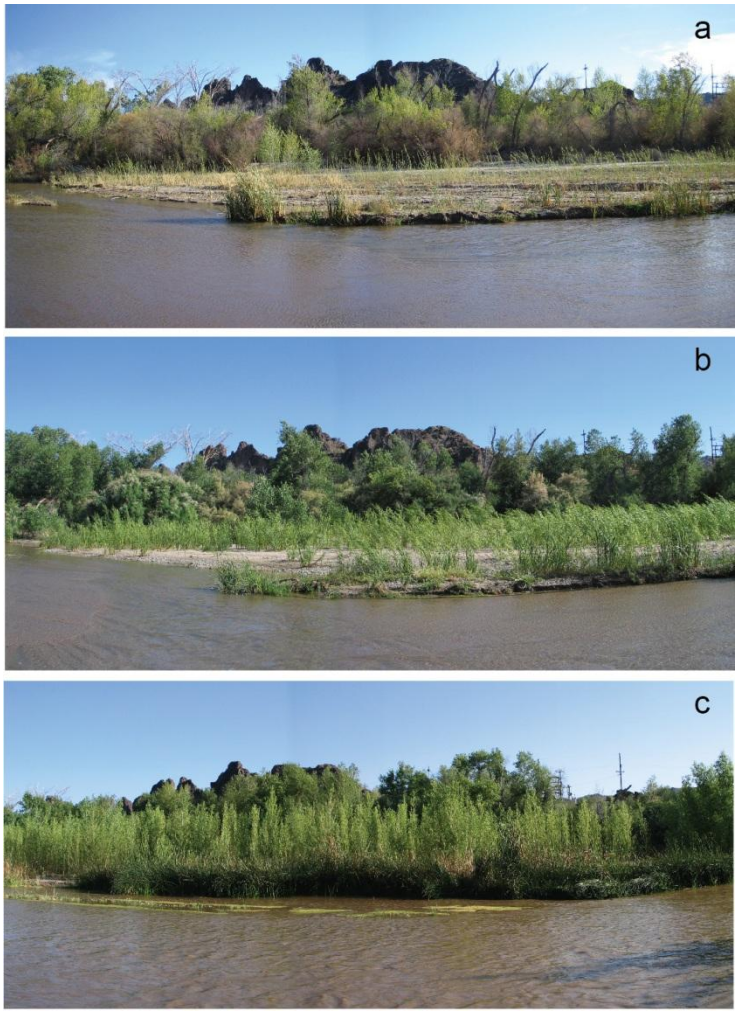

Figure 5. Repeat photographs of vegetation study bar in Mineral reach, looking from channel toward river left: (a) February 2006, (b) May 2006, (c) April 2007. Sequence illustrates growth of seedlings surviving floods and associated bar stabilization.

for willow seedlings in Mineral and Rankin, respectively. Tamarisk was eliminated from 33% of plots that originally contained tamarisk at Mineral and 30% at Rankin post-flood, whereas willow was eliminated from 17% of plots that originally contained willow at Mineral and 23% at Rankin. Flood-induced seedling mortality was limited to low-elevation bars in the active channel (<1m above the thalweg); no changes were observed on higher vegetated surfaces.

Measurements completed before the 2007 event indicated differences in vegetation evolution since 2006 between reaches. At Rankin, stem densities of both willow and tamarisk had increased since the post-2006 event measurements (Figure 6), suggesting that some new colonization and resprouting had occurred in this reach. Whereas willow densities exceeded pre-2006 levels (at Rankin), tamarisk densities did not. At Mineral, in contrast, stem densities showed little change since the post-2006 measurements, suggesting that new colonization or resprouting had been minimal.

Stem-density reductions associated with the 2007 event were significantly lower than in 2006 (Table 2). As in 2006, flood-induced mortality was greater for tamarisk than willow (Table 2, Figure 6), which continued the trend of an increase in the ratio of willow to tamarisk, from 0.07 at the beginning of the study period (pre-2006) to 0.55 after the 2007 event. The 2007 event did not inundate study plots in the lower (Mineral) reach, and field observations confirmed that plant mortality was minimal at Mineral.

We found that, for both the 2006 and 2007 events, antecedent vegetation density (projected plant area per unit volume; mean±sd=0.1±0.09 m^{-1} in Rankin, 0.06±0.05 m^{-1} in Mineral) had highly significant effects on flood-induced mortality (Table 2).

Table 2. Results of statistical tests of flood-induced reductions in stem density as a function of species (tamarisk, willow), reach (Rankin, Mineral), year (2006, 2007), and antecedent vegetation density (stem density * stem diameter).

Model	Factor	Degrees of freedom	Sum of squares	Mean square	F value	P value
2006[a]	Species	1	79.4	79.4	138.6	<0.0001
	Reach	1	5.4	5.4	9.4	0.003
	Vegetation density	1	43.2	43.2	75.4	<0.0001
	Species*vegetation density	1	14.4	14.4	25.4	<0.0001
	Residuals	101	57.9	0.57		
Rankin[b]	Species	1	35.4	35.4	30.9	<0.0001
	Year	1	7.2	7.2	6.3	0.014
	Vegetation density	1	22.7	22.7	19.8	<0.0001
	Residuals	73	83.6	1.1		

a. Species*reach, reach*vegetation density interactions not significant
b. Two-way interactions not significant

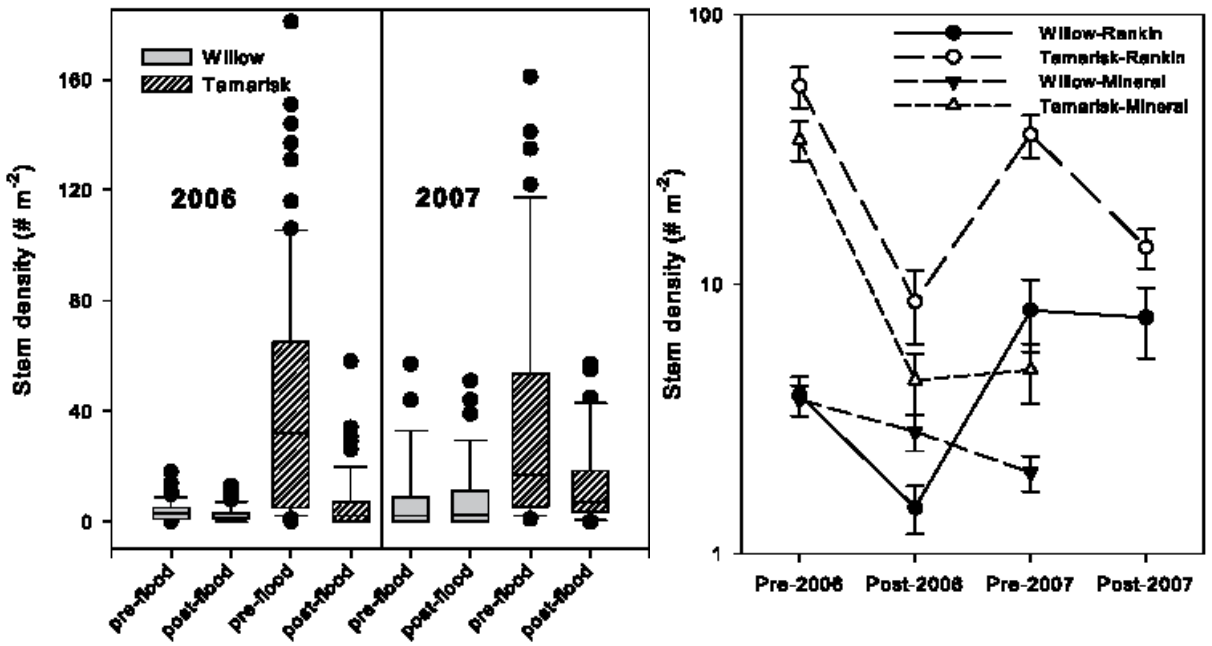

Figure 6. Stem densities of willow and tamarisk before and after 2006 and 2007 floods. Left panel shows distributions of measured densities, with 2006 data from Rankin and Mineral combined and 2007 data from Rankin only (boxes bound 25th and 75th percentiles, solid lines in boxes illustrate medians, and whiskers bound 10th and 90th percentiles). Right panel shows mean and standard error of stem densities, differentiated among species and reaches. Densities for post-2007 in Mineral were not measured because the 2007 event did not inundate vegetation plots in that reach.

The average diameter and height of willow seedlings was 2–5 times greater than tamarisk during all field measurement periods (Figure 7). These seedlings were recruited during the 2004–2005 floods and thus show very high growth rates. By the time of the 2007 event, vegetation that had established in 2005 and survived the 2006 event had grown sufficiently (Figure 4c, 5c, 7) to mediate the geomorphic effects of that event and to in turn influence flood-induced seedling mortality (antecedent vegetation density=0.12±0.08 m^{-1}). This dynamic, whereby seedlings surviving one flood grow and produce greater drag in subsequent floods, continued in the 2010 event, as discussed further below. Comparison of histograms of plant height between survey periods illustrates flood effects on vegetation structure, whereby the greatest mortality occurred among seedlings <40 cm in height and <4 mm in ground diameter, as evidenced by a dramatic reduction in the numbers of those smaller plants (Figure 8). In contrast, plants >70 cm in height and >6 mm in diameter showed little change as a result of flooding. Two sample K-S tests show that the shift in seedling size distributions associated with truncation of smaller sizes was significant for the 2006 flood ($p<0.001$ for both diameter and height; $D=0.47$ for diameter and $D=0.49$ for height, where D is a test statistic describing the maximum distance between the pre- and post-flood distribution functions). These results suggest a threshold of plant resistance to flooding for these events and antecedent conditions.

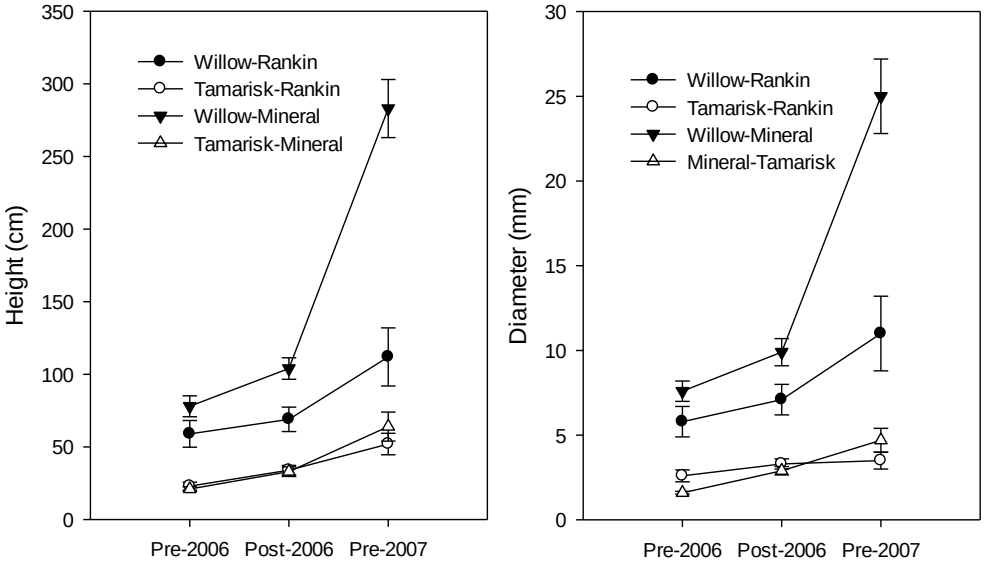

Figure 7. Seedling height and diameter (mean and standard error) measured in February 2006 (pre-flood), May 2006 (post-flood) and April 2007 (pre-flood), for willow and tamarisk, in Rankin and Mineral study reaches. Because vegetation measurements following the 2007 event were taken within one week of the pre-flood measurements, a time period in which minimal plant growth would have occurred, diameter and height were not measured after the 2007 event.

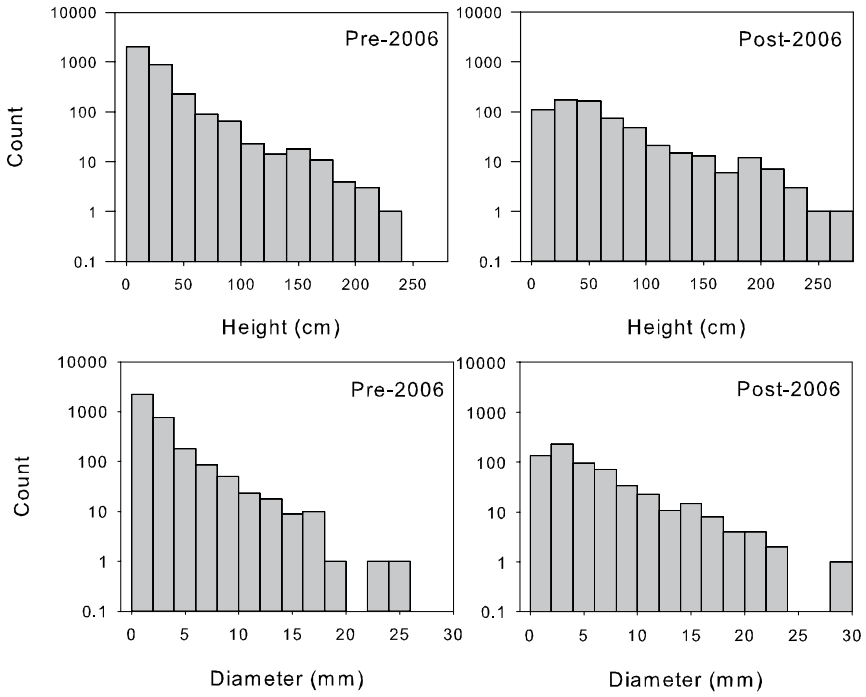

Figure 8. Histograms of plant heights (top) and diameters (bottom) measured in February and May 2006, before and after the 2006 flood, with reaches (Mineral and Rankin) and species (tamarisk and willow) combined. Data are based on repeat measurements of the same study plots. The histograms illustrate size-dependent mortality during the 2006 flood, primarily occurring among plants <40 cm in height and <4mm diameter.

Flood-induced geomorphic changes

Despite similar bed gradients (0.0028 in Rankin, 0.0026 in Mineral), the two study reaches experienced different geomorphic responses to floods, which in turn contributed to the different vegetation responses described above. In the reach closer to the dam (Rankin), the 2006 flood caused scour and shifting of bars and changes in the position of the base flow channel. Along our 15 cross sections, local erosion and deposition offset each other laterally, such that the average of post-flood minus pre-flood elevations was small (ΔZ=0.09±0.04 m; range=0.02–0.14 m). Of our two vegetation sample bars in the Rankin reach, the upstream one that supported the majority of seedlings surveyed pre-flood was scoured and trimmed (ΔZ= -0.09±0.09 m for vegetation transects along this bar, e.g., cross section 90 in Figure 9) such that only a narrow line of vegetation remained. On the downstream bar, net elevation change was limited (ΔZ= 0.05±0.09 m for vegetation transects along this bar, e.g., cross sections 30 and 50 in Figure 9), even in areas with substantial reductions in stem density. Scour chains that were recovered indicated mean scour depths of approximately 0.3 m on the bar surface and subsequent fill. Some of the scour chains could not be relocated, possibly as a result of deeper scour.

In the Mineral reach, we observed differences in topographic response between vegetated and unvegetated areas of the bed (Figure 5, 9). In February 2006, our sample bar had two distinct levels: a lower, vegetated surface bordering the channel, and a higher unvegetated surface (e.g., cross sections 70, 90, and 110 in Figure 9). Surveys after the 2006 flood showed aggradation on the lower, vegetated surface of the bar (ΔZ= 0.20±0.11 m for vegetated portions of 8 cross sections; range =0.07–0.33 m). This aggradation buried smaller seedlings and produced the mortality described above. The upper surface of the bar changed little, such that the vegetated and unvegetated surfaces had similar post-

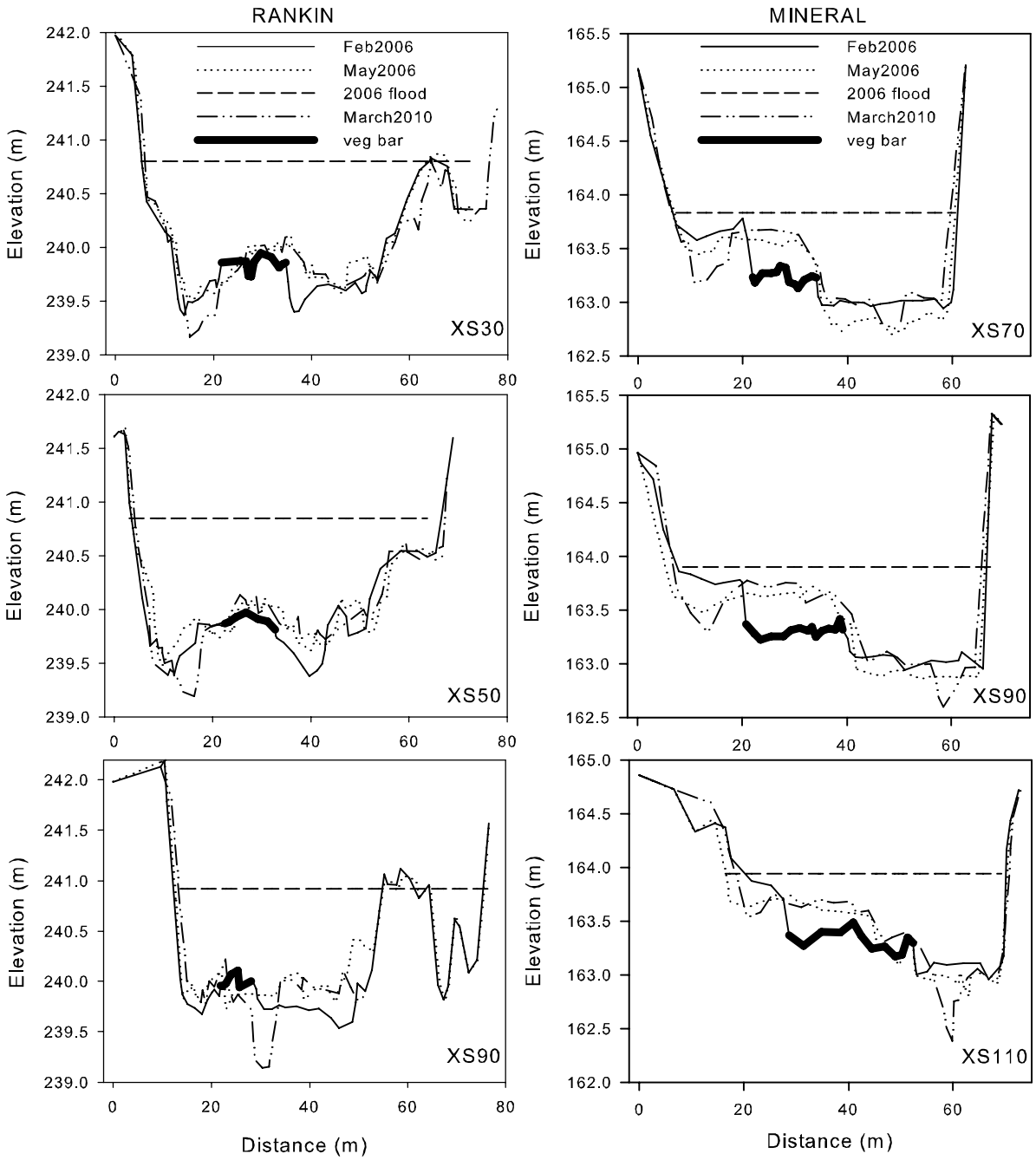

Figure 9. Changes in morphology across study period (February 2006, May 2006, March 2010) for representative cross sections: Rankin 30,50,90 (left) and Mineral 70,90,110 (bottom). Cross section numbers refer to their distance in meters from downstream end of study reach. Water surface elevation for 2006 flood and location of vegetation transects within cross sections (veg bar) also shown. These plots illustrate lateral shifting, aggradation, and/or degradation resulting from flood-induced scour or deposition along low-elevation portions of cross sections.

flood elevations but were perched higher above the low-flow channel (Figure 5, 9). This difference in relative elevation was exacerbated by incision of the low-flow channel bed adjacent to the vegetated sample bar (ΔZ= -0.13±0.03 m for the same 8 cross sections noted above). Aggradation of the vegetated portion of the bar and channel incision were offsetting in terms of average elevation change in the Mineral reach (ΔZ= -0.06±0.04 m for 24 cross sections).

The 2007 flood produced only limited geomorphic changes in the Rankin reach (ΔZ=0.04±0.04 m, for the average of post-2007 cross section measurements minus May 2006 surveys). As noted above, the 2007 event had almost entirely attenuated by the time it arrived at Mineral and therefore did not alter channel morphology there.

The 2010 flood, despite being the largest of the 2006–2010 period (Table 1), produced little topographic change. Cross section surveys documented small amounts of localized scour and fill (e.g., Figure 9) but no reach-wide patterns of net topographic change (ΔZ=0.02±0.06 m, for the average of post-2010 minus pre-2010 cross section elevations in Rankin). In both reaches the larger magnitude of the 2010 flood was offset by the increases in vegetation size and density, limiting its geomorphic effectiveness.

An additional source of geomorphic change during the latter years of our study period was the expansion of beaver, especially in the Rankin reach. Beaver activity produced variability in longitudinal profiles, with dams and impoundments producing up to 1.2 m-high steps in the profile by 2010 in Rankin (Figure 10). In both reaches, thalwegs were more entrenched relative to surrounding bars by 2010 compared to February 2006, in part as a result of beaver activity (Figures 9 and 10).

Neither reach experienced changes in active channel width in any of the floods. Bank erosion potential is limited in these reaches by vegetation, including armoring of steeper banks by mats of arrowweed and energy dissipation by dense, near-bank stands of cattail. Early in the study period the effects of these species were confined to the banks (in the case of arrowweed) and within a few meters of the banks (in the case of cattail; e.g., Figure 4), although cattail had expanded further into the channel by 2010.

With respect to bed-material size, bed sediments at Rankin are coarser than at Mineral throughout their size distributions (Figure 11). At the beginning of the study period D_{50} values averaged over each reach were 2.7 and 0.7 mm in Rankin and Mineral, respectively. The Rankin reach includes many gravel lenses and patches, whereas bed sediments were more unimodal in the coarse sand range in Mineral (Figure 11). Initial (pre-flood) differences in D_{50} between vegetated and unvegetated portions of transects were not significant ($F_{1,25}$=0.4, p=0.5), although fractions of finer sediments (0.0625–0.5 mm) were higher in vegetated transects. The 2006 event did not produce significant changes in grain sizes, in either D_{50} or fraction of sample mass within different size categories. Tests of how post-flood minus pre-flood difference in grain size varied among reaches and as a function of vegetation found that these factors were not significant for D_{50} and most size categories. The post-flood minus pre-flood fraction within the fine tail of grain size distributions (0.0625–0.5 mm) did show significant variation between reaches ($F_{1,25}$=7.1, p=0.013) and between vegetated and unvegetated transects, with the reduction being greater in unvegetated than in vegetated areas ($F_{1,25}$=9.5, p=0.005).

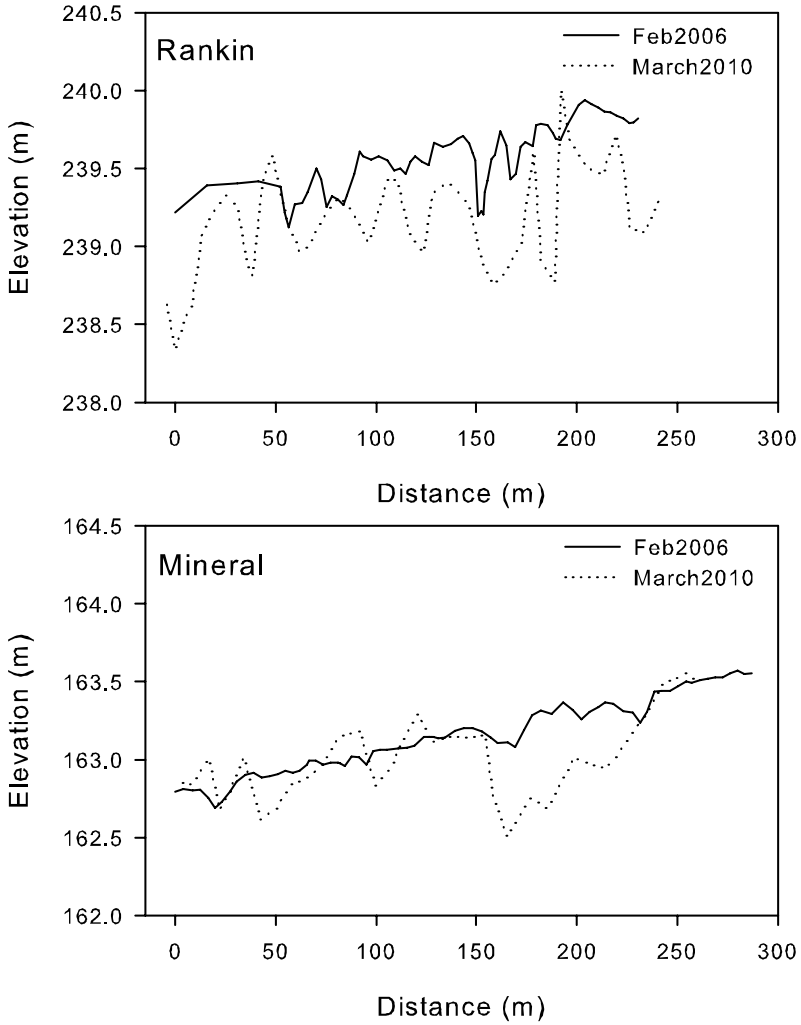

Figure 10: Longitudinal profiles of Rankin (top) and Mineral (bottom) study reaches at start (February 2006) and end (March 2010) of study period, where 0 on the x-axis is the downstream end of each study reach.

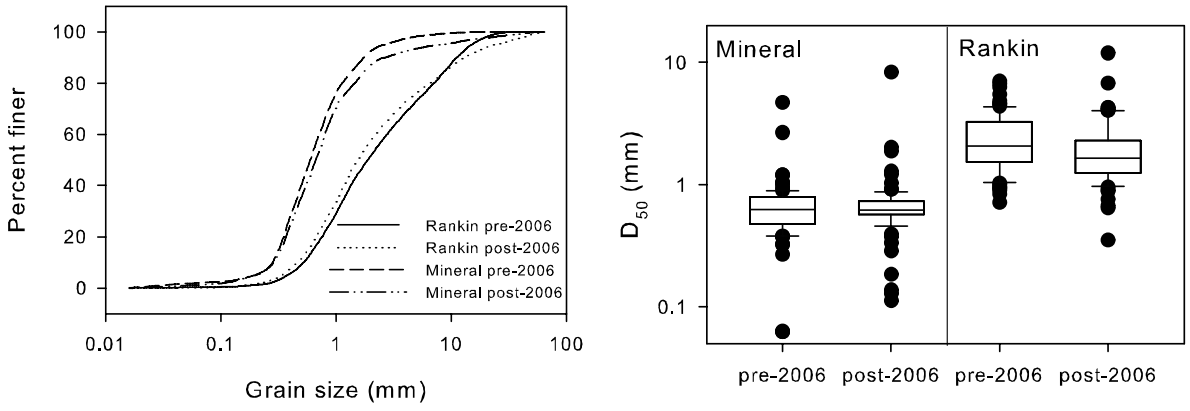

Figure 11. Grain size data from Rankin and Mineral before and after 2006 flood: left panel shows size distributions of composited bulk samples, and right panel shows median grain size (D_{50}) for all samples.

Flood hydraulics

Velocity data collected at multiple scales provides evidence of vegetation effects on flow conditions during BWR floods. Velocities averaged over the 18 km reach between Alamo Dam and our upstream reach for the 2006, 2007, and 2010 events, based on the time between flow releases at the dam and arrival at Rankin, were 0.8, 0.6, and 0.5 m s^{-1}, respectively (Figure 12). These velocities do not show the expected relationship with Q (i.e., hydraulic geometry would suggest a power-law relationship with a positive exponent). We attribute this discrepancy to the increasing height and density of both woody seedlings and cattail, from 2006 when plants were small and sparse to 2010 when vegetation was dense and tall. Although we did not quantitatively survey vegetation in the 18-km reach between Alamo Dam and the Rankin reach, field and aerial photo observations show a similar pattern in the 18-km reach as in our Rankin reach: a steady increase in the size and density of both woody plants and cattail from 2006 to 2010. The lag between peaks of the different flood events at the Alamo and Parker gages shows similar patterns as those outlined above. However, flood travel times and attenuation between Alamo and Parker are affected by not only changes in vegetation density and size, but also by surface water-groundwater interactions.

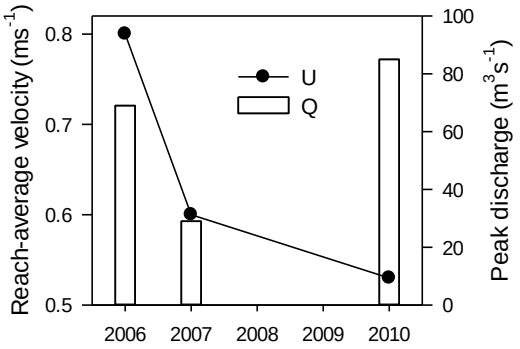

Figure 12. Velocities averaged over the 18-km reach from Alamo Dam to the Rankin reach, based on the time between flow releases at Alamo (from USGS gauge data) and their arrival at Rankin (from pressure transducer and/or visual records); right axis shows corresponding peak discharges released at Alamo. The pattern reflects increasing vegetation drag.

Velocity data collected in and around vegetation patches showed a significant 2-way interaction between year and measurement location ($F_{2,27}$=6.7, p=0.004), indicating that the magnitude of the location effect (within, near, or away from vegetation patches) depended upon year. Pairwise comparisons among factors showed that in 2006, differences were not significant at α=0.05 among velocities within, near, and away from vegetation patches ($\bar{u}$=0.90±0.35 m s^{-1}, 0.87±0.27 m s^{-1}, and 0.74±0.12 m s^{-1} within these three groups, respectively). In 2007, however, velocities were significantly lower (at α=0.05) within vegetation patches ($\bar{u}$=0.67±0.26 m s^{-1}) than in positions near vegetation ($\bar{u}$=1.0±0.22 m s^{-1}) and away from vegetation ($\bar{u}$=1.3±0.13 m s^{-1}).

DISCUSSION

Ecogeomorphic feedbacks

Our observations illustrate an evolution of the strength and nature of vegetation-morphodynamic feedbacks between 2005 and 2010. Early in the study period, one-way effects of hydrogeomorphic processes on vegetation were evident. The 2005 floods reset channel form, scoured

vegetation from the active channel, and resulted in recruitment of a cohort of new pioneer vegetation. The 2006 flood, although much smaller than the 2005 floods, encountered a river system with only small seedlings in the active channel (Figure 4a, 5a). As a result, the 2006 flood was geomorphically effective, exceeding sediment transport thresholds, producing associated channel change by scour or aggradation, and causing vegetation mortality. Evidence of vegetation feedbacks was mixed for the 2006 event. On the one hand, antecedent vegetation density strongly influenced seedling mortality, and aggradation occurred in vegetated portions of the Mineral reach but not in unvegetated areas. On the other hand, vegetation effects on local (ADV-measured) velocities and grain size changes were not significant for this event.

The survival of some seedlings in the 2006 event and their subsequent growth, combined with new recruitment, strengthened vegetation effects on channel morphology and later flows. Although the small size of the 2007 flood makes it difficult to tease out influences of hydrogeomorphic processes on vegetation and vice versa for this event, our observations of flood-induced mortality of small seedlings (as in 2006) but persistence of larger plants, limited geomorphic change, and significant vegetation effects on local velocities are suggestive of increasingly bidirectional vegetation-hydrogeomorphic effects. By the time of the 2010 flood, vegetation was large and dense enough to have been relatively insensitive to scour and burial. The competitive advantage shown by willow in the 2006 and 2007 events persisted; the willow that recruited in 2005 and survived the 2006 event were many meters high as of late 2010 (e.g., Figure 4d). Moreover, cattail density greatly increased along the BWR after 2007. The net effect of increases in cattail density and larger woody seedlings was to produce substantial drag that mediated the geomorphic effectiveness of the 2010 event, which caused minimal topographic change despite its 30% larger magnitude than the 2006 flood.

Corenblit et al.'s [2007] conceptual model describing the temporal evolution of feedbacks between hydrogeomorphic processes and riparian vegetation applies well to the BWR. The 2005 floods triggered a "geomorphic phase" in which the effect of vegetation on channel form was limited. The period surrounding the 2006 floods corresponded to a "pioneer phase"; pioneer vegetation was present but small enough to have limited feedback effects. Seedlings that survived the 2006 event then shifted the system toward an "ecogeomorphic" phase by the time the 2007 flood occurred, with more bidirectional vegetation-hydrogeomorphic effects. Observations of the 2010 flood suggest that by then the system had moved toward a phase in which vegetation strongly influences physical processes, analogous to the fourth stage described by *Corenblit et al.* [2007]. Transitions among these phases may be especially rapid in the BWR because of how the dam elevates base flows and vegetation growth rates.

The trend of increasing biotic influences in the absence of large floods has not been restricted to vegetation; beaver activity has also expanded substantially in the BWR [*Andersen and Shafroth*, 2010; *Andersen et al.*, 2011]. These conditions will likely persist until a large flood (analogous to the 2005 floods) can scour cattail and other vegetation, remove beaver dams, induce avulsion, or otherwise reset the system. The observed cattail encroachment and expansion of beaver highlight several other complexities of ecogeomorphic feedbacks, including the influence of shifts in the composition of the vegetation community and the potentially significant role of non-woody (but dense and stiff) vegetation.

Our observations also illustrate how feedbacks can vary spatially. The mechanism of density reductions differed longitudinally (between reaches) as a result of geomorphic processes (aggradation-induced burial versus scour) and flood attenuation, helping explain differences in response between sites. In the Mineral reach, aggradation of the vegetation study bar produced by the 2006 flood increased the elevation difference between the bar and the base flow channel, perching the bar above the water surface elevation of the 2007 event. Seedlings that survived the 2006 aggradation were those that were tall enough not to have been buried; although we expected resprouting of buried seedlings, we did not observe this. In contrast, in the Rankin reach, erosion of the bed and low-elevation bars

removed seedlings. This highlights the legacy effects of geomorphic changes caused during one flood on the morphodynamics of subsequent events.

The effects of the flows we observed were limited in lateral extent, such that flow forces exceeded thresholds for bed erosion and seedling mortality within the active channel but did not erode banks. Banks along our study reaches, although rich in sand and therefore lacking the cohesion of more clay-rich banks, are armored by vegetation that produces drag and focuses flow energy along the bed of the active channel. This vegetation growth along banks, which has been facilitated by dam-related flow reductions, shifts the threshold for bank erosion and channel widening to larger flood events and results in a scaled-down, equilibrium channel form compared to the pre-dam condition. Other studies from the region have evaluated relationships between vegetation, bank strength, and floods. In Canyon de Chelly, AZ, an undammed system where tamarisk removal occurred, the presence of clay in streambanks limited flood-induced widening [*Jaeger and Wohl*, 2011]. In contrast, flooding that followed tamarisk removal along the Rio Puerco, NM produced massive bank erosion [*Vincent et al.*, 2009].

Surface water-groundwater exchange dynamics also produce spatial variations in morphodynamics and their feedbacks with vegetation [e.g., *Webb and Leake*, 2006]. Discontinuities in surface flows during base flow conditions are common features in arid and semiarid rivers [*B R Davies et al.*, 2009], but gain or loss of surface water to groundwater can also alter high flows and associated sediment dynamics. The attenuation of high flows by Planet Valley, and associated flow differences between the upstream (Alamo) and downstream (Parker) gauges in the BWR (Table 1), illustrate linkages among routing of high flows, antecedent water-table levels, and flood duration. The resulting variations in geomorphic and vegetation changes among our upstream and downstream reaches highlight how releases from dams can have vastly different downstream effects as a result of flow losses.

Implications for flow management

Our study is representative of the type of large-scale flow experiments discussed by *Konrad et al.* [2011], encompassing both manipulative elements, in which we provided input to the nature and timing of flow releases and measured specific biological and physical responses, and mensurative elements, in which we measured system responses over a longer time period reflecting the effects of a suite of high and low flows. The results presented above show that sequenced flood pulses favor native willow seedlings over non-native tamarisk by causing differential levels of mortality and thus increasing the relative density of willow over tamarisk. This complements findings elsewhere that increases in relative density of cottonwood seedlings over tamarisk seedlings provide cottonwood with a competitive advantage [*Sher et al.*, 2000; *Sher et al.*, 2002] and that cottonwood seedlings can outcompete tamarisk seedlings following mechanical manipulations [*Bhattacharjee et al.*, 2009]. This flood-induced change in seedling composition, combined with the much larger size of the willow plants, increases the likelihood that willow will outcompete tamarisk and dominate these sites, provided water availability remains high [*Stromberg et al.*, 2007].

This result suggests that under certain conditions, flow releases that scour or bury tamarisk seedlings before they are well established can be an effective tool to provide native taxa with a competitive advantage over tamarisk. Such scour-oriented flow releases, combined with flow management intended to promote establishment of native vegetation [*Mahoney and Rood*, 1998], could be an addition to the suite of tools used to manage tamarisk and restore native riparian vegetation [*Rood et al.*, 2005; *Shafroth et al.*, 2005; *Shafroth et al.*, 2008; *Merritt et al.*, 2010]. Flow releases to scour tamarisk would have a limited time window before tamarisk became large enough to withstand scour. For example, floods in ephemeral channels in semi-arid southeast Spain that killed herbaceous vegetation and small shrubs did not cause mortality of tamarisk and other trees [*Sandercock and Hooke*, 2010], in agreement with other studies documenting the resilience of tamarisk to floods [e.g., *Graf*, 1978]. Our data on the change in the size distribution of plants caused by floods suggests that tamarisk

are especially susceptible to scour at heights <40 cm in height and <4 mm in diameter, although this threshold of plant height versus scour potential will vary as a function of flood discharge and local hydraulic conditions, including drag associated with larger plants.

In sand-bed rivers such as the BWR, even small managed flood releases can achieve geomorphic work of erosion, deposition, and morphologic change in the active channel. Because these processes set the template for many ecosystem processes, this geomorphic work can therefore make the floods ecologically effective along low-elevation bars in the active channel. Sand-bed rivers have been termed "labile" [*Church*, 2006] because thresholds for mobilization of bed material and sediment transport are easily exceeded. In gravel-bed rivers, in contrast, bed materials are close to mobilization thresholds during bankfull events and larger floods are typically needed to affect channel change [e.g., *Church*, 2006]. For example, in the Trinity River, CA, another dammed river where managed high-flow releases have been used to achieve downstream objectives, even relatively large (greater than bankfull) floods are unlikely to fully mobilize the bed [*May et al.*, 2009].

Beyond the active channel, however, small managed floods are unlikely to cause geomorphic and vegetation changes because of both limited lateral inundation extents and the ratchet effect of vegetation along channel banks. Managed flood releases are therefore only effective for achieving ecosystem goals in the scaled-down context of the active channel rather than the entire valley bottom [*Stillwater Sciences*, 2002]. In contrast, using flows to achieve objectives such as floodplain scour, triggering avulsions, and other forms of channel reorganization that occur under reference conditions [*Trush et al.*, 2000] is not likely to be feasible in most dammed rivers. This limitation has implications for vegetation community structure on floodplains [*Lytle and Merritt*, 2004].

Our results illustrate how the geomorphic and ecological effectiveness of a given flood event is dependent not only on the flood magnitude and duration, but also on the recent sequencing of high-flow events. Although literature on geomorphic hydrology recognizes the importance of recent flood history [e.g., *Kochel*, 1988], discussions of the attributes of flow regimes that influence aquatic ecosystems [e.g., *Poff et al.*, 1997] typically do not address sequencing. Sequencing of flood pulses can influence the establishment dynamics and evolution of vegetation communities. Releasing pulses in consecutive years, even if they are relatively small, can provide a competitive advantage to natives and prevent choking of the active channel with vegetation. In contrast, periods of extended base flow without floods, especially in systems where base flow is elevated above natural levels by dam releases, can allow vegetation encroachment in the active channel [*Shafroth et al.*, 2002]. High base flow releases designed to benefit target native species (e.g., cottonwood and willow) can have unintended consequences by benefitting non-target species (e.g., beaver and cattail).

Flood releases can have substantial downstream variations in effectiveness. Such longitudinal variations have been previously considered with respect to the effects of tributary inputs on water and sediment, which can reduce imbalances in sediment supply and transport capacity caused by dams [*Schmidt and Wilcock*, 2008]. Groundwater dynamics and vegetation characteristics can also greatly influence the downstream effects of a given flood release, as discussed above, highlighting a challenge of prescribing a single flow out of a dam for a long reach of river and the need for variability in flow prescriptions.

An open question in the BWR and other dammed rivers is how reductions in sediment supply (1) influence vegetation and its feedbacks with morphodynamics and (2) should be factored into controlled flood releases. The influence of sediment supply on fluvial processes is a fundamental tenet of fluvial geomorphology [*Parker*, 2004; *Schmidt and Wilcock*, 2008] that has been underlined by research on controlled flood releases on the Colorado River through Grand Canyon [*Hazel et al.*, 2006; *Wright et al.*, 2008; *Melis et al.*, 2012]. Manifestations of reduced supply in dammed rivers, such as coarsening of bed material and incision, are well documented [e.g., *Williams and Wolman*, 1984], but their effects on vegetation are not. Dam-induced coarsening could influence vegetation both by altering the capacity of

substrates to retain moisture and by increasing the critical shear stress of bed materials, thus reducing the frequency of bed (and seedling) scour. Vegetation, in turn, by altering drag and sediment deposition, can mediate relationships between sediment supply, flow, and bed material size. In the BWR, effects of supply limitation are evident immediately downstream of Alamo Dam, where the channel is coarse (gravel-cobble, compared to sand in upstream reaches) and incised several meters below its floodplain, but the downstream extent and ecosystem implications of such changes are uncertain [*Dekker*, 2012]. Sediment transport monitoring and sediment budget construction would provide further insight into how dam-induced changes in sediment supply may influence the erosional effects of floods and vegetation dynamics and, in turn, into how sediment supply should be accounted for in planning managed flow releases in dammed rivers.

CONCLUSIONS

We observed spatial variations in mechanisms of seedling mortality and temporal variations in the strength and direction of vegetation-morphodynamic feedbacks and associated responses to managed floods. Our results illustrate how the effect of floods or other components of hydrologic regimes on riparian vegetation are mediated by geomorphic processes on both a reach scale, where coupled vegetation and geomorphic characteristics influence scour and deposition, and on a basin scale, where spatial variations of flow and sediment supply may have important influences on morphologic and vegetation responses. Our finding that controlled flood releases caused differential mortality of native willow versus nonnative tamarisk illustrate the potential to manage streamflow to influence riparian vegetation dynamics, including establishment and mortality of native versus alien species. Our investigations suggest that in sand-bed rivers, even small flood releases can affect ecogeomorphic change, albeit at a reduced scale compared to larger natural floods. Our observations also show that the geomorphic and ecological effectiveness of flow releases varies longitudinally, with distance downstream, and as a function of antecedent conditions. Dam-released floods can provide both a means of achieving downstream ecosystem objectives and of conducting experiments to develop quantitative insights into relationships between morphodynamics and ecosystem processes.

ACKNOWLEDGMENTS

We thank Paul Kinzel, James Johnsen, Tom Bates, Doug Andersen, Donna Shorrock, Vanessa Beauchamp, Stan Culling, John Hickey, and Robert Pleszewski for field assistance; Jill Majerus and Matthew Gilbert for sediment sieving; and Brian Steele, Jonathan Nelson and Gregor Auble for guidance. We also thank Anne Lightbody, John Stella, and three anonymous reviewers for comments that greatly improved the manuscript. This work was funded by US Army Corps of Engineers, US Geological Survey, US Fish & Wildlife Service and National Science Foundation (EAR-1025076). A portion of this research was performed while the lead author held a National Research Council Postdoctoral Research Associateship at the U.S. Geological Survey's Geomorphology and Sediment Transport Laboratory in Golden, CO. Any use of trade, product, or firm names is for descriptive purposes only and does not imply endorsement by the U.S. Government.

REFERENCES CITED

Allred, T. M., and J. C. Schmidt (1999), Channel narrowing by vertical accretion along the Green River near Green River, Utah, *Geological Society of America Bulletin*, *111*(12), 1757-1772.

Andersen, D. C., and P. B. Shafroth (2010), Beaver dams, hydrological thresholds, and controlled floods as a management tool in a desert riverine ecosystem, Bill Williams River, Arizona, *Ecohydrology*, *3*(3), 325-338, doi: 10.1002/eco.113.

Andersen, D. C., P. B. Shafroth, C. Pritekel, and M. O'Neill (2011), Managed flood effects on beaver pond habitat in a desert riverine ecosystem, Bill Williams River, Arizona USA, *Wetlands*, *31*(2), 195-206, doi: 10.1007/s13157-011-0154-y.

Arthington, A. H., S. E. Bunn, N. L. Poff, and R. J. Naiman (2006), The challenge of providing environmental flow rules to sustain river ecosystems, *Ecological Applications*, *16*(4), 1311-1318.

Asaeda, T., and L. Rajapakse (2008), Effects of spates of different magnitudes on a Phragmites japonica population on a sandbar of a frequently disturbed river, *River Research and Applications*, *24*(9), 1310-1324, doi: 10.1002/rra.1128.

Asaeda, T., P. I. A. Gomes, K. Sakamoto, and M. H. Rashid (2011), Tree colonization trends on a sediment bar after a major flood, *River Research and Applications*, *27*(8), 976-984, doi: 10.1002/rra.1372.

Auble, G. T., and M. L. Scott (1998), Fluvial disturbance patches and cottonwood recruitment along the upper Missouri River, Montana, *Wetlands*, *18*(4), 546-556.

Bhattacharjee, J., J. Taylor, L. Smith, and D. Haukos (2009), Seedling competition between native cottonwood and exotic saltcedar: implications for restoration, *Biological Invasions*, *11*(8), 1777-1787, doi: 10.1007/s10530-008-9357-4.

Birken, A. S., and D. J. Cooper (2006), Processes of *Tamarix* invasion and floodplain development along the lower Green River, Utah, *Ecological Applications*, *16*(3), 1103-1120.

Braudrick, C. A., W. E. Dietrich, G. T. Leverich, and L. S. Sklar (2009), Experimental evidence for the conditions necessary to sustain meandering in coarse-bedded rivers, *Proceedings of the National Academy of Sciences*, *106*(40), 16936-16941, doi: 10.1073/pnas.0909417106.

Church, M. (2006), Bed material transport and the morphology of alluvial river channels, *Annual Review of Earth and Planetary Science*, *34*, 325-354.

Cleverly, J. R., S. D. Smith, A. Sala, and D. A. Devitt (1997), Invasive capacity of *Tamarix ramosissima* in a Mojave Desert floodplain: the role of drought, *Oecologia*, *111*(1), 12-18, doi: 10.1007/s004420050202.

Cooper, D. J., D. C. Andersen, and R. A. Chimner (2003), Multiple pathways for woody plant establishment on floodplains at local to regional scales, *Journal of Ecology*, *91*(2), 182-196.

Cooper, D. J., D. M. Merritt, D. C. Andersen, and R. A. Chimner (1999), Factors controlling the establishment of Fremont cottonwood seedlings on the upper Green River, USA, *Regulated Rivers-Research & Management*, *15*(5), 419-440.

Corenblit, D., E. Tabacchi, J. Steiger, and A. M. Gurnell (2007), Reciprocal interactions and adjustments between fluvial landforms and vegetation dynamics in river corridors: A review of complementary approaches, *Earth-Science Reviews*, *84*(1-2), 56-86, doi: 10.1016/j.earscirev.2007.05.004.

Davies, B. R., M. C. Thoms, K. F. Walker, J. H. O'Keefe, and J. A. Gore (2009), Dryland Rivers: Their Ecology, Conservation and Management, in *The Rivers Handbook: Hydrological and Ecological Principles, Volume Two* edited by P. Calow and G. E. Petts, pp. 484-511, Blackwell Science, Ltd, Oxford, UK.

Davies, N. S., and M. R. Gibling (2011), Evolution of fixed-channel alluvial plains in response to Carboniferous vegetation, *Nature Geoscience*, *4*(9), 629-633, doi: 10.1038/ngeo1237.

Dean, D. J., and J. C. Schmidt (2011), The role of feedback mechanisms in historic channel changes of the lower Rio Grande in the Big Bend region, *Geomorphology*, *126*, 333-349.

Dekker, F. J. (2012), Sediment dynamics in a dryland river: Grain-size variations, erosion rates, sediment mixing, and dam effects, MS thesis, 78 pp, University of Montana, Missoula, MT.

Dixon, M. D., M. G. Turner, and C. F. Jin (2002), Riparian tree seedling distribution on Wisconsin River sandbars: Controls at different spatial scales, *Ecological Monographs*, *72*(4), 465-485.

Edmaier, K., P. Burlando, and P. Perona (2011), Mechanisms of vegetation uprooting by flow in alluvial non-cohesive sediment, *Hydrology and Earth System Sciences*, *15*(5), 1615-1627, doi: 10.5194/hess-15-1615-2011.

Edwards, T. K., and G. D. Glysson (1999), Field methods for measurement of fluvial sediment, edited, Techniques of Water-Resources Investigations of the U.S. Geological Survey, Reston, VA.

Everitt, B. (1980), Ecology of saltcedar—A plea for research, *Environ. Geol.*, *3*(2), 77-84, doi: 10.1007/bf02473474.

Freeman, G. E., W. J. Rahmeyer, and R. R. Copeland (2000), Determination of resistance due to shrubs and woody vegetation, 62 pp, U.S. Army Corps of Engineers ERDC/CHL; TR-00-25, Washington D.C.

Friedman, J. M., and G. T. Auble (1999), Mortality of riparian box elder from sediment mobilization and extended inundation, *Regulated Rivers-Research & Management*, *15*(5), 463-476.

Friedman, J. M., G. T. Auble, P. B. Shafroth, M. L. Scott, M. F. Merigliano, M. D. Preehling, and E. K. Griffin (2005), Dominance of non-native riparian trees in western USA, *Biological Invasions*, *7*(4), 747-751, doi: 10.1007/s10530-004-5849-z.

Gladwin, D., and J. Roelle (1998), Survival of plains cottonwood (*Populus deltoides* subsp.*Monilifera*) and saltcedar (*Tamarix ramosissima*) seedlings in response to flooding, *Wetlands*, *18*(4), 669-674, doi: 10.1007/bf03161681.

Graf, W. L. (1978), Fluvial adjustments to the spread of tamarisk in the Colorado Plateau region, *Geological Society of America Bulletin*, *89*(10), 1491-1501.

Grams, P. E., and J. C. Schmidt (2002), Streamfow regulation and multi-level flood plain formation: channel narrowing on the aggrading Green River in the eastern Unita Mountains, Colorado and Utah, *Geomorphology*, *44*(3-4), 337-360.

Gran, K., and C. Paola (2001), Riparian vegetation controls on braided stream dynamics, *Water Resources Research*, *37*(12), 3275-3283.

Green, J. C. (2005), Modelling flow resistance in vegetated streams: review and development of new theory, *Hydrological Processes*, *19*(6), 1245-1259.

Hazel, J. E., D. J. Topping, J. C. Schmidt, and M. Kaplinski (2006), Influence of a dam on fine-sediment storage in a canyon river, *Journal of Geophysical Research-Earth Surface*, *111*(F1), F01025, doi: 10.1029/2004jf000193.

Hereford, R. (1984), Climate and ephemeral-stream processes: Twentieth-century geomorphology and alluvial stratigraphy of the Little Colorado River, Arizona, *Geological Society of America Bulletin*, *95*(6), 654-668.

Hey, R. D., and C. R. Thorne (1986), Stable channels with mobile gravel beds, *Journal of Hydraulic Engineering*, *112*(8), 671-689.

House, P. K., P. B. Shafroth, and V. B. Beauchamp (2006), Hydrology and fluvial geomorphology, in *Defining ecosystem flow requirements for the Bill Williams River, Arizona*, edited by P. B. Shafroth and V. B. Beauchamp, pp. 9-30, U.S. Geological Survey Reston, VA.

Hupp, C. R., and W. R. Osterkamp (1996), Riparian vegetation and fluvial geomorphic processes, *Geomorphology*, *14*(4), 277-295.

Jackson, W., and P. Summers (1988), Bill Williams River Field Assessment: Hydrology, Hydrogeology, and Geomorphology, US Bureau of Land Management, Denver, CO.

Jaeger, K. L., and E. Wohl (2011), Channel response in a semiarid stream to removal of tamarisk and Russian olive, *Water Resources Research*, *47*(2), W02536, doi: 10.1029/2009wr008741.

Johnson, W. C. (1994), Woodland expansion in the Platte River, Nebraska: patterns and causes, *Ecological Monographs*, *64*(1), 45-84.
Johnson, W. C. (2000), Tree recruitment and survival in rivers: influence of hydrological processes, *Hydrological Processes*, *14*(16-17), 3051-+.
Kean, J. W., and J. D. Smith (2005), Generation and verification of theoretical rating curves in the Whitewater River basin, Kansas, *Journal of Geophysical Research-Earth Surface*, *110*(F4), doi: F04012
10.1029/2004jf000250.
Kochel, R. C. (1988), Geomorphic impact of large floods: Review and new perspectives on magnitude and frequency, in *Flood geomorphology*, edited by V. R. Baker, R. C. Kochel and P. C. Patton, pp. 169-188, Wiley.
Konrad, C. P., A. Warner, and J. V. Higgins (2012), Evaluating dam re-operation for freshwater conservation in the Sustainable Rivers Project, *River Research and Applications*, *28*(6), 777-792, doi: 10.1002/rra.1524.
Konrad, C. P., J. D. Olden, D. A. Lytle, T. S. Melis, J. C. Schmidt, E. N. Bray, M. C. Freeman, K. B. Gido, N. P. Hemphill, M. J. Kennard, L. E. McMullen, M. C. Mims, M. Pyron, C. T. Robinson, and J. G. Williams (2011), Large-scale flow experiments for managing river systems, *BioScience*, *61*(12), 948-959, doi: 10.1525/bio.2011.61.12.5.
Levine, C. M., and J. C. Stromberg (2001), Effects of flooding on native and exotic plant seedlings: implications for restoring south-western riparian forests by manipulating water and sediment flows, *Journal of Arid Environments*, *49*(1), 111-131.
Lytle, D. A., and D. M. Merritt (2004), Hydrologic regimes and riparian forests: A structured population model for cottonwood, *Ecology*, *85*(9), 2493-2503.
Magilligan, F. J., and K. H. Nislow (2005), Changes in hydrologic regime by dams, *Geomorphology*, *71*(1-2), 61-78, doi: 10.1016/j.geomorph.2004.08.017.
Mahoney, J. M., and S. B. Rood (1998), Streamflow, requirements for cottonwood seedling recruitment - An interactive model, *Wetlands*, *18*(4), 634-645.
May, C. L., B. Pryor, T. E. Lisle, and M. Lang (2009), Coupling hydrodynamic modeling and empirical measures of bed mobility to predict the risk of scour and fill of salmon redds in a large regulated river, *Water Resources Research*, *45*, W05402, doi: 10.1029/2007wr006498.
Melis, T. S., J. Korman, and T. A. Kennedy (2012), Abiotic & biotic responses of the Colorado River to controlled floods at Glen Canyon Dam, Arizona, USA, *River Research and Applications*, *28*(6), 764-776, doi: 10.1002/rra.1503.
Merritt, D. M., and N. L. Poff (2010), Shifting dominance of riparian Populus and Tamarix along gradients of flow alteration in western North American rivers, *Ecological Applications*, *20*(1), 135-152.
Merritt, D. M., M. L. Scott, N. L. Poff, G. T. Auble, and D. A. Lytle (2010), Theory, methods and tools for determining environmental flows for riparian vegetation: riparian vegetation-flow response guilds, *Freshwater Biology*, *55*(1), 206-225, doi: 10.1111/j.1365-2427.2009.02206.x.
Micheli, E. R., and J. W. Kirchner (2002), Effects of wet meadow riparian vegetation on streambank erosion. 2. Measurements of vegetated bank strength and consequences for failure mechanics, *Earth Surface Processes and Landforms*, *27*(7), 687-697, doi: 10.1002/esp.340.
Nagler, P. L., E. P. Glenn, C. S. Jarnevich, and P. B. Shafroth (2011), Distribution and abundance of saltcedar and Russian olive in the western United States, *Critical Reviews in Plant Sciences*, *30*(6), 508-523, doi: 10.1080/07352689.2011.615689.
Nepf, H. M. (1999), Drag, turbulence, and diffusion in flow through emergent vegetation, *Water Resources Research*, *35*(2), 479-489.
Palmer, M. A., and E. S. Bernhardt (2006), Hydroecology and river restoration: Ripe for research and synthesis, *Water Resources Research*, *42*(3), W03s07, doi: 10.1029/2005wr004354.

Parker, G. (2004), 1D Sediment Transport Morphodynamics with Applications to Rivers and Turbidity Currents, edited, pp. e-book, Saint Anthony Falls Laboratory, University of Minnesota.

Petryk, S., and G. I. Bosmajian (1975), Analysis of flow through vegetation, *Journal of the Hydraulics Division-ASCE*, *101*(HY7), 871-884.

Poff, N. L., J. D. Allan, M. B. Bain, J. R. Karr, K. L. Prestegaard, B. D. Richter, R. E. Sparks, and J. C. Stromberg (1997), The natural flow regime: A paradigm for river conservation and restoration, *BioScience*, *47*(11), 769-784.

Polzin, M. L., and S. B. Rood (2006), Effective disturbance: Seedling safe sites and patch recruitment of riparian cottonwoods after a major flood of a mountain river, *Wetlands*, *26*(4), 965-980.

Powell, D. M., R. Brazier, J. Wainwright, A. Parsons, and M. Nichols (2006), Spatial patterns of scour and fill in dryland sand bed streams, *Water Resour. Res.*, *42*(8), W08412, doi: 10.1029/2005wr004516.

Richter, B. D., R. Mathews, and R. Wigington (2003), Ecologically sustainable water management: Managing river flows for ecological integrity, *Ecological Applications*, *13*(1), 206-224.

Rominger, J. T., A. F. Lightbody, and H. M. Nepf (2010), Effects of added vegetation on sand bar stability and stream hydrodynamics, *Journal of Hydraulic Engineering*, *136*(12), 994-1002.

Rood, S. B., G. M. Samuelson, J. H. Braatne, C. R. Gourley, F. M. R. Hughes, and J. M. Mahoney (2005), Managing river flows to restore floodplain forests, *Frontiers in Ecology and the Environment*, *3*(4), 193-201.

Sandercock, P. J., and J. M. Hooke (2010), Assessment of vegetation effects on hydraulics and of feedbacks on plant survival and zonation in ephemeral channels, *Hydrological Processes*, *24*, 695-713, doi: 10.1002/hyp.7508.

Schmidt, J. C., and P. R. Wilcock (2008), Metrics for assessing the downstream effects of dams, *Water Resources Research*, *44*(4), W04404, doi: 10.1029/2006wr005092.

Schnauder, I., and H. Moggridge (2009), Vegetation and hydraulic-morphological interactions at the individual plant, patch and channel scale, *Aquatic Sciences*, *71*(3), 318-330, doi: 10.1007/s00027-009-9202-6.

Sciences, S. (2002), Merced River corridor restoration plan, Prepared by Stillwater Sciences, Berkeley, California for CALFED Bay-Delta Program, Sacramento, California.

Scott, M. L., J. M. Friedman, and G. T. Auble (1996), Fluvial process and the establishment of bottomland trees, *Geomorphology*, *14*(4), 327-339.

Shafroth, P. B., and V. B. Beauchamp (Eds.) (2006), *Defining ecosystem flow requirements for the Bill Williams River, Arizona*, 135 pp., U.S. Department of Interior, U.S. Geological Survey, Reston, VA.

Shafroth, P. B., J. C. Stromberg, and D. T. Patten (2002), Riparian vegetation response to altered disturbance and stress regimes, *Ecological Applications*, *12*(1), 107-123.

Shafroth, P. B., G. T. Auble, J. C. Stromberg, and D. T. Patten (1998), Establishment of woody riparian vegetation in relation to annual patterns of streamflow, Bill Williams River, Arizona, *Wetlands*, *18*(4), 577-590.

Shafroth, P. B., V. B. Beauchamp, M. K. Briggs, K. Lair, M. L. Scott, and A. A. Sher (2008), Planning riparian restoration in the context of Tamarix control in western North America, *Restor Ecol*, *16*(1), 97-112.

Shafroth, P. B., J. R. Cleverly, T. L. Dudley, J. P. Taylor, C. Van Riper, E. P. Weeks, and J. N. Stuart (2005), Control of Tamarix in the Western United States: Implications for water salvage, wildlife use, and riparian restoration, *Environmental Management*, *35*(3), 231-246, doi: 10.1007/s00267-004-0099-5.

Shafroth, P. B., A. C. Wilcox, D. A. Lytle, J. T. Hickey, D. C. Andersen, V. B. Beauchamp, A. Hautzinger, L. E. McMullen, and A. Warner (2010), Ecosystem effects of environmental flows: modelling and experimental floods in a dryland river, *Freshwater Biology*, *55*, 68-85.

Sheppard, P. R., A. C. Comrie, G. D. Packin, K. Angersbach, and M. K. Hughes (2002), The climate of the US Southwest, *Climate Research*, *21*, 219-238.

Sher, A. A., D. L. Marshall, and S. A. Gilbert (2000), Competition between native *Populus deltoides* and invasive *Tamarix ramosissima* and the implications for reestablishing flooding disturbance, *Conservation Biology*, *14*(6), 1744-1754.

Sher, A. A., D. L. Marshall, and J. P. Taylor (2002), Establishment patterns of native *Populus* and *Salix* in the presence of invasive nonnative *Tamarix*, *Ecological Applications*, *12*(3), 760-772.

Stella, J. C., J. J. Battles, B. K. Orr, and J. R. McBride (2006), Synchrony of seed dispersal, hydrology and local climate in a semi-arid river reach in California, *Ecosystems*, *9*(7), 1200-1214, doi: 10.1007/s10021-005-0138-y.

Stella, J. C., M. K. Hayden, J. J. Battles, H. Piegav, S. Dufour, and A. K. Fremier (2011), The role of abandoned channels as refugia for sustaining pioneer riparian forest ecosystems, *Ecosystems*, *14*, 776-790.

Stromberg, J. C. (2001), Restoration of riparian vegetation in the south-western United States: importance of flow regimes and fluvial dynamism, *Journal of Arid Environments*, *49*(1), 17-34, doi: 10.1006/jare.2001.0833.

Stromberg, J. C., B. D. Richter, and D. T. Patten (1993), Response of a Sonoran riparian forest to a 10-year return flood, *Great Basin Naturalist*, *53*, 118-130.

Stromberg, J. C., P. B. Shafroth, and A. F. Hazelton (2012), Legacies of flood reduction on a dryland river, *River Research and Applications*, *28*(2), 143-159, doi: 10.1002/rra.1449.

Stromberg, J. C., S. J. Lite, R. Marler, C. Paradzick, P. B. Shafroth, D. Shorrock, J. M. White, and M. S. White (2007), Altered stream-flow regimes and invasive plant species: the Tamarix case, *Global Ecology and Biogeography*, *16*(3), 381-393, doi: 10.1111/j.1466-8238.2007.00297.x.

Tal, M., and C. Paola (2007), Dynamic single-thread channels maintained by the interaction of flow and vegetation, *Geology*, *35*(4), 347-350, doi: 10.1130/g23260a.1.

Tal, M., K. Gran, A. B. Murray, C. Paola, and D. M. Hicks (2004), Riparian vegetation as a primary control on channel characteristics in multi-thread rivers, in *Riparian Vegetation and Fluvial Geomorphology*, edited by S. J. Bennett and A. Simon, pp. 43-58, American Geophysical Union, Washington D.C.

Tooth, S., and G. C. Nanson (2000), The role of vegetation in the formation of anabranching channels in an ephemeral river, Northern plains, arid central Australia, *Hydrological Processes*, *14*(16-17), 3099-3117.

Trush, W. J., S. M. McBain, and L. B. Leopold (2000), Attributes of an alluvial river and their relation to water policy and management, *Proceedings of the National Academy of Sciences of the United States of America*, *97*(22), 11858-11863.

Vincent, K., J. Friedman, and E. Griffin (2009), Erosional consequence of saltcedar control, *Environmental Management*, *44*(2), 218-227.

Webb, R. H., and S. A. Leake (2006), Ground-water surface-water interactions and long-term change in riverine riparian vegetation in the southwestern United States, *Journal of Hydrology*, *320*(3-4), 302-323, doi: 10.1016/j.jhydrol.2005.07.022.

Williams, G. P. (1978), The case of the shrinking channels—the North Platte and Platte Rivers in Nebraska, *U.S. Geological Survey Circular 781*.

Williams, G. P., and M. G. Wolman (1984), Downstream effects of dams on alluvial rivers, 83 pp, United States Geological Survey Professional Paper 1286.

Wright, S. A., J. C. Schmidt, T. S. Melis, D. J. Topping, and D. M. Rubin (2008), Is there enough sand? Evaluating the fate of Grand Canyon sandbars, *GSA Today*, *18*(8), 4-10, doi: 10.1130/GSATG12A.1.

Appendix 1: Sediment transport measurements, 2006 and 2010 floods

We collected a limited amount of suspended sediment data during the 2006 and 2010 floods. These data were designed to provide insights into spatial and temporal variations in concentrations, as a proxy for sediment supply, rather than for calculation of loads. In 2006, we collected six Isco pump samples at Rankin (taken at one-hour intervals, at 5 m from the water's edge and ~0.5 m below the surface) and four grab samples at Mineral (taken over a 5-hour period, at 2 m from the water's edge and ~0.6 m below the surface). We compare the suspended sediment concentrations we measured to those from a downstream site, at the mouth of the BWR in Lake Havasu, sampled by Wiele et al. [2009, 2011]. In 2010 we collected cross-section and depth-integrated suspended sediment samples, at 9 different times across the flood hydrograph,along a transect 1 km downstream of our Rankin reach. Samples were collected using a DH-74 sampler from a cataraft using a tagline.

Measurements of suspended sediment transport in 2006 showed downstream variation in total suspended sediment (TSS) concentrations (Figure 1-1). At Rankin, we measured concentrations of 130±7 mg L^{-1} over a 6-hour period during the flood peak. Further downstream, at Mineral, we measured TSS of 270±15 mg L^{-1} over a 5-hour period during the 2006 flood peak, which is similar to USGS-measured TSS values from a downstream site at that time [Wiele et al., 2009]. Sampling at Rankin in 2010 documented the highest sediment concentrations on the rising limb of the flood hydrograph (5600 mg L^{-1}), with values of 810±90 mg L^{-1} over a 5-hour period during the flood peak

Limited sediment transport data collected both by us and USGS [Wiele et al., 2009; Wiele et al., 2011] during recent floods provide evidence of spatially varying supply limitation. The suspended sediment concentrations measured during the 2006 event were lowest near Alamo Dam, suggesting that supply becomes more available as the river passes through wide alluvial basins such as Planet Valley. Measurements at Rankin in 2010 show an initial spike of sand and silt transport on the rising limb at the beginning of high-flow events, followed by sharp decline, a hysteresis pattern consistent with supply limitation. Measurements by USGS during the 2005 and 2006 events at the mouth of the BWR, in Lake Havasu, show an analogous but more muted hysteresis [Wiele et al., 2009]. More generally, sediment transport monitoring and construction of sediment budgets that quantify the relative influences of dams, tributaries, and downstream morphology on sediment supply would provide further insight into how sediment supply may influence the erosional effects of floods and vegetation dynamics and, in turn, into how sediment supply should be accounted for in planning managed flow releases in dammed rivers.

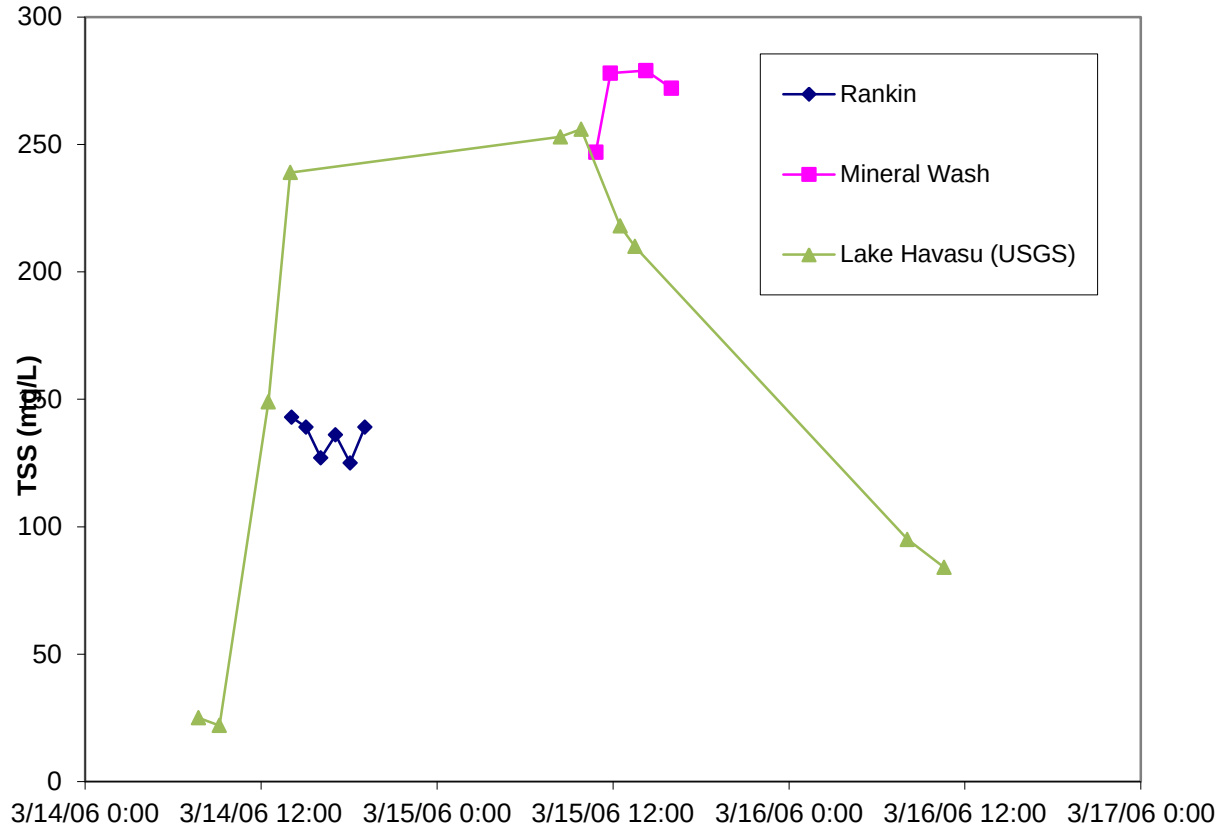

Figure 1-1. Suspended sediment transport measurements during March 2006 flood on Bill Williams River, including our measurements at Rankin and Mineral Wash and USGS measurements at the mouth of the BWR in Lake Havasu (Wiele et al., 2009).

References cited

Wiele, S. M., R. J. Hart, H. L. Darling, and A. B. Hautzinger (2009), Sediment transport in the Bill Williams River and turbidity in Lake Havasu during and following two high releases from Alamo Dam, Arizona, in 2005 and 2006, *U.S. Geological Survey Scientific Investigations Report*, *2009-5195*, 22 p.

Wiele, S. M., J. P. Macy, H. L. Darling, R. J. Hart, and A. B. Hautzinger (2011), Discharge and sediment concentration in the Bill Williams River and turbidity in Lake Havasu during and following high releases from Alamo Dam, Arizona, in March and April 2010, *U.S. Geological Survey Open-File Report 2011-1129*, 10 p.

Appendix 2: Other products associated with this project

Project results have been disseminated to the public and the scientific community, including:

- Completion of M.S. thesis at the University of Montana:
    - Dekker, F. J. 2012. "Sediment Dynamics in a Dryland River: Grain-Size Variations, Erosion Rates, Sediment Mixing, and Dam Effects." M.S Thesis, Geosciences. Available for download: http://etd.lib.umt.edu/theses/available/etd-08312012-091636/
- Submission of one manuscript to a peer-reviewed scientific journal.
    - Wilcox, A. C. and P. B. Shafroth. In revision. "Coupled hydrogeomorphic and woody-seedling responses to controlled flood releases in a dryland river." Submitted to *Water Resources Research* (reviewers recommended publication after minor revisions; the *In revision* version of this paper is included in this report).
- Presentation of results at international scientific conferences:
    - Bywater-Reyes, S., A. Wilcox, A. Lightbody, K. Skorko, J. C. Stella. 2012. "Uprooting force balance for pioneer woody plants: A quantification of the relative contribution of above- and below-ground plant architecture to uprooting susceptibility." *EOS Trans. AGU* Fall Meet. Suppl. Abstract EP41A-0867.
    - Shafroth, P.B., D.M. Merritt, and A.C. Wilcox. 2012. "Effects of river hydrology and fluvial processes on riparian vegetation establishment, growth, and survival." *EOS Trans. AGU* Fall Meet. Suppl. Abstract EP43C-03.
    - Wilcox, A.C., P.B. Shafroth, A. Lightbody, J.C. Stella, S. Bywater-Reyes, L. Kiu, and K.Skorko. 2012. "Feedbacks among floods, pioneer woody vegetation, and channel change in sand-bed rivers: Insights from field studies of controlled flood releases and models." Geophysical Research Abstracts Vol. 14, EGU General Assembly, Vienna, Austria.
    - Dekker, F. and A.C. Wilcox. 2011. "Dam impacts on downstream sediment grain size in a dryland river." *EOS Trans. AGU.* Fall Meet. Suppl. Abstract EP51A-0831.
- Research talks by Wilcox (*"Feedbacks between Riparian Vegetation and River Morphodynamics"*)
    - Montana Institute on Ecosystems Rough Cut Seminar Series. University of Montana, 15 October; Montana State University, 17 October 2012.
    - Institut de Physique du Globe – Paris, 4 April 2012.
    - Free University of Bozen-Bolzano, Italy, 29 March 2012.
    - Ecole Normale Supérieure de Lyon, France, 20 April 2012.
    - University College Cork, Ireland, 13 March 2012.

The University of Montana investigators have successfully leveraged other resources for studies devoted entirely or partly toward the BWR

- National Science Foundation. "Collaborative Research: Quantifying feedbacks between fluvial morphodynamics and pioneer riparian vegetation in sand-bed rivers." EAR-1025076, 2010-2013
- National Center for Airborne Laser Mapping Graduate Student Seed grant: An airborne lidar survey of 40 km^2 along the Santa Maria River will be performed in 2013 as a result of a grant from NCALM, a NSF-funded source of high-quality LiDAR, to UM. These data will be open-source and hosted on NCALM's website and OpenTopography.
- EPA STAR graduate fellowship to U. Montana student Sharon Bywater-Reyes (working on BWR)
- Geological Society of America Graduate Research Grant to Franklin Dekker

- PRIME Lab. “Quantifying erosion and sediment dynamics at variable time scales in a dryland river.” Seed grant for cosmogenic nuclide analysis of BWR sediments at Purdue Rare Isotope Measurement Laboratory, 2011

Appendix 3: Supporting information

A. Example mixing equation calculation

The following is an example mixing calculation for (equation 3, Catchment erosion rate chapter) with uncertainty propagation:

Equation for Nuclide concentration upstream of Alamo Dam:

$$\langle \mathrm{N_{Confluence}} \rangle = \frac{(\mathrm{N_{BS}E_{BS}A_{BS}} + \mathrm{N_{SM}E_{SM}A_{SM}})}{(\mathrm{E_{BS}A_{BS}} + \mathrm{E_{SM}A_{SM}})} \quad (3)$$

Equation notations:

$\langle N_{confluence} \rangle$ = Mixing calculation result for nuclide concentration at BWR confluence (at g^{-1})
N_{BS} = BS (*Big Sandy River*) nuclide concentration (at g^{-1})
E_{BS} = BS erosion rate (t km^{-2} yr^{-1})
A_{BS} = BS catchment area (km^2)
N_{SM} = SM (*Santa Maria River*) nuclide concentration (at g^{-1})
E_{SM} = SM erosion rate (t km^{-2} yr^{-1})
A_{SM} = SM catchment area (km^2)

Equation input values:

$N_{BS} = 1.45\times10^5$ at g^{-1}
E_{BS} = 159.5 t km^{-2} yr^{-1}
A_{BS} = 7,428 km^2
$N_{SM} = 1.77\times10^5$ at g^{-1}
E_{SM} = 114.9 t km^{-2} yr^{-1}
A_{SM} = 3,707 km^2

$\langle N_{Confluence} \rangle$ Calculation:

$$\langle \mathrm{N_{Confluence}} \rangle = \frac{(1.45\times10^5 \boldsymbol{at\ g^{-1}})(159.5\ \cancel{t\ km^{-2}yr^{-1}})(7{,}428\ \cancel{km^{-2}}) + (1.77\times10^5 \boldsymbol{at\ g^{-1}})(114.9\ \cancel{t\ km^{-2}yr^{-1}})(3{,}707\ \cancel{km^{-2}})}{\left((159.5\ \cancel{t\ km^{-2}yr^{-1}})(7{,}428\ \cancel{km^{-2}}) + (114.9\ \cancel{t\ km^{-2}yr^{-1}})(3{,}707\ \cancel{km^{-2}})\right)}$$

$\langle \mathrm{N_{Confluence}} \rangle = 1.54\times10^5$ at g^{-1}

Propagation of uncertainty equations:

Notation:
u_x = an absolute uncertainty
$\%u_x$ = a relative uncertainty
r_x= a result with uncertainty

Addition and subtraction:

$$u_{12} = \sqrt{u_1^2 + u_2^2}$$

Percent uncertainty:

$$\%u_1 = 100 \times \frac{u_1}{r_1}$$

Multiplication and division:

$$\%u_{12} = \sqrt{(\%u_1)^2 + (\%u_2)^2}$$

***Propagation of uncertainty for <$N_{Confluence}$>Calculation**:*

Notation:

u<$N_{confluence}$> = Mixing calculation result absolute uncertainty (at g^{-1})

uN_{BS} = BS nuclide concentration absolute uncertainty (at g^{-1})

$\%uN_{BS}$ = BS nuclide concentration percent uncertainty

uE_{BS} = BS erosion rate absolute uncertainty (t km^{-2} yr^{-1})

$\%uE_{BS}$ = BS erosion rate percent uncertainty

A_{BS} = BS catchment area (km^2)

uN_{SM} = SM nuclide concentration absolute uncertainty (at g^{-1})

$\%uN_{SM}$ = SM nuclide concentration percent uncertainty

uE_{SM} = SM erosion rate absolute uncertainty (t km^{-2} yr^{-1})

$\%uE_{SM}$ = SM erosion rate percent uncertainty

A_{SM} = SM catchment area (km^2)

Uncertainty in mixing calculation:

$$\langle \mathbf{uN_{Confluence}} \rangle = \frac{(\mathbf{uN_{BS}uE_{BS}A_{BS}} + \mathbf{uN_{SM}uE_{SM}A_{SM}})}{(\boldsymbol{u}\mathbf{E_{BS}A_{BS}} + \mathbf{uE_{SM}A_{SM}})}$$

Steps for Solving Uncertainty

Numerator:

$$(\mathbf{uN_{BS}uE_{BS}A_{BS}} + \mathbf{uN_{SM}uE_{SM}A_{SM}})$$

(1) Uncertainty multiplication

$$\text{numerator left} = \left(\frac{\left(\sqrt{(\%uN_{BS})^2 + (\%uE_{BS})^2}\right)}{100} \times (\mathrm{N_{BS}E_{BS}}) \right) \times \mathrm{A_{BS}}$$

$$\text{numerator right} = \left(\frac{\left(\sqrt{(\%uN_{SM})^2 + (\%uE_{SM})^2}\right)}{100} \times (\mathrm{N_{SM}E_{SM}}) \right) \times \mathrm{A_{SM}}$$

(2) Uncertainty addition

$$\text{Numerator uncertainty} = \sqrt{(numerator\ left)^2 + (numerator\ right)^2}$$

Denominator:

$$(\mathbf{E_{BS}A_{BS}} + \mathbf{E_{SM}A_{SM}})$$

(1) Uncertainty addition

$$Denominator\ uncertainty\ = \sqrt{(\mathrm{E_{BS}A_{BS}})^2 + (\mathrm{E_{SM}A_{SM}})^2}$$

Final Division:

$$\%u < N_{Confluence} >= \sqrt{\left(\frac{numerator\ uncertainty}{numerator\ result\ value} \times 100\right)^2 + \left(\frac{demoinator\ uncertainty}{denominator\ result\ value} \times 100\right)^2}$$

Conversion to absolute uncertainty from percent *uncertainty:*

$$< N_{Confluence} > = \left[\frac{(\%u < N_{Confluence} >)}{100}\right] \times \langle \mathrm{N_{Confluence}} \rangle$$

B. Mafic rock extent in sample watersheds

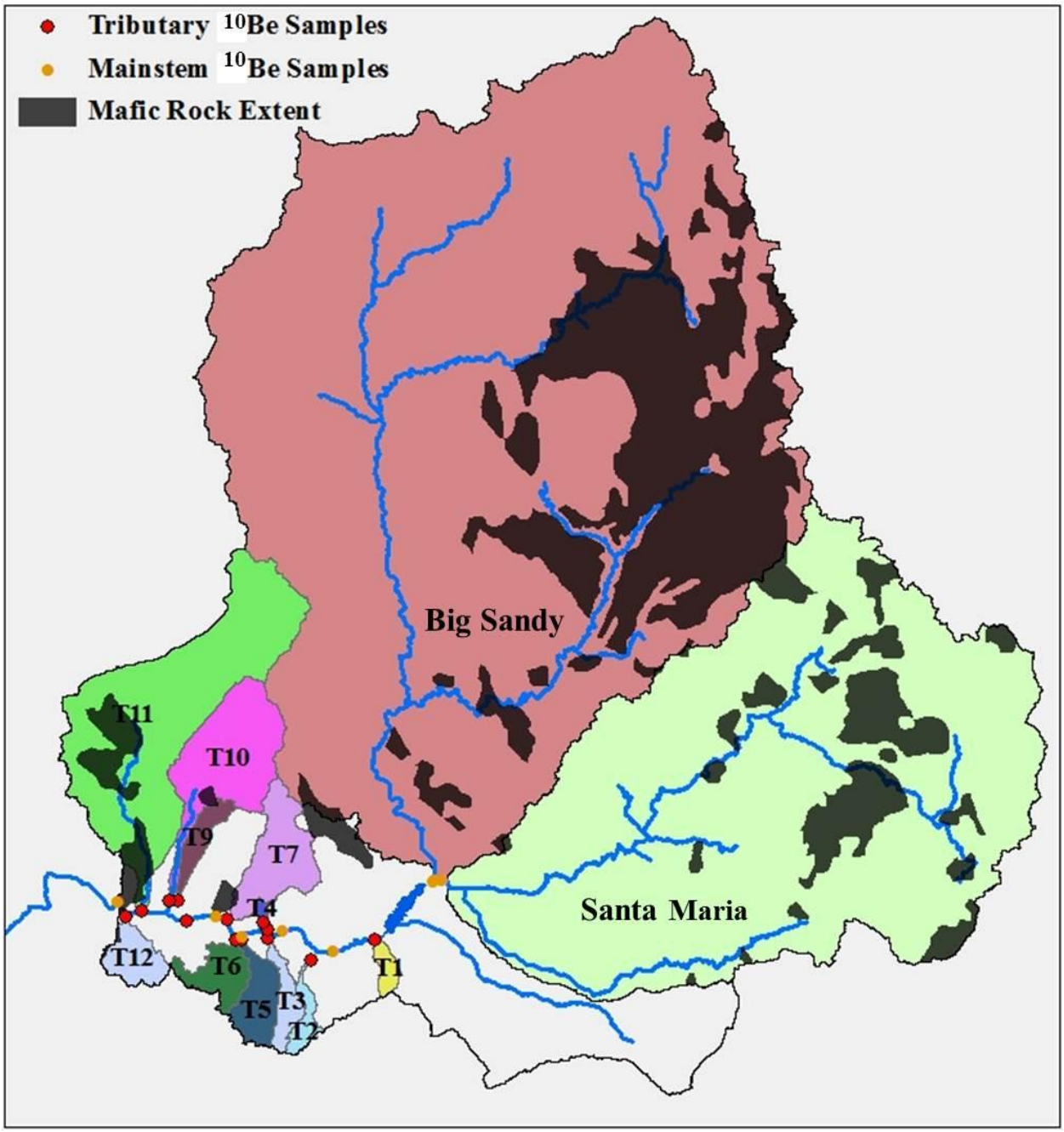

Figure B-1. The extent of mafic rock in the Bill Williams River watershed (Richard et al., 2000). A high percentage of mafic rock that is low in quartz could cause greater uncertainty in catchment nuclide concentration and erosion rate.

Table B-1. The percent area of mafic rock and average elevation in each sampled catchment. (Excluding DS_1-5).

Sample	Mafic Rock Percent Area (%)	Average Mafic Rock Elevation (m)	Average Elevation (m)	Elevation Difference (m)
BS	21.5	1542	1314	228
SM	13.6	1354	1136	218
BWR_C	18.8	1448	1255	193
T1	0	N/A	681	N/A
T2	0	N/A	588	N/A
T3	0	N/A	497	N/A
T4	0	N/A	398	N/A
T5	0	N/A	476	N/A
T6	0	N/A	450	N/A
T7	1.7	452	587	-135
T8	0	N/A	232	N/A
T9	0.8	603	452	151
T10	2.4	566	678	-112
T11	14.7	535	714	-179
T12	4.6	413	418	-5

C. Modern bathymetric survey erosion rate

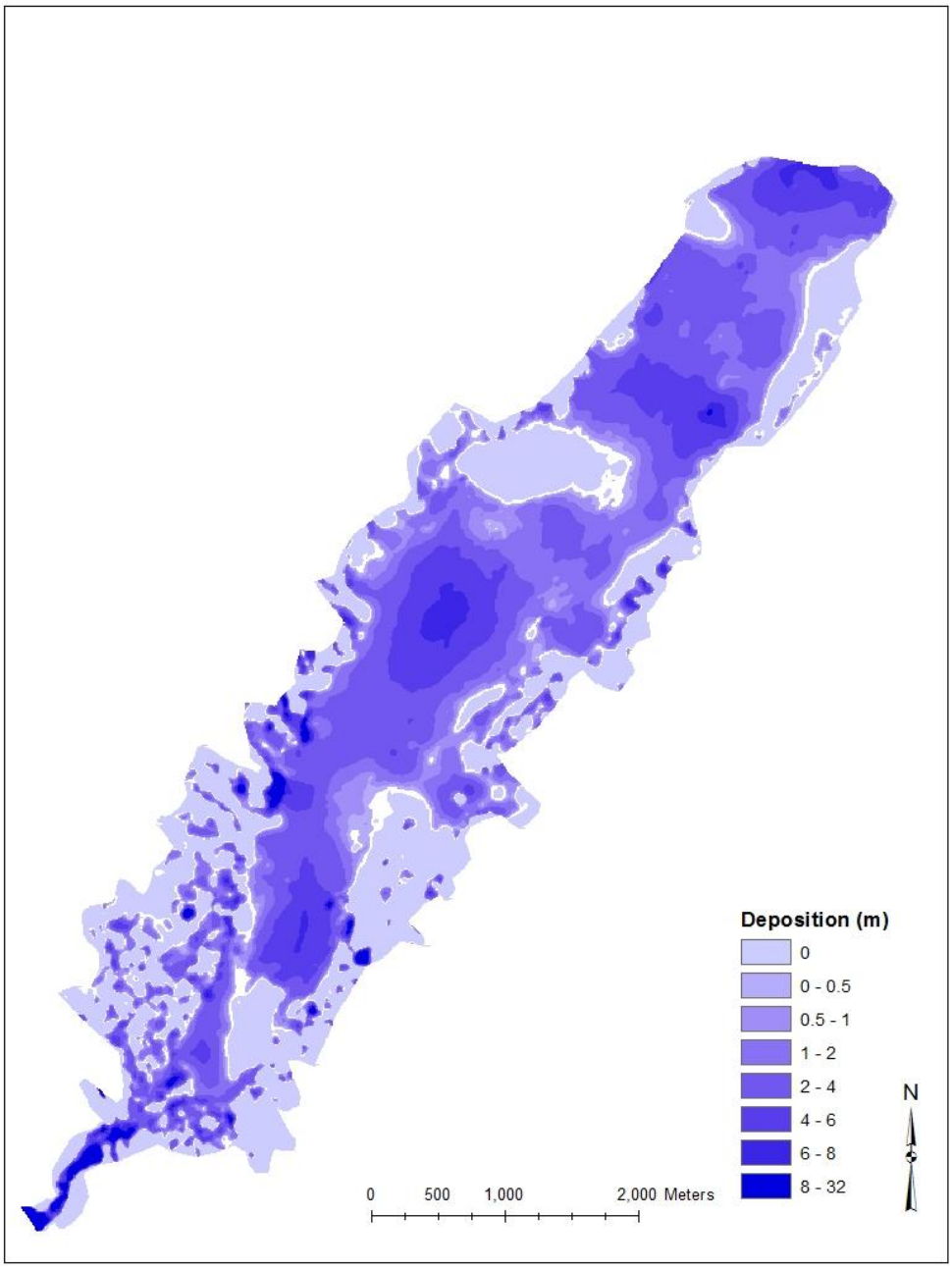

Figure C-1. Sediment deposition in Alamo Lake between 1968 and 1985 found by comparison of digital elevation models (DEMs) (US Army Corp of Engineers, 1963; US Army Corp of Engineers, 1985). Erosion rate found from the total deposition in those 17 years was 270 ± 20 t/km^2/yr. This is greater than the long-term rates of erosion found from cosmogenic nuclide analysis.

D. Supporting information for grain-size analysis study

Figure D-1. Left: small and medium grain-size photo mounts used for digital analysis of grain size; Right: photos of bed material taken with those mounts.

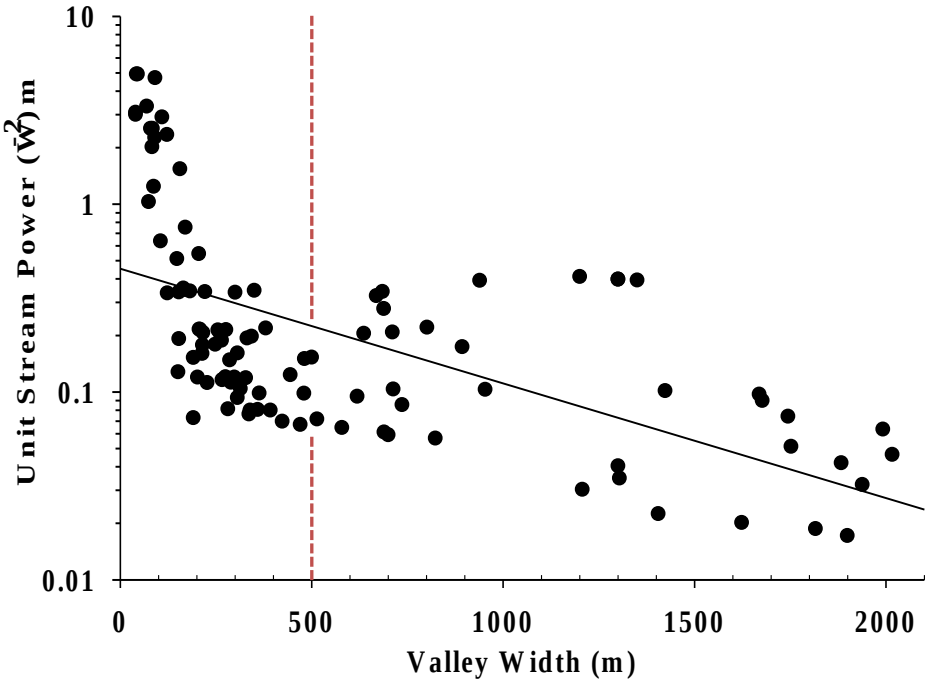

Figure D-2. Unit stream power for the BWR plotted with associated valley width. Valleys with greater than 500 m were studied in more detail because 500 m valley width is near an inflection point for unit stream power and only 4 valleys of that size exist on the BWR.

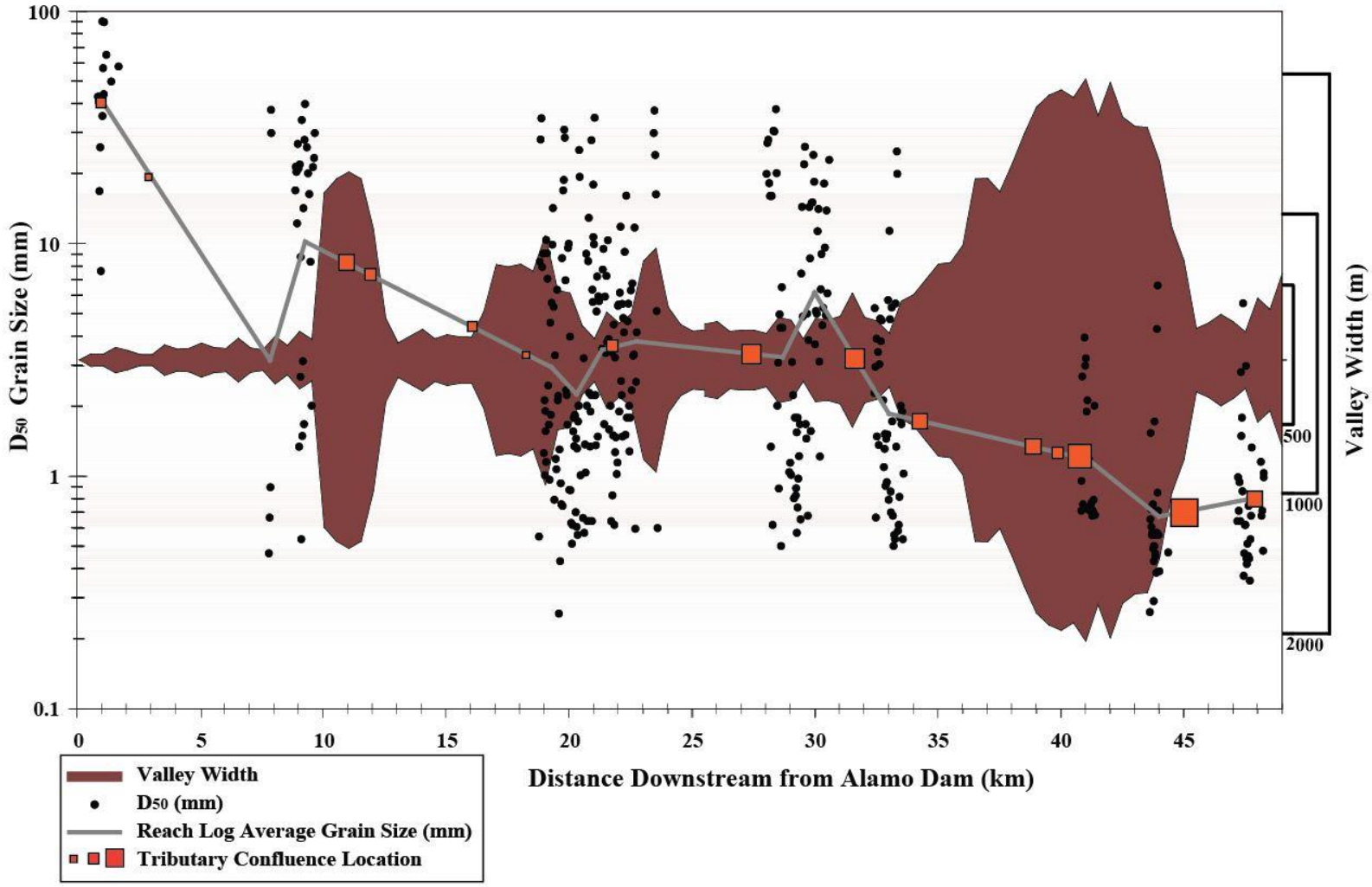

Figure D-3. Valley width (right y-axis), grain size (left y-axis) and tributary confluences are plotted with distance downstream from the dam. The grey line shows reach log averages of D_{50} grain size (mm). Boxes showing tributary confluences are roughly scaled to their catchment area. The coarse grain size just downstream from Alamo Dam is an indication of sediment deficit, while valley width control on grain size is evident in the floodplain reach centered at 40km where several large tributaries also join the mainstem.

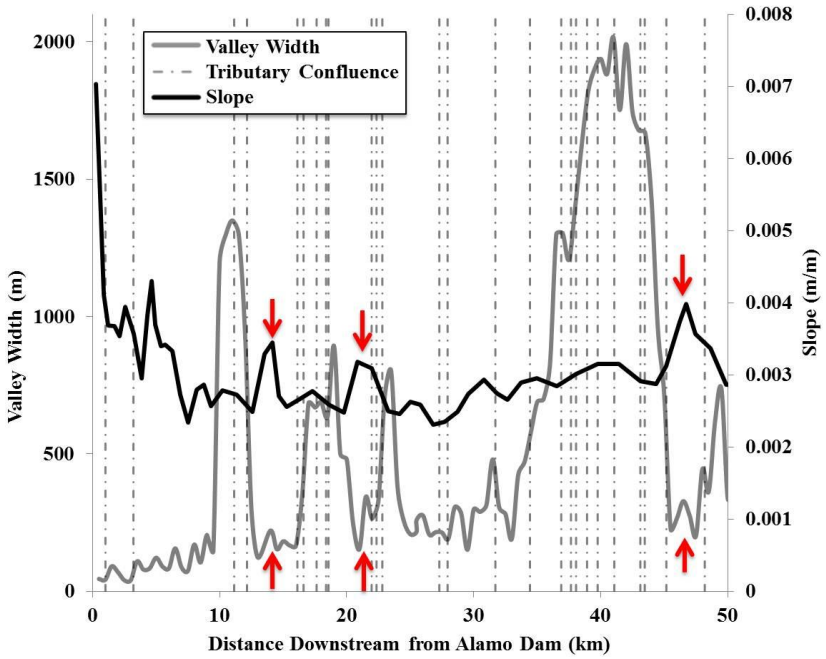

Figure D-4. Valley width and slope shown with distance downstream tributary confluence locations are represented by vertical dashed lines. Red arrows indicate areas of confinement that corresponded with increased slope.

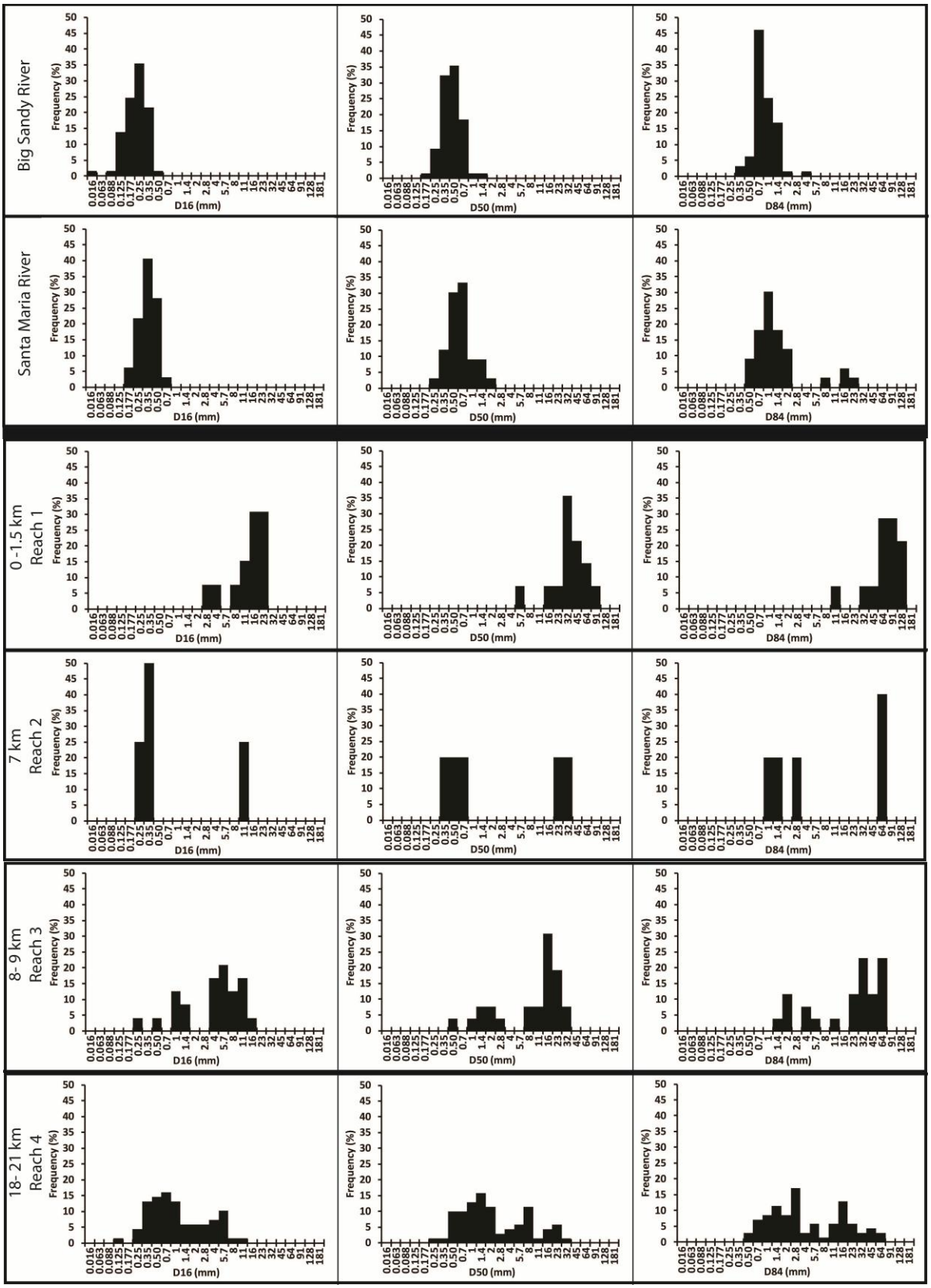
Big Sandy River
Santa Maria River
0 -1.5 km
Reach 1
7 km
Reach 2
8- 9 km
Reach 3
18- 21 km
Reach 4
Frequency (%)
D16 (mm)
D50 (mm)
D84 (mm)

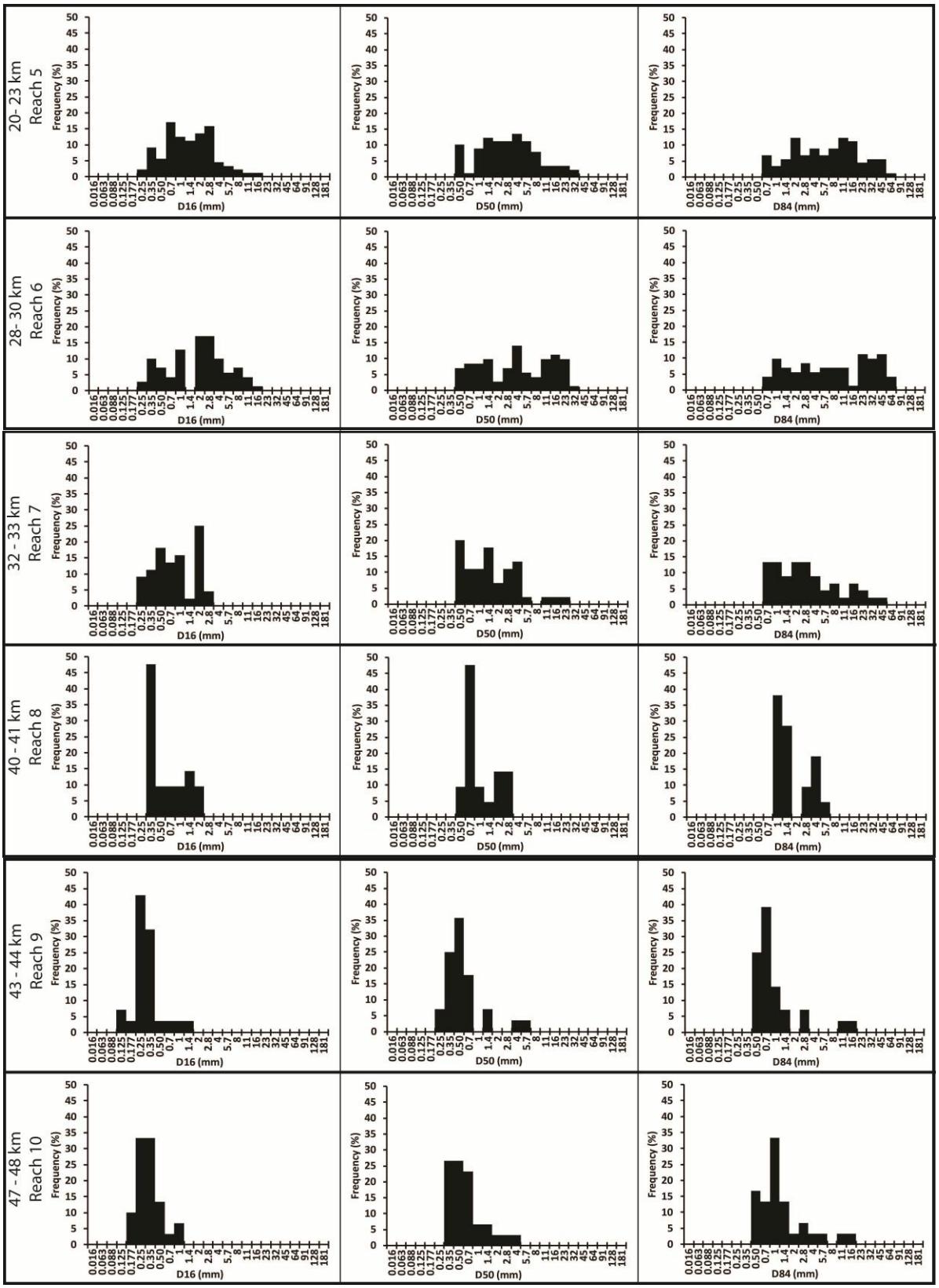

Figure D-5. Histograms with the frequency of D_{16}, D_{50} and D_{84} grain sizes in each reach. Size is by half phi class.

E. Aerial photograph comparisons of Bill Williams River in vicinity of Alamo Dam

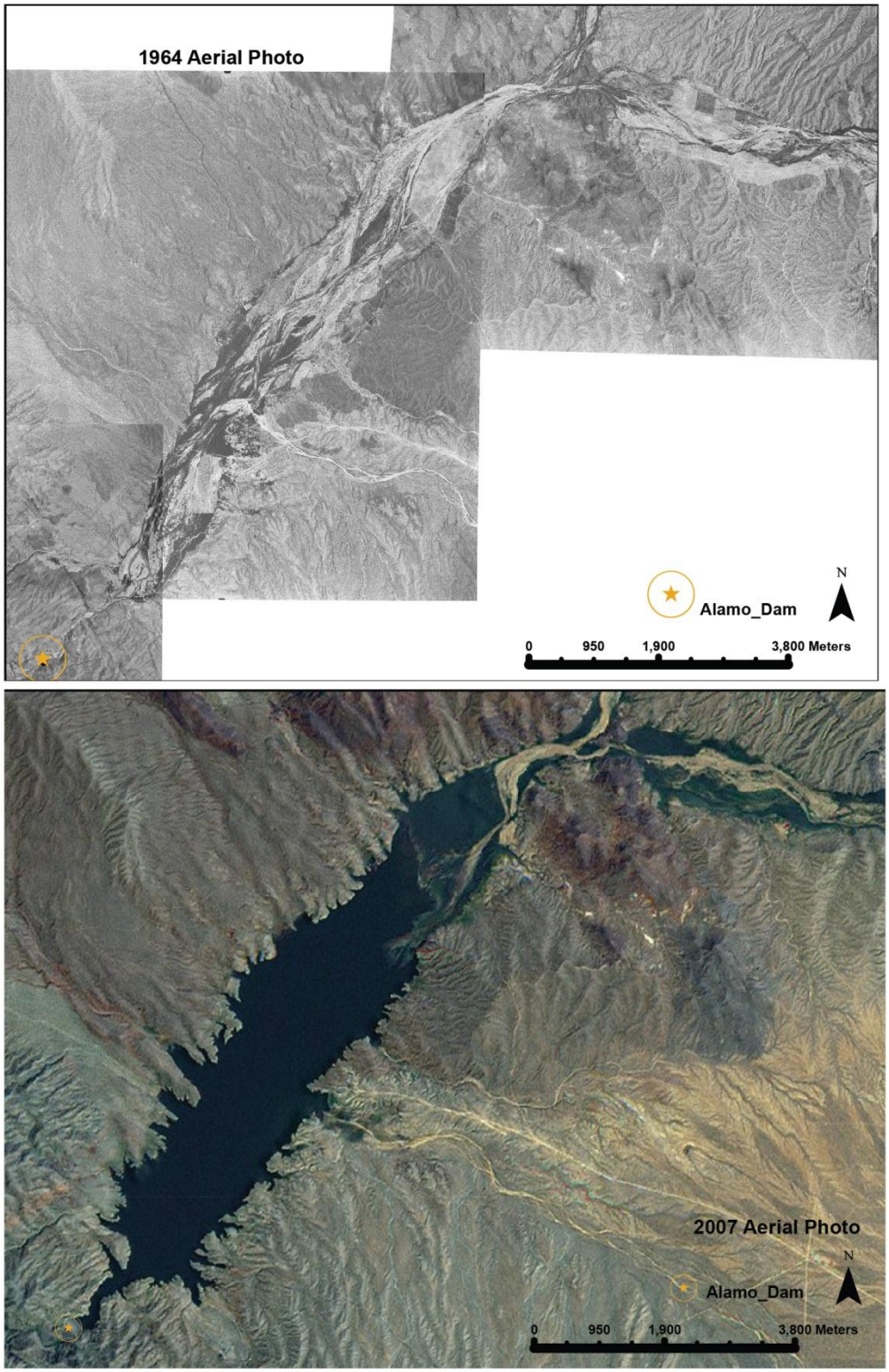

Figure E-1. Aerial photograph comparison of Alamo Valley (1964) and Alamo Reservoir (2007).

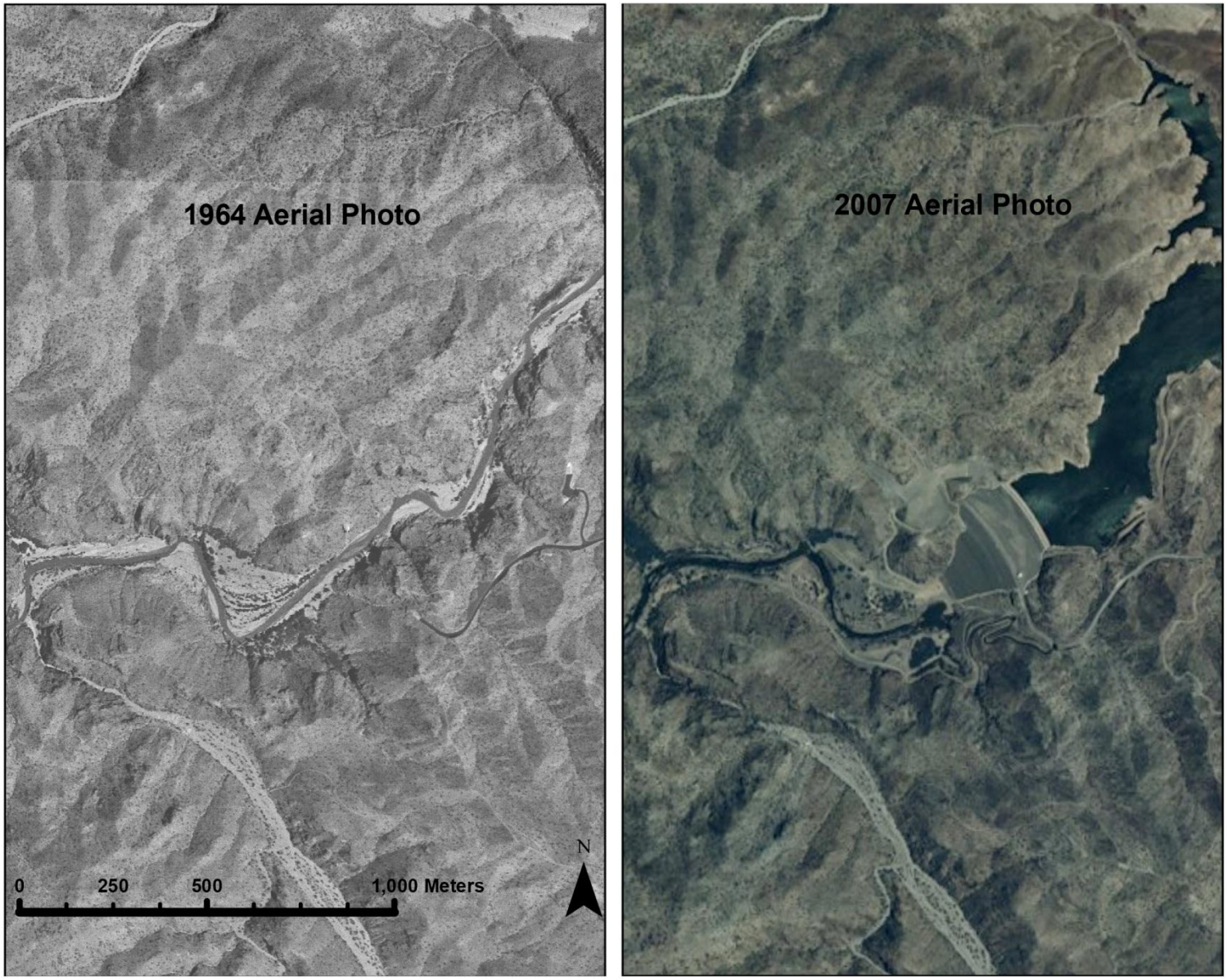

Figure E-2. Aerial photograph comparison of Bill Williams River at Alamo Dam site in 1964 and 2007.

References Cited (Appendix 3)

Richard, S.M., Reynolds, S.J., Spencer, J.E., and Pearthree, P.A., 2000, Geologic map of Arizona: Arizona Geological Survey Map, v. 35, no. 1, p. 1–000.

United States. Army. Corps of Engineers. Los Angeles District, 1973, Foundation report for Alamo Lake : Colorado River Basin, Bill Williams River, Arizona, flood control: Army Engineer District, Los Angeles, Los Angeles.

US Army Corp of Engineers, 1985, Alamo Lake Bathymetric Survey:.

US Army Corp of Engineers, 1963, Alamo Reservoir General Plan of Reservoir:.